3

UNEP/DEWA/RS.02-3

UNEP

Center for Clouds, Chemistry and Climate

The Asian Brown Cloud: Climate and Other Environmental Impacts

Report commissioned by the United Nations Environment Programme (UNEP) and
prepared by the Center for Clouds, Chemistry and Climate (C^4) funded by
the UNEP, National Science Foundation, USA, the G. Unger Vetlesen Foundation, and the
Alderson Chair funds to the Scripps Institution of Oceanography, University of California, San Diego.

UNEP Expert Panel

G.R. Cass *(Deceased; Georgia Institute of Technology, Atlanta)*
S.K. Chhabra *(Patel Chest Institute, New Delhi)*
W.D. Collins *(National Center for Atmospheric Research, Boulder)*
P.J. Crutzen *(Scripps Institution of Oceanography, UCSD; Max-Planck Institute for Chemistry, Mainz)*
N. Kalra *(Indian Agriculture Research Institute, New Delhi)*
T.N. Krishnamurti *(Florida State University, Tallahassee)*
J. Lelieveld *(Max-Planck Institute for Chemistry, Mainz)*
A.P. Mitra *(National Physical Laboratory, New Delhi), Chair*
H.V. Nguyen *(Scripps Institution of Oceanography, UCSD)*
V. Ramanathan *(Scripps Institution of Oceanography, UCSD)*
J.M. Samet, M.D. *(School of Public Health, Johns Hopkins University, Baltimore)*
D.R. Sikka *(National Physical Laboratory, New Delhi)*

UNEP Resource Experts

K. AchutaRao *(Lawrence Livermore National Laboratories, Livermore)*
C.E. Chung *(Scripps Institution of Oceanography, UCSD)*
A. Jayaraman *(Physical Research Laboratory, Ahmedabad)*
R. Krishnan *(Indian Institute of Tropical Meteorology, Pune)*
I.A. Podgorny *(Scripps Institution of Oceanography, UCSD)*

Peer Reviewers

L. Bengtsson *(Max Planck Institute of Meteorology, Hamburg, Germany)*
S. Gadgil *(Indian Institute of Science, Bangalore, India)*
T. Nakajima (*University of Tokyo, Japan*)
H. Rodhe *(University of Stockholm, Sweden)*

ABC Project Team

UNEP
Klaus Töpfer
Surendra Shrestha
Mylvakanam Iyngararasan

C^4
Veerabhadran Ramanathan
Paul J. Crutzen
Hung V. Nguyen

© UNEP and C^4 2002

ISBN: 92-807-2240-9

This publication may be reproduced for educational purposes without special permission from UNEP, provided that acknowledgement of the source is made. UNEP would appreciate receiving a copy of any publication that uses this publication as a source.

No use of this publication may be made for resale or for any other commercial purpose whatsoever without prior permission in writing from the United Nations Environment Programme.

For bibliographic and reference purposes this publication should be referred to as:

UNEP and C^4 (2002). The Asian Brown Cloud: Climate and Other Environmental Impacts UNEP, Nairobi

This report is available from:
United Nations Environment Programme
Regional Resource Centre for Asia and the Pacific (UNEP RRC.AP)
Outreach Building, Asian Institute of Technology
P.O. Box: 4, Klong Luang, Pathumthani 12120
Thailand
Tel:+(66-2) 516 2124
Fax:+(66-2) 516 2125
E-mail:grid@ait.ac.th
URL:http://www.rrcap.unep.org

DISCLAIMER
The contents of this volume do not necessarily reflect the views or policies of UNEP or contributory organizations.

Table of Contents

Executive Summary 1

Part I: The South Asian Haze: Air Pollution, Ozone and Aerosols

1. Introduction 8
2. The Indian Ocean Experiment 14
3. Air Pollution and Ozone 16
4. Spatial and Temporal Variations of the Haze 21

Part II: Climate and Environmental Impacts

5. Overview 24
6. Radiative Forcing and Latent Heating 26
7. Climate and Hydrological Cycle 31
8. Agriculture Effects 38
9. Health Effects 42

Part III: Global and Future Implications

10. Global and Future Implications 47

References 50

Executive Summary

About 60% of the world's population of 6000 million lives in Asia. The recent decades witnessed impressive economic development in the region. Fueled by growing population, globalization and the information technology revolution, this development has resulted in higher demands for energy, mobility and communications. The scope and magnitude of the environmental consequences of these demands are far reaching, especially with respect to air pollution at local and regional levels. The problem of air pollution is no longer confined only at local scale. The new scenario encompasses complex interlinkages of several issues, including air pollution, haze, smog, ozone and global warming. The most visible impact of air pollution is the haze, a brownish layer of pollutants and particles from biomass burning and industrial emissions that pervades many regions in Asia (Figure A). A recent international study, the Indian Ocean Experiment (INDOEX), has revealed that this haze is transported far beyond the source region, particularly during December to April. The INDOEX findings pertain mainly to the period from December to April referred to in this report as the dry season. The seasonal classification followed by the Indian meteorologists is as follows: January to February is the "winter"; March to May is the "pre-monsoon"; June to September is the "south west monsoon"; and October to December is the "winter monsoon" or the "north east monsoon".

This UNEP report is the first comprehensive study of the South Asian haze and its impact on climate. It is largely based on the studies of the INDOEX science team of over 200 scientists from Europe, India and USA. It provides a summary of the large brownish haze layer and its impact on the radiative heating of the atmosphere and the surface for South Asia and the adjacent Indian Ocean during the INDOEX campaign. It also discusses *preliminary findings* with respect to the impact of this haze on regional temperatures, precipitation, agriculture and health.

The INDOEX campaign began in 1995 with ship observations and culminated in a major field campaign launched from the Maldives during January to April of 1999, with ships, aircraft, satellites and surface observations. An aerosol-chemistry-climate observatory was established on an island in the Maldives. The government of the Maldives, which also provided generous logistic support, received the field operations and this observatory enthusiastically.

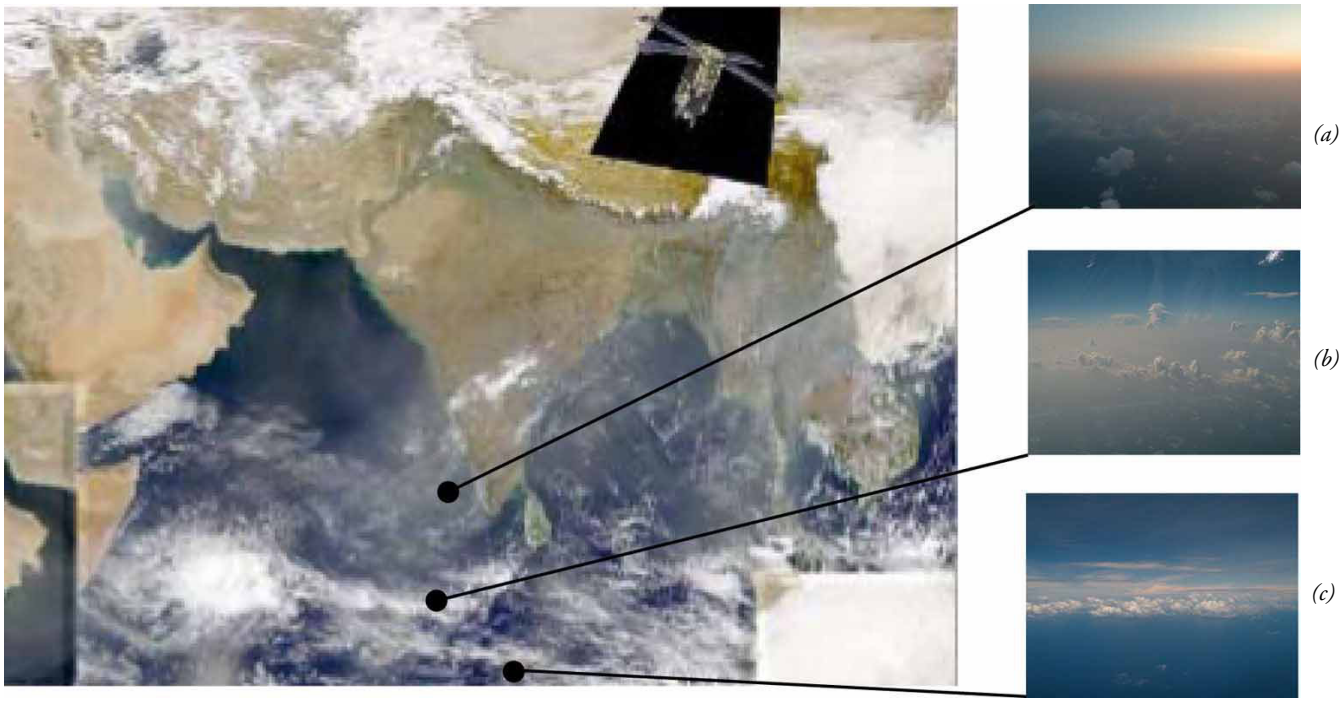

(Courtesy of N. Kuring, NASA Goddard Space Flight Center)

Figure A: Synoptic view of the Asian during INDOEX, top left, from the SEAWiFS satellite. The three photographs on the right taken from the C-130 research aircraft show images of (a) the dense haze in the Arabian Sea, (b) the trade cumuli embedded in the haze and (c) the pristine southern Indian Ocean.

The discovery during INDOEX of the so-called South Asian haze (Figure A) is clear evidence of the magnitude of the aerosol pollution problem. Three dimensional aerosol-assimilation models reveal this haze to extend over South, Southeast and East Asia. At present, biomass burning and fossil fuel burning are the major sources of air pollution. Due to lack of observations of emissions at the source regions in South Asia, it was infeasible to determine with confidence the relative contribution of biomass and fossil fuel burning to the observed haze. But our tentative conclusion is that biomass burning plays a major role in gaseous pollution (such as carbon monoxide), while fossil fuel combustion and biomass burning contribute to particulate (aerosol) pollution.

The affected region is the most densely populated in the world characterized by a monsoon climate, high levels of pollution, and increasing problems of water stress, agricultural productivity and health. The haze can impact all of these aspects directly. It can also impact them indirectly through its effects on atmospheric and surface temperatures and the hydrologic cycle.

Its most direct effect, as documented during INDOEX, is a significant reduction in the solar radiation reaching the surface; a 50 to 100% increase in solar heating of the lower atmosphere. Possible direct effects also include a reduction in the precipitation efficiency by inhibiting the formation of larger raindrop size particles; reduction in agricultural productivity by reducing available sunlight for photosynthesis; and adverse health effects. The direct effects are restricted mainly to the regions beneath the haze layer (south Asia in this case).

Indirect effects of the haze include cooling of the land surface; increase in the frequency and strength of the thermal inversion that can trap more pollution; perturbation of the winter time rainfall patterns; and an overall reduction in the average tropical (20° N to 20° S) evaporation and precipitation. The impact of these pollution particles on the hydrological cycle of the tropics and the sub-tropics has implications to water availability and quality, which are the major environmental concerns for this century.

The aerosol effects on surface temperature and hydrological cycle are of opposite sign to that of greenhouse gases (GHG). While GHGs warm the surface and increase rainfall, aerosols exert a cooling and drying effect. In this regard, it is significant that most regions in Asia experienced a decreasing trend in precipitation since the 1960s. The agricultural impact of aerosol-induced drying, coupled with the reduction in photo-synthetically active solar radiation, is of major concern to Asia, the largest agricultural continent with 60 to 90% of the world's agricultural population (Fu et al., 1998) and producer of 80 to 90% of the world's rice. In what follows, we summarize the specific details of our findings. First, we would like to note the following important caveats.

The findings in this report regarding the climate impacts of the haze are based on limited sets of modeling studies. For example, the studies do not include the effects of increase in greenhouse gases. While definitive conclusions cannot be drawn from these studies, these studies illustrate the potential importance of the haze to the region's climate, water budget and agriculture and also illustrate the great need for further studies of this important environmental problem facing most of the Asian region.

We are at the very early stages of our understanding of regional climate changes, in particular, how regionally and seasonally concentrated climate forcing terms (e.g. the haze forcing) influence regional and global climate. The climate change problem is made considerably complex because aerosols can directly alter the hydrological cycle (by suppressing evaporation and rainfall), which in turn can feedback on temperatures since latent heat released in rainfall regulates the general circulation and the wind patterns around the globe. We are probably at least a decade or more away from comprehending these effects quantitatively. In spite of these reservations, we have used sensitivity studies with three-dimensional models (the same models used for global warming studies) to make quantitative estimates. However these models are global models with coarse horizontal resolution and regional climate studies require a factor of 5 to 10 higher spatial resolution to resolve important monsoon features. Quantitative estimates of rainfall changes cited in this report merely indicate possibilities and such estimates may be revised substantially along with improvement in understanding of the haze phenomenon. Another major limitation of our report is that it is restricted primarily to the dry season, from December to April. The vertical and horizontal distribution of aerosols during May to November are not known, excepting over the oceans where satellite data give the column integrated optical depths, and furthermore the anthropogenic contribution is not known over the oceans or the land.

Composition of the Pollution "Cloud" and Haze

Emission Strength: For the INDOEX region, the fossil energy related CO_2 per capita is nearly an order of magnitude lower than in North America and Europe, but the emissions are growing at a rate 5-6 times larger. The CO emissions, however, are comparable. India emits about 110 Tg/yr (tera (10^{12}) grams per year) compared with about 107 Tg/yr from North America. Although simultaneous emissions of NO_x lead to enhanced ozone, and thereby OH, concentrations, altogether it is likely that hydroxyl (OH) concentrations are reduced because of the reaction of OH with CO. Because almost all of the gases that are emitted to the atmosphere by human activities and natural processes are removed by reaction with OH, and OH can be reduced furthermore by the presence of the haze layer, the air pollution in South and Southeast Asia does negatively impact on the self-cleaning (oxidation) efficiency of the atmosphere, on regional and on global scales.

SO_2 emissions (which are converted to sulfate aerosols) are 5 Tg/yr of sulfur for India, 28 Tg/yr for China and 25 Tg/yr for North America. Emission sources of other aerosol components such as organics, black carbon, fly ash and dust are very poorly characterized. For black carbon, available estimates suggest that the Asian region may contribute about 30 to 50% of the total world emissions.

Composition: Direct chemical measurements were used to show that anthropogenic sources contribute as much as 75% to the observed haze. The sub micrometer anthropogenic aerosol typically has a chemical composition (by mass) of 10-15% black carbon, 26% organic, 32% sulfate, 10% mineral dust, 5% fly ash, and smaller fractions of various other chemicals. Over the Indian Ocean, hundreds to a thousand kilometers downwind of the sources, aerosol mass loading was comparable to suburban air pollution in North America and Europe. Aerosol optical depth in visible wavelengths varies from about 0.05 in the Southern Indian Ocean (typical of unpolluted air) to between 0.4 and 0.7 (very polluted) north of the equator over the Arabian Sea and the Bay of Bengal. Over adjacent continental areas, optical depths are even larger. Several three-dimensional aerosol-assimilation models were used to extend the experiment domain to reveal that the time-mean optical depth exceeds 0.4, indicating heavy aerosol pollution, over central and northern Asia, portions of Southeast Asia and eastern China.

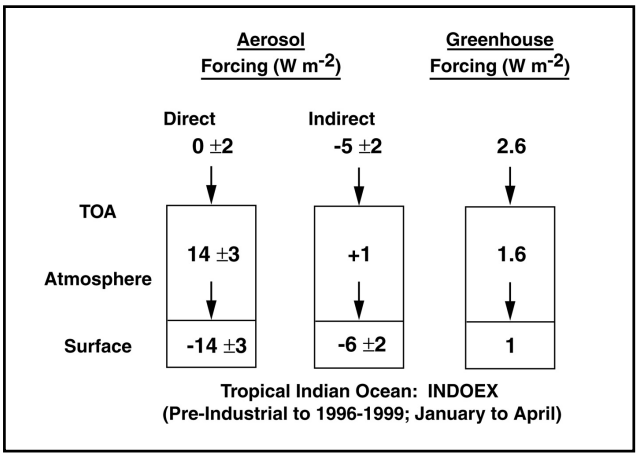

Figure B: Comparison of the aerosol forcing with the greenhouse forcing. The direct forcing is due to scattering and absorption of solar radiation by anthropogenic haze. The indirect forcing is due to the nucleation of more cloud drops by aerosols and the resulting increase in cloud albedo or reflectance. The greenhouse forcing includes the effects of all anthropgenic greenhouse gases (Ramanathan et al., 2001b).

Impacts on the Climate System

Radiative Forcing: The impacts of the South Asian haze are listed below. This aerosol haze causes a reduction in the spatial and temporal mean solar energy at the earth's surface by about14 Wm^{-2}, about 10% of natural levels, and an additional heating of the planetary boundary layers by about 14 Wm^{-2} (doubling the lower atmosphere solar heating). These values should be compared with the greenhouse forcing (from the pre-industrial to the present) of about 1 Wm^{-2} at the surface and 1.6 Wm^{-2} heating of the atmosphere. The result is a solar radiative disturbance over a substantial fraction

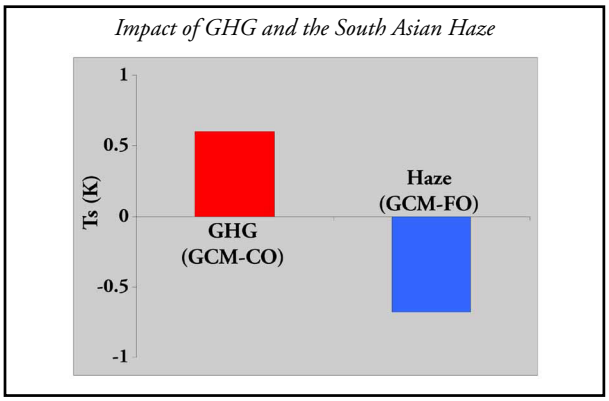

Figure C: The relative impact of Greenhouse gases (GHG) and the South Asian Haze on the average (land only) Indian subcontinent surface temperature as estimated by a GCM-CO (for GHGs) and a GCM-FO. The GCM-CO is described in Washington and Meehl (1996) and the GCM-FO simulation with the South Asian haze is described in Chung, Ramanathan and Kiehl (2002). Both the GHG and the Haze temperature changes are for the January to March period. The values for both the GHG and haze are the difference in the model surface temperature between the pre-industrial to the 1990s.

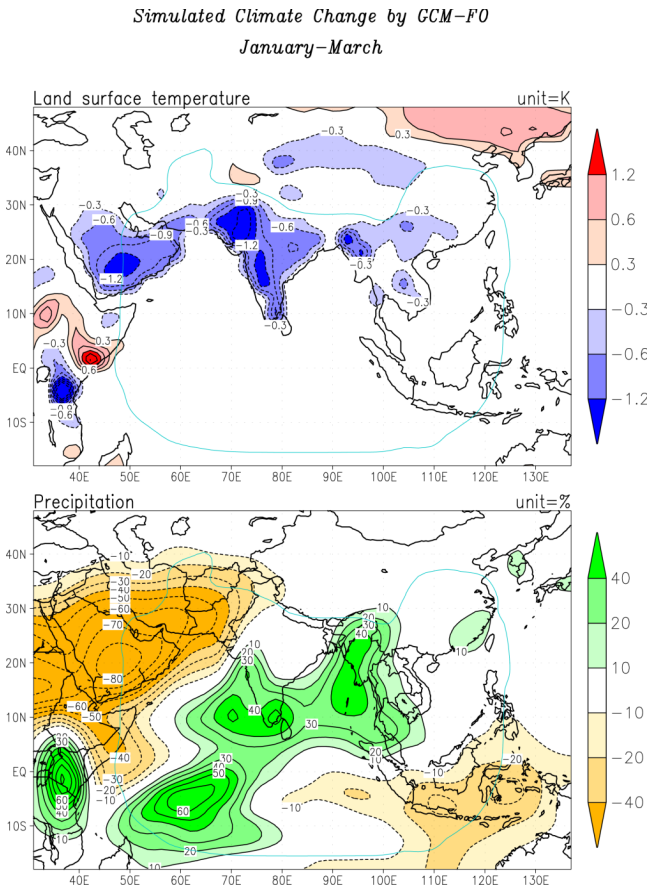

Simulated climate change (January-March) simulated with NCAR/CCM3 and with observed sea surface temperature (SST). Land surface temperature change (upper panel) in units of K. Precipitation change (lower panel) is displayed in units of percentage (Chung et al., 2002).

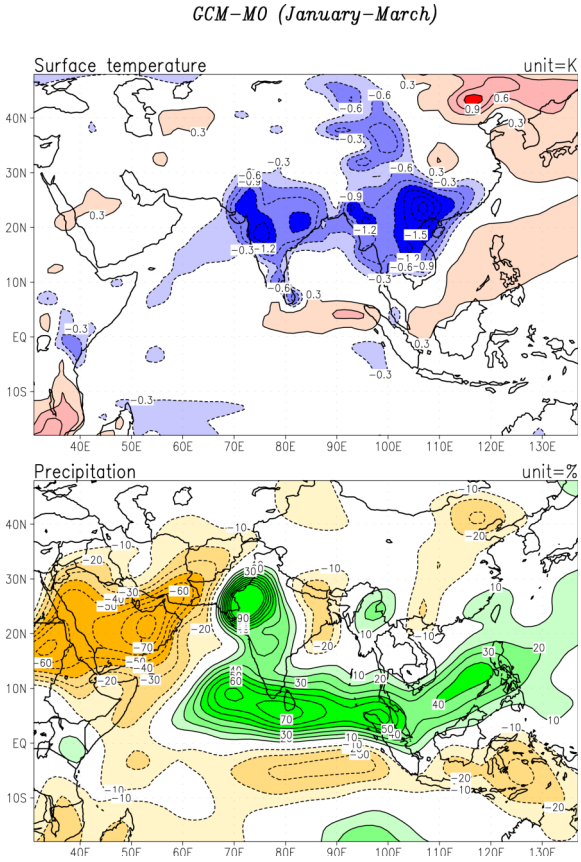

Surface temperature change (January-March) simulated with the CCM3 and Slab Ocean Model (Kiehl et al., 2000).

Figure D: Effect of the South Asian Haze on Dry Season Surface Temperature and Rainfall

of South Asia during the dry winter monsoon period (January - April), about an order of magnitude larger than that coming from CO_2 and the other "greenhouse gases" (Figure B). These INDOEX findings have been extensively reported in peer-reviewed international publications including three special issues of American and Indian journals that were dedicated to INDOEX.

Temperature Effects: The impact of INDOEX aerosols on the climate of South Asian region is estimated to be substantial. The panel initiated a series of sensitivity studies with three-dimensional climate models (with and without interactive oceans) in collaboration with the National Center for Atmospheric Research (J.T. Kiehl, J.J. Hack and W.M. Washington). As of publication of this report, general circulation model (GCM) studies with fixed ocean temperature (referred as GCM-FO for fixed ocean temperature) and a mixed layer slab ocean (GCM-MO for mixed layer ocean) have been completed and sent for publication (Chung et al., 2002 and Kiehl et al., 2000). We have also completed simulations of the haze effects with a fully coupled ocean model (referred as GCM-CO) and preliminary analysis supports the temperature changes derived from the simpler models.

In spite of the fact that the top-of-atmosphere (TOA) direct radiative forcing is nearly zero (Figure B); the computed surface cooling is substantial (Figure C), thus demonstrating the importance of the surface forcing. All three, GCM-FO, -MO and -CO, models indicate an overall decrease of surface air temperature over the Indian subcontinent, the Indo-China region and eastern China during January to March. The seasonal and land surface averaged temperature change is about –0.5K (GCM-FO and -MO). The estimated winter/spring (January to April) cooling due to the haze is comparable to the estimated (by GCM-CO) greenhouse warming as shown in Figure C.

There is strong observational support for this model result. For example, the surface temperatures (averaged over the Indian sub-continent) during June to December show a strong warming trend (very similar to the global average warming trend) where as during January to April, the surface temperatures show practically zero trend from 1950 to 2000, thus supporting our finding that the cooling by the absorbing haze has nearly cancelled the GHG warming. In contrast, in the lower troposphere (1 to 3 km), there is local heating by about 0.5 K. The surface cooling accompanied by atmospheric warming stabilizes the boundary layer, which can lead to more trapping of pollution and increased lifetimes of the haze.

Implications to the Role of Black Carbon: The large surface cooling, in spite of the substantial increase in solar heating of the lower atmosphere (Figure B) by black carbon is significant, particularly in view of its potential policy implications. The first implication is that the TOA forcing, by itself, is not sufficient to judge the climate impacts of aerosols, at least, regionally. The regional surface temperature changes, even its sign, depend on the sign and magnitude of the surface forcing. Since absorption of solar radiation by absorbing aerosols (black carbon, fly ash and dust) contributes about 75% of the reduction in solar radiation at the surface, these absorbing aerosols lead to surface cooling (and not a warming), at least over South Asia and the tropical Indian Ocean region. This deduction raises the disturbing possibility that a reduction in the haze (motivated by air quality and health concerns) may significantly amplify global warming over Asia, at least during the dry season.

Hydrological Cycle: The haze has been found to substantially perturb the hydrological cycle. Introduction of the haze in the GCM results in a reduction in the tropical (20˚ N to 20˚ S) mean evaporation and precipitation by about 1 to 2%. Regional precipitation patterns in the GCM-FO and GCM-MO versions of the model changed significantly. Model simulations with the haze show significant redistribution of rainfall with large increases (20 to 40%) in some regions, which in turn are compensated by comparable decreases in other regions. For example, the GCM-FO simulations suggest that, while the rainfall in the near equatorial rainfall regime may increase and the enhanced activity may extend farther northward up to the southern fringe of the peninsular India, there may be corresponding decrease over the sub-tropical belt over NW India, Pakistan, Afghanistan, and the adjoining western central Asian region (not unlike the observed trends of the last 4 decades). This is possible through the enhancement of the ascending branch of the regional Hadley cell and its descending branch over the sub-tropics.

Winter precipitation over NW India contributes 20-40% of the annual rainfall and over northern Pakistan, Afghanistan, and adjoining central western Asia; its contribution is even 50-70% of the annual. Such a reduction in rainfall is very likely to cause water stress as the winter precipitation is through snowfall and the decreased snow melting in summer would deplete the water resources over the region of impact. Even the man-made irrigation resources in the affected region would suffer due to reduced snowmelt. Reduction in irrigation water is likely to cause long-term impact on agricultural production though in the wheat model used this aspect has not been explicitly considered as winter-spring wheat is mostly (over 80%) irrigated over the region.

The results could be taken as possibilities as the models have the capabilities to simulate the winter climate well. However they are not certainties as the natural climate system on the regional scale could be impacted through other natural variability's and human-induced activities, such as the green house gases warming. Although the model results are still preliminary, having neglected, for instance, the effects of growing concentrations of the greenhouse gases and feedbacks with the ocean whose temperatures were kept constant, they clearly indicate that the effects of anthropogenic aerosol can be large on regional scales.

Agriculture Impacts

Haze can impact agriculture productivity in a variety of direct and indirect ways.

Direct Effects: 1) Reduction of total solar radiation (sum of direct and diffused) in the photo-synthetically active part of the spectrum (0.4 to 0.7 micron) reduces photosynthesis, which in turn leads to a reduction in productivity. 2) Settling of aerosol particles (e.g. fly ash, black carbon and dust) on the plants can shield the leaves from solar radiation. 3) In addition, aerosol deposition can increase acidity and cause plant damage.

Indirect Effects: 1) Changes in surface temperature can directly impact the growing season. In the tropics, a surface cooling (such as expected from aerosols) can extend the growing season (while a greenhouse warming can shrink it). 2) Changes in rainfall or surface evaporation can have a large impact.

In this report we have accounted only for the direct effect of solar reduction that too using just one crop model developed by the Indian Agriculture Research Institute of India. The major effect was found for rice productivity (the dominant winter time crop grown South India) and a negligible decrease for productivity of winter wheat. When the haze effects on surface solar radiation were included in the crop model, rice productivity decreases by about 5 to 10% (Figure E). A more realistic picture would emerge when these studies are coupled with GCM scenarios with changing concentrations of greenhouse gases and aerosols.

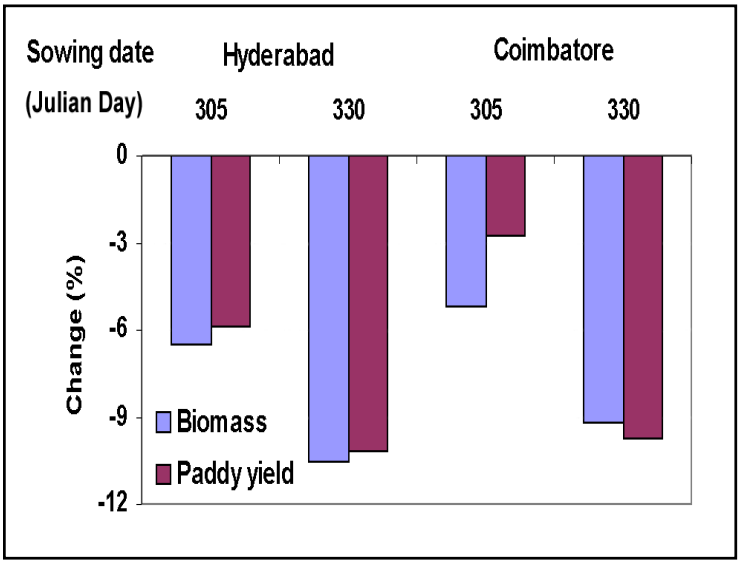

Figure E: Impact of the direct radiative effect of the haze on rice productivity. Results were estimated from the crop model of the Indian Agriculture Research Institute (courtesy of N. Kalra), showing the impacts for two cities in south India with two hypothetical sowing starting dates. Date 305 is November 1 and 330 refers to November 26.

Health Effects

There is now a growing body of literature linking air pollution with short and long term effects on human health. Populations at risk from inhaled particles are those most susceptible to pulmonary and heart diseases, infants and elderly people. A 1997 joint study of the World Health Organization (WHO), the World Resources Institute (WRI) and the US Environmental Protection Agency (EPA) estimated that nearly 700,000 deaths worldwide are related to air pollution and that this number can escalate to 8 million deaths by 2020 (Working Group, 1997). Occurrences of respiratory diseases in South Asia resulting from air pollution both indoors and outdoors, is estimated to be quite substantial. In each of the 23 cities with a million plus population in India, air pollution levels exceed WHO standards. It has been estimated that in India alone about 500,000 premature deaths are caused by indoor pollution, for mothers and their children who are under 5 years of age (Smith, 2000). Serious respiratory disease related problems have been identified for both indoor and outdoor pollution in Calcutta, Delhi, Lucknow, Bombay, Ahmedabad, and several countries in East Asia including China, Thailand and Korea. There is still inadequate knowledge of the relative effectiveness of sub micron particles compared with larger particles, or the specific roles of black carbon and organic carbon. Such studies need to be performed in the future.

Summary

Some of the results listed in this report are preliminary in nature but do indicate possibilities of substantial changes in climate scenario and impacts even when GHGs are considered. In spite of the advances by INDOEX, significant scientific uncertainties remain. First, we need to estimate the haze amount and its radiative forcing during May to December. We need studies with coupled ocean-atmosphere models to address the following questions: How does the solar heating in the haze affect the monsoon rainfall? How does the reduction of solar energy to the surface affect the water budget and soil moisture? Does the haze amplify or ameliorate the warming due to greenhouse gases? How does air pollution from Asia affect the worldwide concentrations of ozone and other pollutants? On the policy side, the evidence of long-range transport of the haze complicates potential prescriptions for dealing with the problem, as responses must be coordinated among sovereign nations. It is also important to note that the same actions that can reduce the buildup of GHGs in burning of fossil fuels can also contribute to reduction of particulate matter.

It is our perception that air pollution ranks among the top environmental issues in the region largely due to its potential effects on health, agriculture and water budget. A survey conducted by the Asian Development Bank a few years ago found that senior environmental policymakers in the region share this perception. As early as 1992, the World Bank, in its annual World Development Report, highlighted the health threat posed by particulate air pollution. With respect to health effects, indoor air pollution is just as important, an issue not considered in the report.

Lastly, there are consequences for the hydrological cycle, climate and the global ozone budget. It is of great interest and relevance to note the enormous range of scales we have to deal with in the study of air pollution and its effects on the environment, ranging from the severe health effects caused by indoor pollution, to those of urban and rural pollution, the impact of the aerosol on regional and even global climate. The climate effects of urban air pollution can no longer be considered as negligible. We conclude this report by suggesting a strategy for understanding the air pollution issue in this broader context and help policymakers arrive at informed decisions (Figure F).

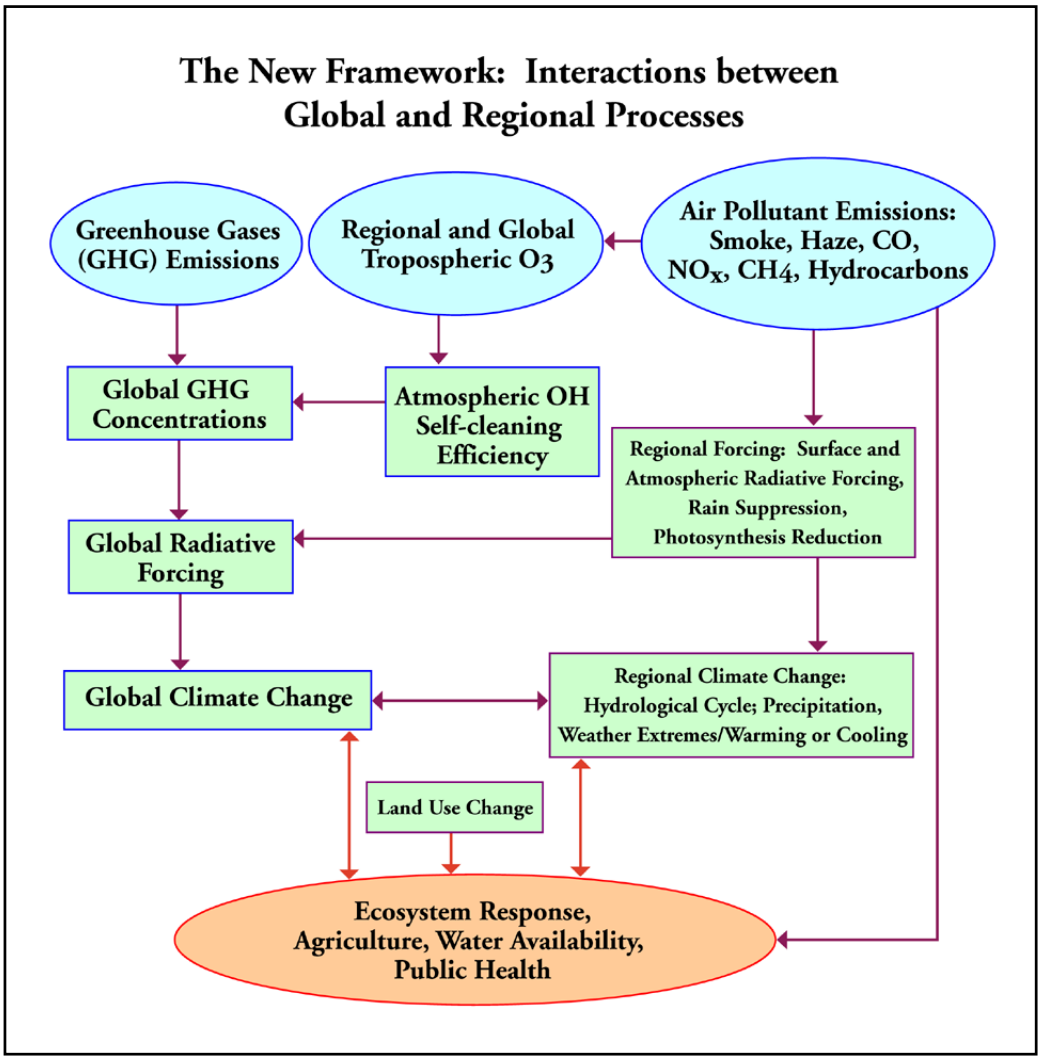

Figure F. Source: Ramanathan and Crutzen, Asian Brown Cloud Concept Paper, 2001.

Part I: The South Asian Haze: Air Pollution, Ozone and Aerosols

1. Introduction

The effects of anthropogenic aerosols on the climate constitute one of the largest sources of uncertainty in quantifying climate change (Working Group 1, IPCC, 2001). The new findings and analyses reported in this study provide a new perspective on this problem, which on the one hand helps reduce the uncertainty in our knowledge of aerosol radiative forcing, and on the other hand reveals the complex ways by which aerosols impact climate. The objectives of this report are three fold:

• To document the South Asian brown haze observed by INDOEX and to consider its potential impacts on climate, hydrological cycle, agriculture, visibility and human health.

• To illustrate the connection and interaction between the climate effects of air pollution and global warming.

• To demonstrate the great importance of arresting further degradation of air quality in Asia.

The primary focus of this report is on the South Asian region. However, the problems we discuss are germane to the entire Asian region. The anthropogenic aerosols released from this region are projected to become the dominant component of anthropogenic aerosols worldwide in the next 25 years (Nakicenovic and Swart, 2000). The air pollution issue in this region should be viewed in a broader context, for valuable lessons can be learned from experiences elsewhere in the world. In particular, we begin with a brief discussion of air pollution problems in London, Los Angeles and China.

1.1. Historical context

Air pollution in Asian cities has grown with the progressing industrialization and urbanization. This recent experience in Asia is predated by similar problems in the western countries at early stages of their economic development. By studying how coal burning produced the London smog problem and how the use of petroleum led to photochemical smog in Los Angeles we can anticipate the types of air pollution problems that can be expected in Asian cities as well. Over the years, great improvements have been made in the air quality in London and Los Angeles. Lessons from both London and Los Angeles help to forecast how serious pollution problems elsewhere eventually will be solved.

1.1.1. Coal use in London

Wood was used for fuel in London up to the 13th century when wood supplies became depleted. By the 1280's, coal was used for fuel in industrial processes including limekilns and metalworking. Coal use in these industries produced smoke concentrations that merited control, sometimes through relocating the industry to the downwind side of town.

By the 1600's, coal became widely used for domestic heating in London in addition to expanded industrial use as the city grew. Concern was registered by local officials due to the soiling of buildings by black soot, including St. Paul's Cathedral. Effects on public health also were debated. In the 1700's, concern was raised about the sulfurous content of urban air. Black smoke and sulfur oxides both are produced when coal is burned, and it is often difficult to attribute ill effects to either pollutant separately as they tend to travel together. Persons adversely affected by the urban air pollution levels were urged to leave the city in order to improve their health. Indications are that smoke concentrations were so heavy in the 1700's in London that some buildings had to be repainted every three years to hide the effects of smoke particle deposition.

The 19th century saw continued growth in coal use in London as population shifted to the city in search of the expanded job opportunities to be found there. Smoke abatement laws were passed but there was little effective control because the technology for control was lacking. Increasing coal use was accompanied by an increasing frequency of fog in the city. Sulfuric acid droplets and particulate sulfates derived from coal combustion effluent as it ages in the atmosphere provide hygroscopic sites for fog droplet nucleation making it easier for fogs to form. The word smog follows from this combination of circumstances, as it is a contraction of the words smoke and fog.

The use of coal and the frequency of fogs both peaked in London in about the year 1900. Upgraded furnaces and use of automatic rather than hand stoking helped to reduce the amount of smoke produced when burning coal. At the turn of the century, London experienced more than 60 foggy days per year, dropping to about 20 days per year in 1950. During this period, it became obvious that increased death rates were associated with the heavily polluted London fogs. In 1952 an extended period of air stagnation lead to an episode of polluted fog that resulted in 4000 excess deaths in London over a several day period. Today the atmosphere in London is much cleaner.

Domestic and small industrial use of coal has been discontinued in favor of use of clean burning natural gas and electric rather than steam driven motors and engines.

1.1.2. Los Angeles photochemical smog

The air pollution problem in Los Angeles grew to unacceptable levels during the period of rapid industrialization that accompanied the Second World War. The most obvious characteristics of this new air pollution problem included severe eye irritation and greatly reduced visibility. The local visibility problem was so severe that there was almost a complete loss of days with extremely clear air. During the period 1932-1937, very clear afternoons with visual range in excess of 35 miles occurred on 21% of the days of the summer season. By 1943-1947, the number of such very clear afternoons dropped to 0.2% of summer days.

In the early 1950's Professor Haagen-Smit of the California Institute of Technology demonstrated that a key feature of Los Angeles smog involved photochemical reactions that occur in the atmosphere when light shines on a mixture of hydrocarbon vapors and oxides of nitrogen. These reactions lead to ozone formation, as well as to the formation of a large variety of co-pollutants including aldehydes, peroxyacyl nitrates (PANs), and fine particles produced from the low vapor pressure products of atmospheric chemical reactions. Ozone is a respiratory irritant and can damage crops, trees and materials such as natural rubber. The aldehydes are eye irritants and could be responsible for much of the reported eye irritation.

Following the discovery of the general nature of photochemical smog, a network of air monitoring stations was established throughout the Los Angeles area. In the late 1950's, peak one-hour average ozone concentrations above the California ozone air quality standard of 0.1 ppm occurred on more than 300 days per year.

Investigation of the oxides of nitrogen emissions to the Los Angeles area atmosphere showed emissions of about 400 tons per day in the late 1940's about half due to motor vehicle exhaust and half due to stationary source fuel use such as at electric utility boilers and petroleum refineries. Hydrocarbon vapor emissions at that time were much higher, more than 1500 tons per day. The largest hydrocarbon source initially was from evaporative losses or leaks from petroleum production, refining, and marketing. Los Angeles contains a number of oil fields and also the petroleum refineries needed to supply all of southern California and parts of Nevada and Arizona. Motor vehicle exhaust contributed the next largest hydrocarbon source, followed by evaporation of solvents used in cleaning, printing, and painting to name but a few of the many sources of solvent loss.

Stringent emission control rules were adopted, many of them directed toward stopping hydrocarbon losses in the petroleum industry. From the 1940's through the mid 1960's there was a large and steady decline in hydrocarbon emissions from the petroleum sector of the economy. At the same time, the population in the air basin surrounding Los Angeles grew from roughly 3 million persons in 1940 to nearly 9 million persons in the mid-1960's. With that increase in population came an increase in the number of automobiles. Hydrocarbon emissions from the expanded motor vehicle fleet grew to more than compensate for the decreased emissions from the petroleum production, refining and marketing sector. Reduced hydrocarbon emissions from cars, and especially the introduction of hydrocarbon oxidation catalysts on cars in 1975 later acted to reduce motor vehicle emissions. Meanwhile, population growth within the air basin surrounding Los Angeles continued, reaching about 14 million persons by the turn of the present century. With that growth came increased emissions of solvents from a variety of small uses in the community such as household cleaning products and paints. Today, the hydrocarbon emissions in Los Angeles are about evenly split between vehicle exhaust and evaporative sources.

Strict emissions controls changed the nature of the hydrocarbon emissions in the Los Angeles area, but the quantity of hydrocarbons emitted daily stayed at high levels of more than 1000 tons per day due to the steadily expanding population within the air basin that surrounds Los Angeles. Close to the source, ozone concentrations depend on the ratio of the various pollutants in the atmosphere more than they depend on the absolute amounts emitted. As population growth continued in the Los Angeles area, oxides of nitrogen emissions from fuel combustion increased from the level of 400 tons per day in the late 1940's to approximately 1600 tons per day by the mid 1970's. Use of 3-way catalysts on newer motor vehicles and application of other nitrogen oxides emissions controls to boilers and heaters subsequently lowered nitrogen oxide emissions in the air basin surrounding Los Angeles to approximately 1000 tons per day. Analysis of the Los Angeles ozone problem shows that reduction of the ratio of hydrocarbon emissions to oxides of nitrogen emissions is the easiest way to reduce ozone concentrations in that city (note that this is not the case in some other

cities where biogenic hydrocarbon emissions place a lower limit on the ability to remove hydrocarbons from the atmosphere). The increased oxides of nitrogen emissions relative to the 1940's combined with a strict hydrocarbon control program reduced the hydrocarbon to oxides of nitrogen ratio in the atmosphere, and a general reduction in emissions density occurred as the population spread over a much larger geographic area over time, resulting in steadily declining peak ozone concentrations over time. By 1990, the number of days per year with peak 1-hr average ozone concentration greater than the Federal air quality standard of 0.12 ppm had declined to roughly 160 per year. That downward trend has continued such that today far less than 100 days per year exceed 0.12 ppm ozone, and days with ozone concentrations above 0.2 ppm are rare indeed.

1.1.3. Air quality in China

Air quality in Chinese cities today more closely resembles the London smog problem than the Los Angeles smog problem, although that could change as present problems with coal smoke are brought under control. Coal is burned for power generation, industrial applications, in small domestic and commercial boilers and as a home heating fuel. Outside of a few major cities such as Beijing and Shanghai, motor vehicle populations and hence petroleum use is small when compared with American cities. Chinese cities experience very high airborne particle concentrations due to airborne dust, primary particles emitted from coal and biomass combustion, motor vehicle exhaust as well as secondary sulfates formed by atmospheric chemical reaction from the sulfur dioxide emitted when coal is burned. Fine particles smaller than 2.5 micrometers in diameter are responsible for most visibility problems and are of health concern because they can penetrate deep into the lung. Recent measurements in downtown Beijing show fine particle concentrations averaging just over 100 micrograms per cubic meter of air compared to about 22 micrograms per cubic meter annual average in Los Angeles. The annual average fine particle air quality standard proposed for the United States is set at 15 micrograms per cubic meter, about one seventh of the level in Beijing. Fine particle concentrations in Beijing approach 300 micrograms per cubic meter on the highest concentration days of the year, and these high concentration events often co-occur with fogs, as in London. Total suspended particulate matter concentrations (airborne particles of all sizes) can reach or exceed one milligram per cubic meter of air on a bad day.

Officials in Beijing are taking aggressive steps to correct this air pollution problem. Natural gas has been brought into the city and is systematically being used to displace coal combustion. Use of natural gas instead of coal was a major feature of the successful cleanup of the London-smog problem. New cars are now equipped with catalytic converters to reduce their exhaust emissions and unleaded gasoline is available for these cars. Catalytic converters are being retrofitted onto pre-catalyst cars built since the mid-1990's. Construction dust suppression measures are in use. Nevertheless, Chinese cities face a difficult problem when it comes to air pollution control. Airborne particle measurements made at background sites in the countryside outside of Beijing show fine particle concentrations more than half as high as in the city. This implies that much of the air pollution in Beijing is already in the air before the air enters the city. Indications are that there is a large-scale regional air pollution problem of great geographic extent covering North China that could frustrate control programs if those control programs are merely local in scope.

1.2. The South Asian region

The South Asian Region includes the Indian subcontinent (India, Pakistan, Bangladesh, Nepal and Bhutan) as well as Sri Lanka, and Maldives. The region is one of the most densely populated in the world, with present population densities of 100-500 persons/km^2. Although total land area comprises only about 3% of the world's land masses, the 1990 population was about 1/5 th of the global total and by 2025 is expected to rise to about 1/4 (Table 1). Three fourths of the region's population live in rural area, of which about one third is living at the threshold of poverty (UNDP, 2000). Deforestation is serious in most of the countries within the region, although in India afforestation efforts have shown some positive results in recent years. Urban population is increasing rapidly (from 27% in 1990 to

Table 1: Population in South Asian Countries (in millions)

Year	India	Pakistan	Bangladesh	Sri Lanka	Nepal
1990	853	123	112	17	19
1995	929	130	120	18	22
2025	1,442	267	235	25	35

an expected 40% in 2020 for India) and is expected to be nearly 50% in 2025 causing destruction of fragile ecosystem and increasing air pollution. The gross domestic product (GDP) growth rates are high, around 5-6%. There is increasing water stress: per capita availability of water has decreased drastically from 5200 m^3/cap/yr in 1950, to a far lower value of 1860 m^3/cap/yr in the year 2000 for India and from 5140 m^3/cap/yr in 1950 to 1200 m^3/cap/yr in Pakistan, that is below water stress level of 1700 m^3/cap/yr in the latter case. There are 5 megacities with population around or above 10 million in the region: Calcutta, Mumbai, Delhi, Dhaka and Karachi.

1.3. The climate in South Asia

The region is characterized by a tropical monsoon climate. Differences in rainfall are of primary significance in defining the climate of the region. The most important feature is the seasonal alteration of atmosphere flow patterns associated with the monsoon. Two monsoon systems operate in the region: the Southwest or summer monsoon (June-September) and the Northeast or winter monsoon (December-April). The rainfall during the summer monsoon largely accounts for the total annual rainfall over most of South Asia (except over Sri Lanka where rainfall of the winter (Northeast) monsoon is dominant) and forms a chief source of water for agriculture and other activities. The monsoon rainfall in South Asia is characterized by large spatial and temporal variability. The arid, semi-arid region encompassing Pakistan and Northwest India receive monsoon rainfall as low as 50 mm while parts of Northeast India and the west coast receive over 1000 mm. This region also features large year-to-year variations in the rainfall frequently causing severe floods/droughts over large areas.

There are two major anomalous regions: the arid and semi-arid parts comprising of large areas of Pakistan and north-western Indian states of Rajasthan, Punjab, Haryana and Gujrat which experience frequent droughts, and the eastern Himalayan sub-region, fed by the Ganga-Brahmaputra-Meghna river system, which are subjected to frequent floods. In India, during the period 1871-2000 there were 22 drought years and 19 flood years. There had been three cases of prolonged drought condition, viz., 1904-05, 1965-66 and 1985-87. Such cases cause great calamity. Similarly, there had been two cases of prolonged flood conditions, viz., 1892-94 and 1916-17. Studies indicate a clear relationship between the occurrence of droughts (floods) in South Asia with the El Niño (La Niña) events in the east Pacific Ocean. It has been observed that, during the period 1856-1997 there were 30 El Niño years in which the averaged monsoon rainfall over India was 7% below normal; in 10 out of these 30 cases, drought conditions prevailed over India. Two years featured flood conditions (1878 and 1983). During the same period there were 16 La Niña years, 9 of which featured flood conditions over India. However, it appears from some of the recent studies that this relationship has been weakening in recent years, possibly due to global warming.

The key parameters for economic development in the region are food and water supply. Both are under stress, especially in the two regions experiencing extreme climates, and this will increase in the future. While India is currently producing adequate food grains (206 MT in 2000-2001; Paroda, 2001), the projected requirement of 330 MT in 2025 will not be easy to achieve. Similarly for Pakistan and Bangladesh, the large future requirements will be difficult to meet.

1.4 Emission Scenario: Fossil fuel and biomass burning

While per capita emissions of greenhouse gases are very low for all countries in this region (0.2 TC/cap for India for 1990) (ALGAS, 1998), the growth rate is high (about 4-6% per year). India is the only country heavily dependent on coal for energy in the region (307 MT in 97/98 vs. 84 MT of oil and 21.5 MT of natural gas). Bangladesh uses primarily natural gas, Pakistan oil and natural gas, and Nepal primarily biomass fuel. Biofuel consumption is also large for India, but the estimates vary widely. Rough estimates are around 150-250 MT fuelwood, 90-100 MT dungcake and 40-100 MT agricultural residue (Bhattacharya and Mitra, 1998). Bio fuels, therefore, could be around one-half of the total fuel for India. The total bio fuel for the entire subcontinent could be anywhere between 300-500 MT as against 300 MT of fossil fuel (90-91 period) – roughly of the same order.

For 1990, CO_2, and CH_4 inventories for this region amounts to about 200Tg C and 25Tg CH_4 respectively. CO_2-equivalent was around 3% of the world emissions. By 97-98, fuel consumption in India has already increased by 50%, amounting to about 800 Tg CO_2/yr for India alone. Sulfur content in Indian coal is low, so SO_2 emission is not as large as one would expect. SO_2 emission for the region is about 5 TgSO2/yr (3% of the world; Lelieveld et al., 2001). Indian CO emissions are large, arising principally from large consumption of biofuels – large forest fires are rare – estimated to be around 60 Tg CO/yr. Black carbon and organic carbon

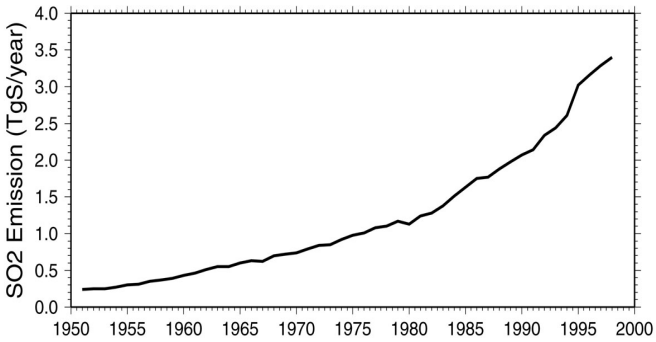

Figure 1.1: SO_2 emission for India shows a steady rise in the last 50 years (Data source: Smith et al., 2001).

emissions amount to 714 Gg and 1036 Gg respectively (Mitra and Sharma, 2001), a very large fraction of the global emissions.

1.5. Pollution scenario

Several of the world's most polluted cities are found in South Asia (Figure 1.2): Calcutta, Delhi, Mumbai, Karachi, and Dhaka are examples of megacities that produce unacceptably high emissions of health endangering gaseous and particulate matter. A study of potential exposure to polluted outdoor air in Asia and the Pacific region (WRI, 1998) showed that the percentage of population in cities exceeding WHO guidelines was as high as 98% for India and 99% for China. Small particulate mater (SPM) values are several times higher than those prescribed by National Air Quality standards. For Delhi, annual average for 1997 was 370 μgm^{-3}, or 2 1/2 times larger than the standard value for the residential area. Though the values of SO_2 and NO_x generally remained within prescribed limits of 60-80 μgm^{-3}, there have been sharp increases in recent years – SO_2 by 109% from 1989 to 1996 and NO_x by 82% (White Paper on Pollution in Delhi, 2000).

Vehicular pollution is a major contributing source – especially two-wheelers and diesel driven heavy trucks. For Delhi alone, vehicular population has increased more than tenfold in 20 years (from 0.2 M to 2.6 M) and account for more than 60% of the particulate pollution.

1.6. Problem areas

Haze is a common phenomenon in the region in wintertime even in high altitude areas: an example of haze seen during an aircraft flight in Nepal at a location close to Mt. Everest is shown in Figure 1.3. There are evidences of sunlight reduction in several places with time: for Pune, there is a reduction by more than 12% during the period 1977-92 (Vashistha and Dikshit, 2000). Although there is doubt

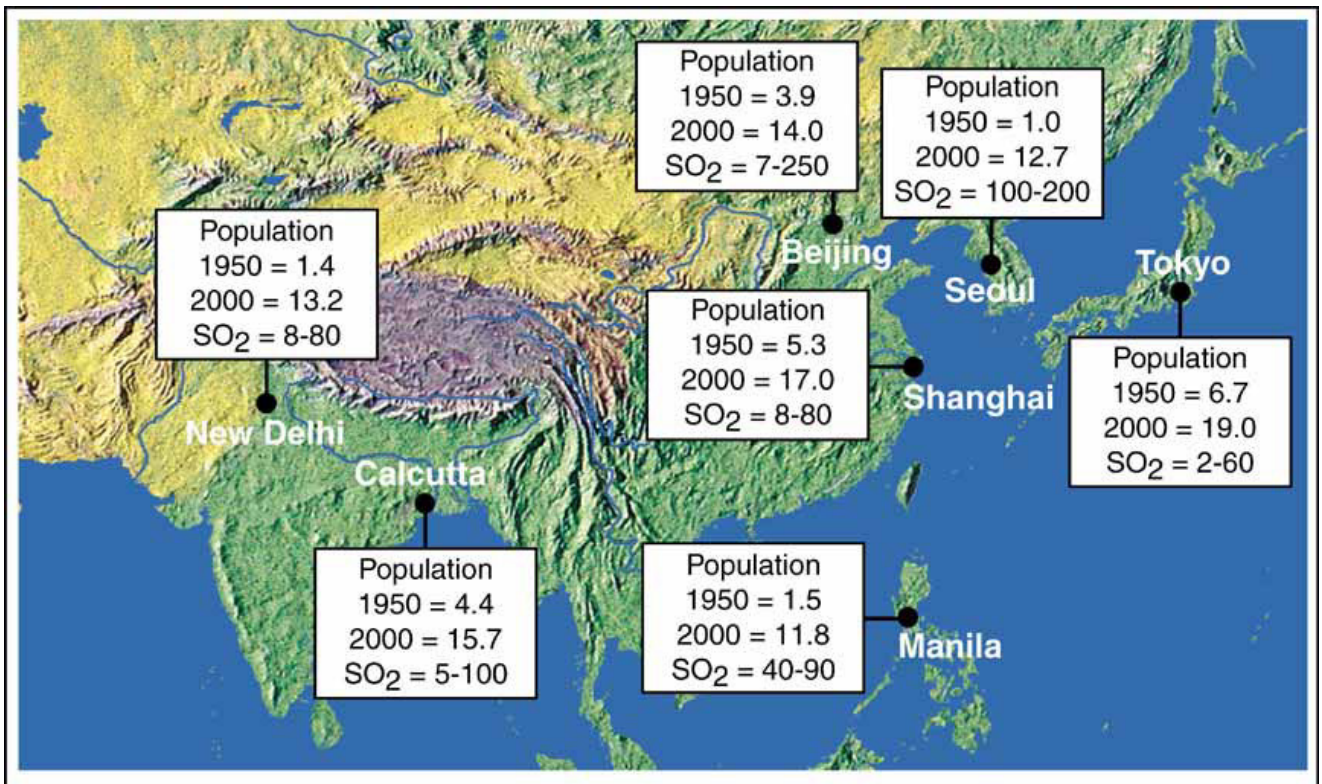

Population in millions. (Source: "Mega-city Growth and Future", Fuchs, R.J. et al. (Eds.), UNU Press, Tokyo, 1994).

Range of annual averages of SO_2 concentrations during 1980-84 period in $\mu g/m^3$ (Source: "Atmospheric Change: An Earth System Perspective," Graedel, T.E. and P.J. Crutzen, W.H. Freeman & Co., New York, 1993).

Figure 1.2

about whether extreme climatic events have increased in frequency or in magnitude in recent years, one should note recent conditions. There have been two consecutive droughts (1999 and 2000) in Pakistan and the northwestern parts of India while increased flooding situations in the high rainfall areas of Bangladesh, Nepal and the northeastern states of India. For Bangladesh, there have been severe floods at intervals of 7 to 10 years, the recent floods occurring in 1988 and 1998. During the 1998 flood, as much as 2/3 of the land area was inundated and nearly 1.6 M hectare of cropland was damaged.

These are serious concerns about the decreasing water availability in the region. Per capita water availability has decreased drastically – for Pakistan it is already less than 1700 m^3/cap i.e. it has reached water stress regime. A substantial part, 70-90% of available surface and groundwater, will continue to be required for agriculture, but there are ways to effect substantial saving in this sector.

There is distinct association between ambient air pollution and respiratory diseases, although estimates of mortality vary. Risk estimates for acute respiratory infections, chronic obstructive pulmonary disease and lung cancer, as well as tuberculosis, asthma (with less confidence) are available. 500,000 premature deaths annually for children below 5 and adult women in India have been attributed to indoor pollution from biomass fuels (Smith, 2000). For south Asia, acute respiratory illness (ARI) deaths are reported to be as large as 1.4 million per year (Murray and Lopez, 1996). Studies in India in a number of locations – Delhi, Calcutta, Mumbai, Lucknow also point to serious hazards from both indoor and outdoor pollution, although there are inherent uncertainties reflecting differences in pollution mixtures, sex, income level and occupational patterns.

C⁴ Archive

C⁴ Archive

Figure 1.3: Photograph of the South Asian Brown haze over the Nepalese town of Phaplu (bottom panel), taken on March 25, 2001, approximately 30 km south of Mt. Everest (top panel), from a flight altitude of about 3 km. Both photographs were taken from the same location, one viewing north (top) and the other south (bottom). During the dry season from January to April, the brown sky seen over Nepal is typical of many areas in South Asia. The dry north east monsoonal winds carry this anthropogenic haze thousands of kilometers south and south eastwards, and spread it over most of the tropical Indian Ocean between 25° N to about 5° S.

2. The Indian Ocean Experiment (INDOEX)

2.1. Scientific objectives for studying aerosols during INDOEX

INDOEX was conducted over the tropical Indian Ocean from 1996 to 1999 during the winter monsoon seasons. The experiment culminated in an intensive field phase (IFP) in January-March 1999 during which an international group of over 200 scientists from the United States, Europe, India, and the Maldives using aircraft, ships, surface stations, satellites and computer models to study how air pollution affects the regional climate (Figure 2.1). INDOEX was designed to measure the characteristics, distribution, and radiative effects of these aerosols under present-day conditions (Ramanathan et al., 1996; Crutzen and Ramanathan, 2001). In addition to the IFP data, several years of chemical, meteorological, and radiative data are available from the (i) Kaashidhoo Climate Observatory (KCO, at 4.965˚ N, 73.466˚ E), (ii) annual cruises by Indian research vessels (e.g., Jayaraman et al., 1998), and (iii) continental surface sites.

The Indian Ocean has been selected for measuring the transport, properties, and radiative effects of aerosols partly because of specific and favorable meteorological conditions. During the winter monsoon, the prevailing low-level winds in the northern Indian Ocean are northeasterly while the prevailing low-level winds in the southern Indian Ocean are southerly (Krishnamurti et al, 1997a). These wind patterns transport continental and anthropogenic aerosols from India and Arabia over large areas of the Arabian Sea and northern Indian Ocean, and from India and Southeast Asia over large areas of the Bay of Bengal (Krishnamurti et al, 1997b). The polluted air is advected as far south as the Inter-Tropical Convergence Zone (ITCZ). The convergence of pristine air from the southern Indian Ocean and polluted air from the northern Indian Ocean establishes a large gradient in aerosol loading close to the ITCZ. The expected geographic gradients in pollutants have been confirmed during pre-INDOEX ship experiments (Rhoads et al., 1997; and Jayaraman et al., 1998).

2.2. Relationship of INDOEX to earlier studies of regional air pollution

The radiative effects of aerosols over the Indian Ocean and Arabian Sea have been examined using observations from previous field programs. The first detailed calculations of the aerosol effects use data collected during the First Global Atmospheric Research program (GARP) Global Experiment (FGGE) and summer Monsoon Experiment (MONEX) (Ackerman and Cox, 1982 and 1987; and Ellingson and Serafino, 1984). These studies focus exclusively on the forcing by soil-dust aerosols from the Saudi Arabian peninsula and Sahara Desert. According to modern inventories of sulfate pollution from India, the flux of sulfur dioxide from India was approximately 1/3 the present-day value during MONEX (Smith et al., 2001). The results show that the dust aerosols enhance the shortwave heating rates (a measure of the absorption of solar radiation) by up to 0.3˚ C/day, a change of 50%, in the lower atmosphere over the Arabian Sea. The effects of anthropogenic aerosols obtained from INDOEX are substantially larger and will be discussed later. The climatic effects of aerosols released by the Kuwait oil fires during the 1991 Gulf War have also been extensively modeled, although of course the source of the aerosols was a transient phenomenon. More recent pre-INDOEX studies have examined the impacts of sulfate and carbonaceous aerosols on continental surface insolation (Venkataraman et al., 1999; Reddy and Venkataraman, 1999). INDOEX, however, represents one of the first sustained international efforts to quantify the regional effects of anthropogenic aerosols from India, Southeast Asia, and China.

The major funding for INDOEX was provided by the following agencies:

- U.S. National Science Foudation (lead agency)
- European Organisation for the Exploitation of Meteorological Satellites
- Indian Space Research Organization, Bangalore
- Laboratoire de Météorologie Dynamique du Centre National de la Recherche Scientifique, Paris
- Max Planck Institute for Chemistry, Mainz
- U.S. Department of Energy
- U.S. National Aeronautics & Space Administration
- U.S. National Oceanic and Atmospheric Administration
- Vetlesen Foundation

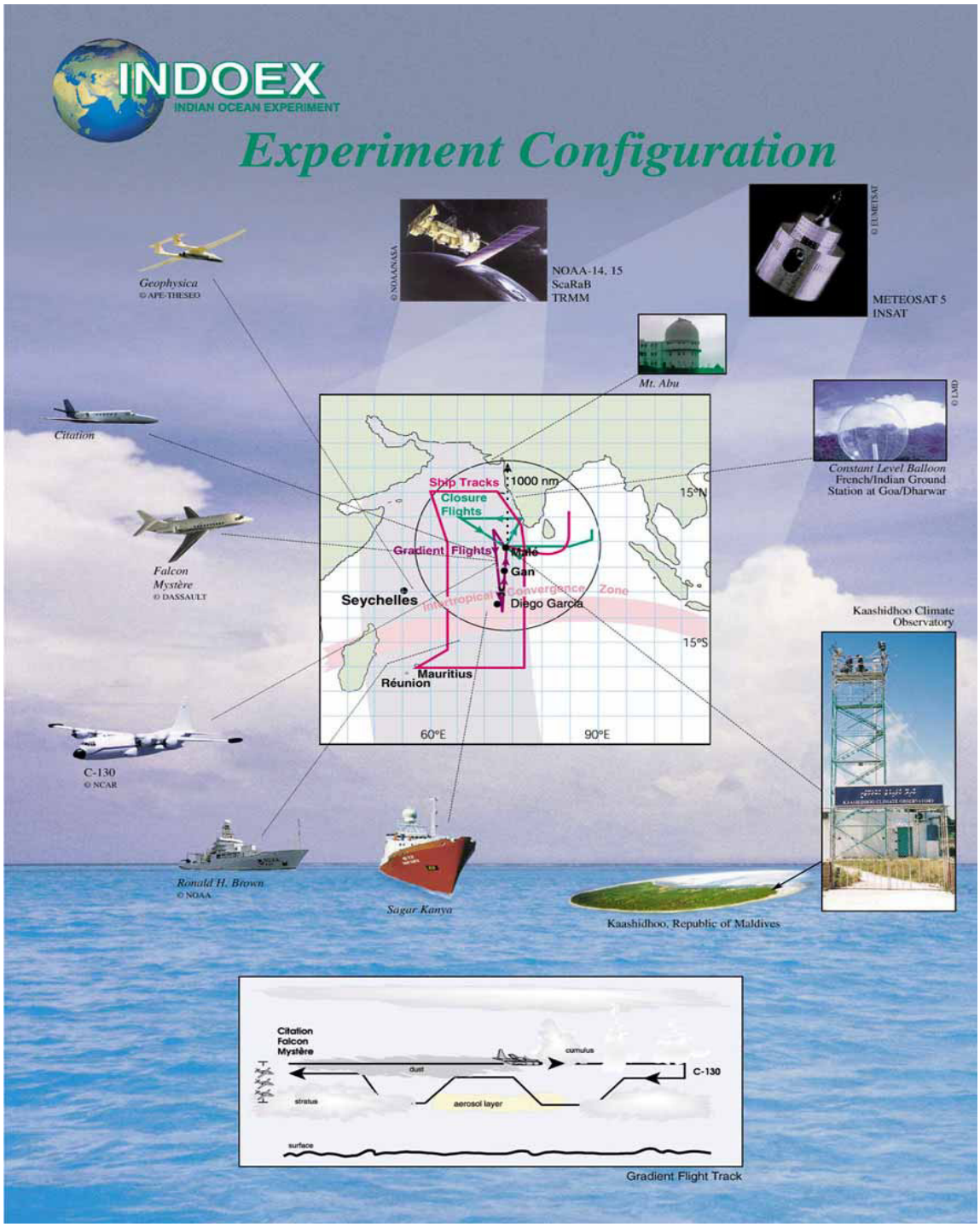

Figure 2.1: The illustration of the INDOEX composite observing system shows the domains of the various platforms. Geostationary satellites (Eumetsat's Meteosat 5 and Indian INSAT) and polar orbiters (NOAA-14, 15 and Russian-French-German ScaraB) provide synoptic view of the entire region. The US NCAR C-130, the Dutch Citation and the French Mystère fly from Hulhule, the Maldives while the Italian-Russian Geophysica and the German Falcon depart from Malé and the Seychelles. These aircraft performed north-south flights from 10N-17S and east-west flights from about 75E-55E measuring solar radiation fluxes, aerosol properties and distribution, cloud microphysics, chemical species and watervapor vertical distribution. The ocean research vessels US NOAA Ronald H. Brown and the Indian Sagar Kanya travel between Goa, Malé, La Reunion and Mauritius transecting the intertropical convergence zone sampling surface solar radiation, aerosol absorption and scattering, chemical species including ozone, winds and watervapor vertical distribution - Sagar Kanya also sails in the source region along the western coast of India. Surface stations in India (including Mt. Abu, Pune and Trivandrum), the Maldives (Kaashidhoo), Mauritius and La Réunion measure chemical and physical properties of aerosols, solar radiation, ozone and trace gases. Closely related to surface platforms, French Constant Level Baloons are flown from Goa, India to track low-level air folw from the Indian subcontinent measuring air pressure, temperature and humidity. (Ramanathan et al., 2001a)

3. Air Pollution and Ozone

3.1. Pollution sources: gases

The South Asian region has substantial populations living in rural locations, where domestic energy consumption depends on biofuels such as wood and cow dung, whereas in urban areas soft coke, kerosine and other liquid fuels are used as well. The economic development of the region, associated with an increasing demand for electricity, and the growing use of cars, cause substantial pollution emissions. At present, about one quarter of the energy use in Asia depends on biofuels while in India this fraction is even larger, close to 50%. Source estimates of air pollution in several Asian regions, as compared with other major source regions in the northern hemisphere, are presented in Figure 3.1.

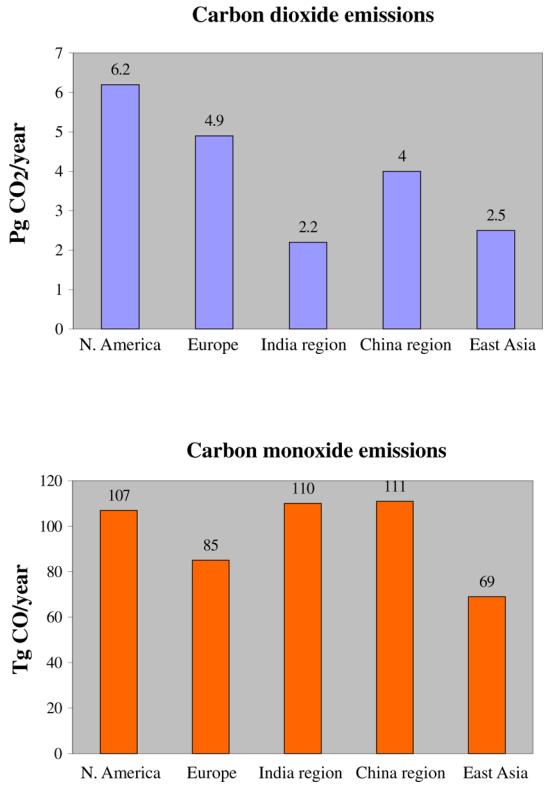

Figure 3.1: Estimated man-made CO_2 (A) and CO (B) emissions, mainly from fossil fuel use and biomass burning (India region includes Bangladesh, Maldives, Sri Lanka, Myanmar (Burma), Nepal, Pakistan; China region includes Cambodia, Vietnam, Laos, Mongolia, N-Korea; E-Asia includes Japan, S-Korea, Indonesia, Malaysia, Philippines, Thailand) (van Aardenne et al., 2001).

Until recently, North America and Europe dominated the use of fossil fuels, associated with strong carbon dioxide (CO_2) emissions and consequent global warming. The fossil fuel related CO_2 release per capita in Asia is nearly an order of magnitude smaller than in North America and Europe. However, Asian emissions are growing. Since about half the world's population lives in this region, the potential for strong pollution emissions is large. At present biomass burning is a main source of air pollution in the tropics. One objective of INDOEX was to improve the information on the mix of emission sources in South and Southeast Asia. It should be emphasized that estimating biomass burning emissions, notably from biofuel use, is difficult since they usually occur scattered over large rural areas. The burning process is not well defined because the fuel type and the combustion phase (flaming, smoldering) strongly affect the exhaust composition. It has been estimated that in India firewood contributes approximately two thirds to biofuel consumption, while the burning of dung and agricultural wastes contribute roughly equally to the remaining one third (Ravindranath and Ramakrishna, 1997; Sinha et al., 1998; Mahapartra and Mitchell, 1999).

The types of compounds that are emitted by combustion processes are very much dependent on the temperature. At high burning temperatures much of the fuel is directly converted into CO_2. At lower temperatures more hydrocarbons and incompletely combusted gases, such as carbon monoxide (CO) and oxygenated hydrocarbons, are emitted. Domestic burning takes place at relatively low temperatures, and because it is a main source of pollution over India, CO concentrations are high in southern Asian air masses. In addition, INDOEX has shown that compounds that are typical for biomass burning are abundant (Lelieveld et al., 2001). Examples of such products observed during INDOEX are acetone (CH_3COCH_3), methyl cyanide (CH_3CN) and methyl chloride (CH_3Cl). Especially methyl cyanide is a tracer of biomass burning emissions. Biomass burning is a strong source of air pollution as it is very inefficient as an energy source.

The INDOEX measurements of CO have been reproduced through computer modeling (Figure 3.2). Several models have subsequently been used to calculate CO concentrations for the entire region. Figure 3.3 shows results for February 1999, indicating that mean CO levels of 300 nmol/mol are exceeded in large areas. The quite good agreement with measurements also indicates that the CO emission estimates as

presented in Figure 3.1 are in the right range since these are used in the model. Figure 3.3B shows that the calculated fraction of CO from biomass burning is very high. Additional support for these model results is provided by a comparison with radiocarbon monoxide (^{14}CO) measurements performed from a ship during INDOEX. Fossil fuels are radiocarbon depleted, and the observed high ^{14}CO fraction indicates that 60-90% of the CO is of biogenic origin, attributed to the human-induced burning of biomass.

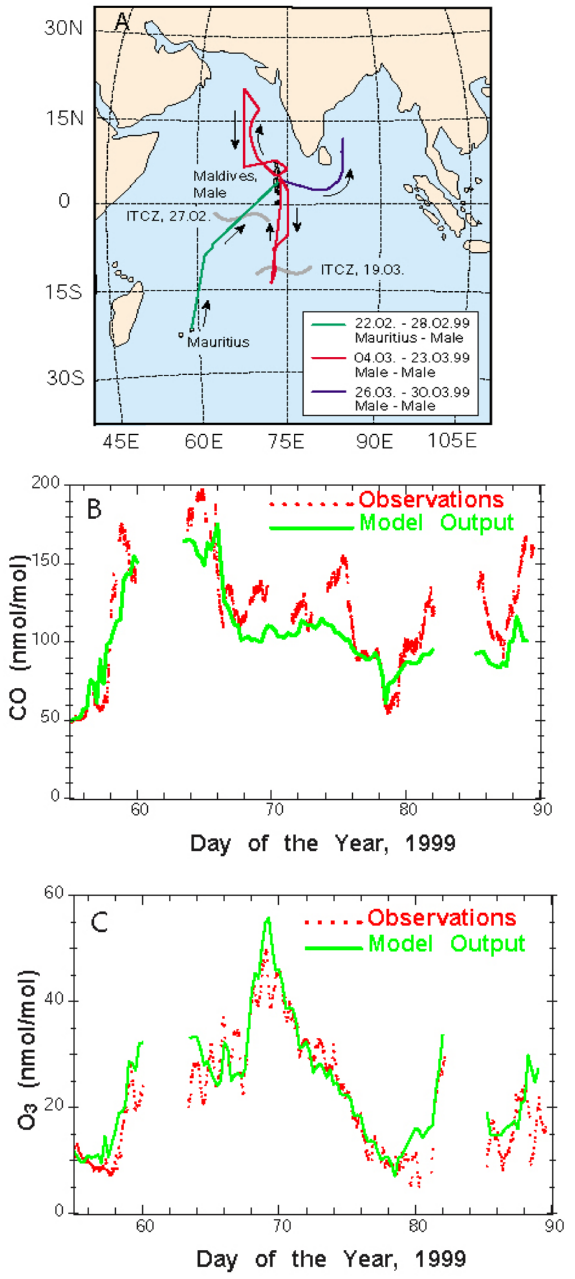

Figure 3.2: Tracks of the research vessel Ron Brown during INDOEX (A). Measured and model calculated carbon monoxide (B) and ozone (C) concentrations (Lal and Lawrence, 2001).

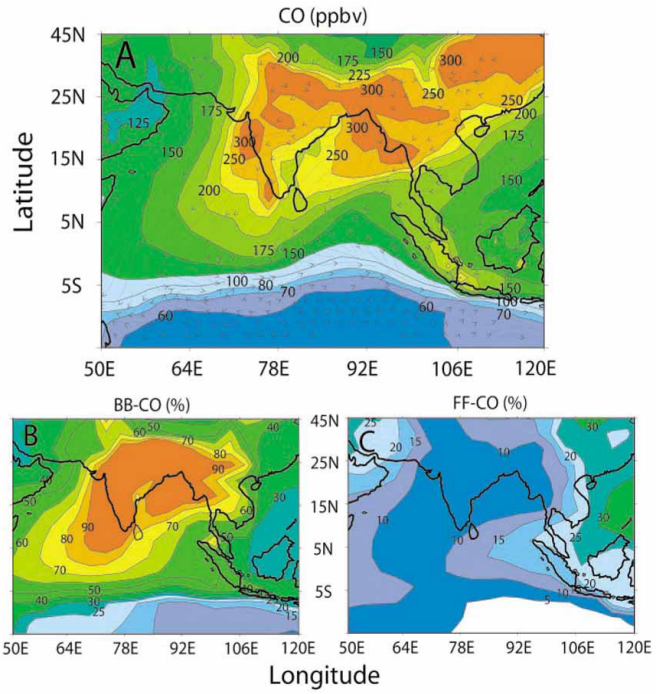

Figure 3.3: (A) Mean CO concentrations near the surface in February 1999, calculated with a chemistry-transport model. Average winds are shown by streamlines. Marked tracers indicate the percentage of CO from biomass burning (B) and fossil fuel combustion (C). (Lelieveld et al., 2001.)

Considering that the pollution occurs at low latitudes with high solar radiation intensity, one expects strong photochemical activity, possibly giving rise to ozone (O_3) buildup. Ozone is an important natural trace gas in the stratosphere (ozone layer) where it protects the Earth from harmful solar ultraviolet radiation. The lower atmosphere (troposphere) contains a much smaller fraction of O_3 (~10%), where it initiates the removal of pollutants through oxidation processes. The combination of CO, hydrocarbons and nitrogen oxides, notably from combustion processes, can lead to the formation of photochemical smog. "Photosmog" is typically associated with high levels of O_3, which (being a strong oxidant) can damage biological tissues, including the human respiratory tracts, agricultural crops and natural ecosystems. Ozone is also a greenhouse gas, so that its increase during industrialization contributes to climate change. Because of its important role in atmospheric chemistry, O_3 was measured from all platforms and ground stations, as well as through balloon soundings from the Kaashidhoo Climate Observatory (KCO) and two ships. Although O_3 concentrations near the Indian coast were about 50-70 nmol/mol and peak values even reached 80-100 nmol/mol, the air quality standards for O_3 were not

strongly violated in polluted air from India. The European Union air quality standard indicates that ozone may only exceed the threshold of 60 nmol/mol during a maximum of 25 days per year. Should values exceed 120 nmol/mol for more than an hour, the population must be warned. After three hours exceeding this value, government is to take countermeasures, for example, driving restrictions. Preliminary measurements in Indian cities indicate that O_3 rarely exceeds 80 nmol/mol, though there is some discrepancy between various measurements (Lal and Lawrence, 2001). This is consistent with the fact that much of the gaseous pollution originates from biomass burning. In particular smoldering fires produce relatively little nitrogen oxides ($NO_x = NO + NO_2$), a necessary catalyst for photochemical O_3 formation. Nevertheless, substantial amounts of nitrate were measured in the aerosol particles (equivalent to several hundred pmol/mol), and NO_x levels of 5-15 nmol/mol have been measured in urban air (Lal et al., 2000), which indicates that NO_x emissions are not negligible.

In spite of the fact that ozone in photosmog was not exceedingly high during INDOEX, it should be emphasized that only limited O_3 measurements are available in urban and none in suburban air, so that definitive statements cannot be made. Importantly, in the next decades emission trends in the region will likely reflect the increased use of fossil fuels, more strongly associated with NO_x emissions, which will boost photochemical O_3 formation, possibly comparable to Europe and the USA during the past decades. Considering the population size, the situation in Asia will likely become even more serious. In general, the South Asian air quality problem will be largest during the winter monsoon (the dry season) in meteorologically stable and cloud free atmospheric conditions. The potential for future photosmog development during the dry monsoon is large. During the wet summer monsoon, however, under unstable and convective conditions, vertical mixing and transport of local pollution will limit the local violation of air quality standards, whereas much of the pollution will be introduced into the large-scale circulation.

3.2. Pollution sources: aerosols

Part of the pollution emissions occur as microscopic particles (aerosols) or in particular as gaseous precursors of aerosols. In the latter case, chemical reactions within the atmosphere convert the primary gaseous pollution into gases with lower volatility some of which rapidly condense into particles. A main example is the release

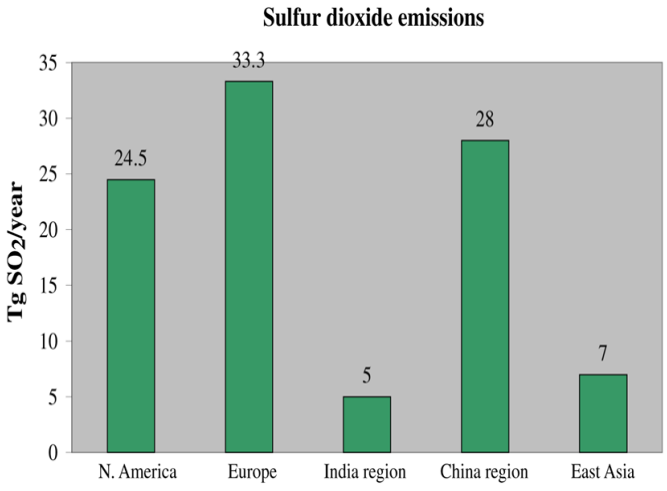

Figure 3.4: Estimated man-made SO_2 emissions (for regions, see caption Figure 3.1).

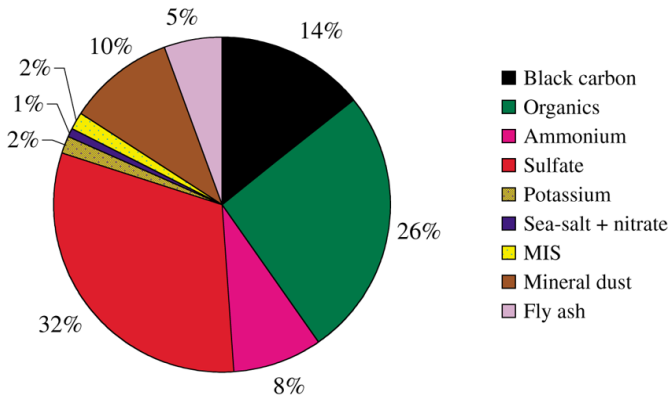

Figure 3.5: Fractional contribution of chemical components to the INDOEX aerosol, as measured over the Indian Ocean by aircraft in February and March 1999. The total mass concentration is 22 μg/m³. MIS is minor inorganic species. These are free troposphere measurements and do not include boundary layer sea-salt.

of sulfur dioxide (SO_2) from fossil fuel combustion. Emission estimates are shown in Figure 3.4, indicating a particularly significant Asian contribution by China due to the heavy use of sulfur-rich coal. In the atmosphere, SO_2 is converted into particulate sulfate, which is largely removed by rain. A major discovery of INDOEX was the presence of a huge aerosol plume over the Indian Ocean, known as the INDOEX "brown cloud", sometimes reaching as far south as 10° S. The large extent of the plume is in part associated with the scarcity of precipitation during the winter monsoon. Evidently the large size of the plume must be related to very high aerosol concentrations near the sources.

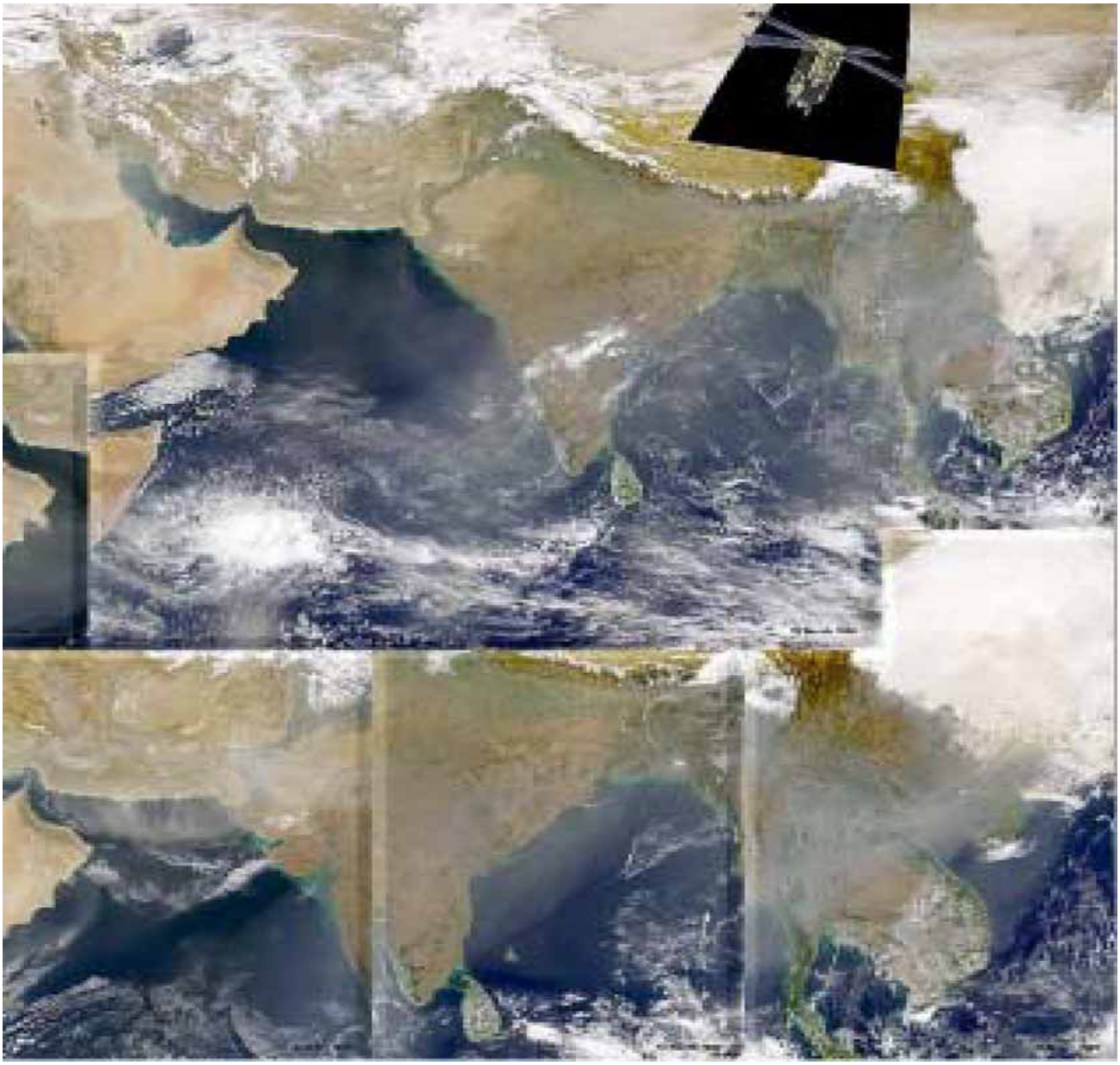

Figure 3.6: Satellite images of the INDOEX pollution cloud over the Indian Ocean. These observations were performed by NASA with the SeaWiFS instrument during INDOEX in the period January-March 1999.

During INDOEX aerosol chemical and optical measurements were performed from the aircraft, ships and KCO. The latter is located on the Maldives about 500 km southwest of India and more than 1000 km from the main pollution centers. The analysis of filter samples collected at KCO shows a high average dry mass concentration of ~17 $\mu g/m^3$, while aircraft measurements indicate even higher concentrations (Figure 3.5). The aerosol plume was typically composed of sulfate, organic compounds, black carbon (soot), mineral dust, ammonium, fly ash and minor compounds such as potassium and nitrate. Mass spectrometric particle analysis shows that the black carbon particles were always mixed with organics and sulfate. Very similar results were obtained from KCO (which will show more sea salt), the aircraft and the ship measurements, which shows that the aerosol composition was remarkably uniform over the northern Indian Ocean.

The aerosol mass loading observed over the Indian Ocean, at least hundreds of kilometers downwind of the sources, is quite comparable to sub-urban air

pollution in N-America and Europe. In N-America and Europe urban fine aerosols typically contain 28% sulfate, 31% organics, 9% BC, 8% ammonium, 6% nitrate and 18% other material (mean mass 32 $\mu g/m^3$), suburban aerosols 37% sulfate, 24% organics, 5% BC, 11% ammonium, 4% nitrate, 19% other material (mean mass 15 $\mu g/m^3$), and remote continental aerosols 22% sulfate, 11% organics, 3% BC, 7% ammonium, 3% nitrate, 56% other material (mean mass 4.8 $\mu g/m^3$). Moreover, the black carbon content was high. This gives the aerosol a strong sunlight absorbing character. Figure 3.6 shows satellite observations (in true color) that confirm the presence of a huge brownish-gray cloud extending from South and Southeast Asia over the Indian Ocean.

The black carbon aerosol and fly ash are unquestionably human-produced since natural sources are negligible. Likewise, the sulfate can be largely attributed to anthropogenic sources. Filter samples collected on board a ship in the clean marine boundary layer over the southern Indian Ocean reveal a fine aerosol sulfate concentration of about 0.5 $\mu g/m^3$, probably from the oxidation of naturally emitted dimethyl sulfide (produced by plankton). The sulfate concentration over the northern Indian Ocean was close to 7 $\mu g/m^3$, and we thus infer an anthropogenic fraction of more than 90%. Similarly, the ammonium concentration over the southern Indian Ocean, from natural ocean emissions, was 0.05 $\mu g/m^3$, indicating an anthropogenic contribution of more than 95% to the nearly 2 $\mu g/m^3$ of ammonium observed in the INDOEX pollution cloud.

It is more difficult to attribute the organic aerosol fraction to a particular source category. Secondary organic particles from natural hydrocarbon sources are probably of minor importance since India is scarcely forested. Moreover, the black carbon/total carbon ratio of 0.5, as derived from the filter samples, is typical for aerosols from fossil fuel combustion. In the aerosol over the clean southern Indian Ocean organic compounds were negligible, whereas over the northern Indian Ocean they amounted to almost 6 $\mu g/m^3$. We thus infer that most of the particulate organics over the northern Indian Ocean were of anthropogenic origin. Free troposphere INDOEX aerosol components of natural origin included a total mass fraction of 1% sea salt and 10% mineral dust. Some of the mineral aerosol likely originated from road dust and agricultural emissions. Taken together, the human-produced contribution to the aerosol was at least 85%.

Similarly to gaseous air pollution, very little chemical information is available about (sub)urban aerosols from direct measurements in South and Southeast Asia. Preliminary observations of total aerosol mass in Calcutta indicate average concentrations of about 200 $\mu g/m^3$, whereas in Bombay average concentrations up to 2000 $\mu g/m^3$ are observed. Such high aerosol mass loadings strongly limit visibility, while air quality standards are exceeded by orders of magnitude. Air quality standards often refer to respirable suspended particulate matter (PM), being aerosols with a diameter smaller than 10 μm (PM10). The air quality standards for PM10 typically range from 10-150 $\mu g/m3$ annually averaged, depending on the particle composition and national legislation. Similarly to O_3, the potential for future increases is large, for example, through the growing use of sulfur containing fuels that also contribute to soot production. Further, it should be emphasized that the improvement of air quality measurements within regional networks, in conjunction with model calculations, addressing both local pollution in (sub)urban areas and downwind of large source areas (for example at KCO) are prerequisite to firmly establish the link between emissions and concentrations of gaseous and particulate air pollution.

4. Spatial and Temporal Variations of the Haze

The reduction of the direct (unscattered) solar radiation at the Earth's surface is related to the aerosol optical depth (AOD). The transmission of the direct solar radiation decreases exponentially with increasing optical depth. AOD is the best measure for column loading of aerosols. During INDOEX, the optical depth was obtained from surface and airborne radiometers, calculated from the chemical speciation using optical models, and derived from multi-spectral measurements combined with radiative transfer codes. The change in aerosol forcing with a unit increase in optical depth is called forcing sensitivity. The forcing sensitivity has been calculated both from INDOEX observations and models (Satheesh and Ramanathan, 2000; Ramanathan et al., 2001a and Collins et al., 2001b). One of the intrinsic properties of aerosols that determines atmospheric forcing is the fraction of sunlight incident on a typical aerosol particle which is scattered rather than absorbed. This property is the single-scattering albedo (SSA). In visible wavelengths SSA for sulfate aerosols is nearly identical to 1, while SSA for soot is approximately 0.3.

4.1. Spatial extent of anthropogenic aerosols

The AOD has been measured in the southern and northern Indian Ocean during the winter months of 1996 to 1999 (Figure 4.1) from the ORV *Sagar Kanya* (Jayaraman et al., 1998). The optical depth in visible wavelengths varies from approximately 0.05 near 20° S to between 0.4 and 0.7 at 15° N (Ramanathan et al., 2001a). The value of 0.05 in the southern Indian Ocean is typical of unpolluted air (Satheesh et al., 1999), while values exceeding 0.2 are characteristic of polluted air. The large latitudinal gradient in optical depth is related to the variation in the number of particles per unit volume of air. The total number of particles changes from 250 cm^{-3} in the southern Indian Ocean to roughly 1500 cm^{-3} in the northern Indian Ocean. The two major natural aerosol species, sea-salt and dust, contribute only 11% and 12% (respectively) of the total optical depth in this region (Satheesh et al., 1999). As a result, approximately 80 (±10)% of the optical depth is obtained from anthropogenic aerosols. There is a transition between the polluted and undisturbed regions at approximately 5-8° S at the location of the ITCZ.

Analysis of satellite observations for 1996 to 2000 indicates that the high optical depths are characteristic of the winter season during the late 1990s. The optical depth averaged over the winter season for ocean regions between 0 to 30° N varies by less than 10% relative to the optical depth obtained during INDOEX in 1999 (Tahnk and Coakley, 2001).

The INDOEX observational estimates of optical depth are confined primarily to the Indian Ocean, Arabian Sea, and Bay of Bengal. Estimates of optical depth over land (Figure 4.2) have been obtained from an aerosol

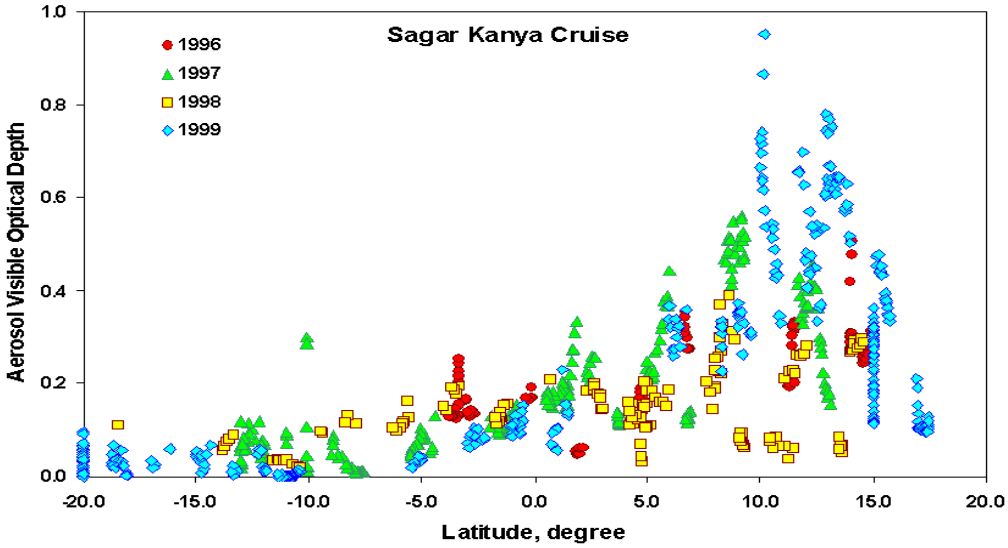

Figure 4.1: Latitudinal variation of aerosol optical depth (0.5 μm) measured by the Indian research vessel Sagar Kanya during 1996 to 1999. The multi-wavelength Sun photometer used for this data is described in Jayaraman et al. (1998). The precision of the measurement is ± 0.03 or 20%, whichever is smaller. Each color represents a different year.

assimilation model (Collins et al., 2001b) that is consistent with in situ measurements and satellite estimates of optical depth over oceans (Ramanathan et al., 2001a). The model is able to reproduce ship and surface measurements of daily-mean optical depth with an error of –0.03 to +0.07. During January through March of 1999, the model shows that the large optical depths over the northern Indian Ocean are accompanied by larger values over the adjacent continental areas where the anthropogenic aerosols originate. The time-mean optical depths over central and northern India, portions of Southeast Asia, and eastern China exceed 0.4 during this period. These values over land are the highest in the region bounded by 30° S to 30° N, 40° E to 120° E, which is consistent with the anthropogenic origin of the aerosols observed during INDOEX.

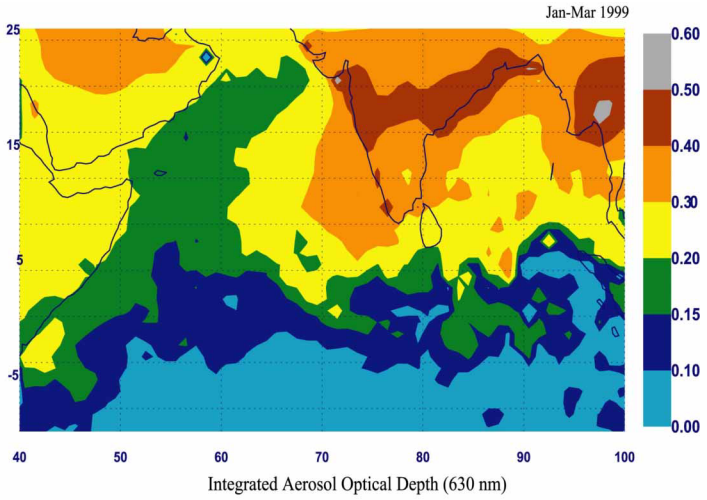

Figure 4.2: The regional map of aerosol visible optical depth (AOD). The AOD values over ocean are retrieved from AVHRR data (Rajeev et al., 2000) and over land are estimated using a 4-D assimilation model (Collins et al., 2000). The figure illustrates the north-south gradient in AOD with values around 0.5 around the coast and less than about 0.1 south of equator. As described in Rajeev and Ramanathan (2001), the standard error of the seasonal average shown in this figure is about ± 0.02 or 15 %, whichever is greater.

4.2. Seasonal and interannual variability

Variations of AODs during the winter monsoon (January to March) and summer monsoons (June to August) (Figure 4.3) have been examined (Li and Ramanathan, 2002). Two major characteristics of the regional distribution can be identified from the maps. During the winter monsoon, the AODs are larger over both the Arabian sea and the Bay of Bengal. As identified in numerous studies (e.g, Rajeev et al., 2000; Satheesh et al., 1999; Ramanathan et al., 2001a) the dominant sources for these aerosols are anthropogenic emissions (both bio-mass burning and fossil fuel combustion). During the summer monsoon, when AODs are much larger over both regions the Arabian Sea and the Bay of Bengal. With the onset of the southwest monsoon, the Arabian plume becomes dominant and AODs off the Arabian and the north African coast reach values as high as 0.5 to 0.6, and spread to most of the Arabian sea. Three factors contribute to the summer time aerosol build up. First is the transport of mineral dust from Arabia and north Africa by the westerly winds at and above 700 mb. Second is the enhancement in the production of sea salt by the strong westerly winds. Lastly, the high humidity of the southwesterly surface winds increase the aerosol size which in turn leads to increase in scattering optical depth.

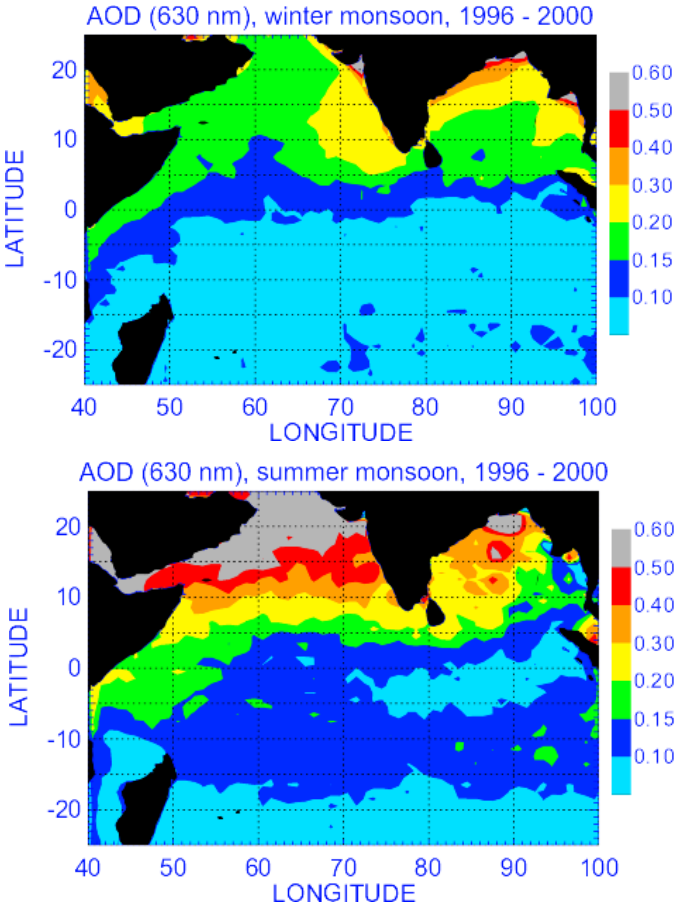

Figure 4.3: Maps of aerosol optical depth (AOD) during the winter monsoon (January, February and March) (top) and during the summer monsoon (June, July and August) (bottom), averaged for the five years from 1996 to 2000. The AOD values are retrieved from AVHRR data (Li and Ramanathan, 2002).

The year to year variability of AODs during the SW monsoon, and the NE monsoon is shown in Figure 4.4 along with the variability of the annual mean values. Interannual variations of the SW monsoon AODs over the Bay of Bengal are largest, with a variability of ±23% of total annual AODs. The value for the region of Arabian Sea is ±7%. It is interesting that the SW monsoon AODs during 1997 were higher over both the Arabian Sea and the Bay of Bengal. For the time series of AODs (1996 ~2000), the Arabian Sea shows a distinct seasonal cycle (Figure. 4.5) with peak values in the summer months. The maximum monthly mean value (~ 0.6) of AOD (0.63μm) during the summer is three times larger than that during the winter (0.2).

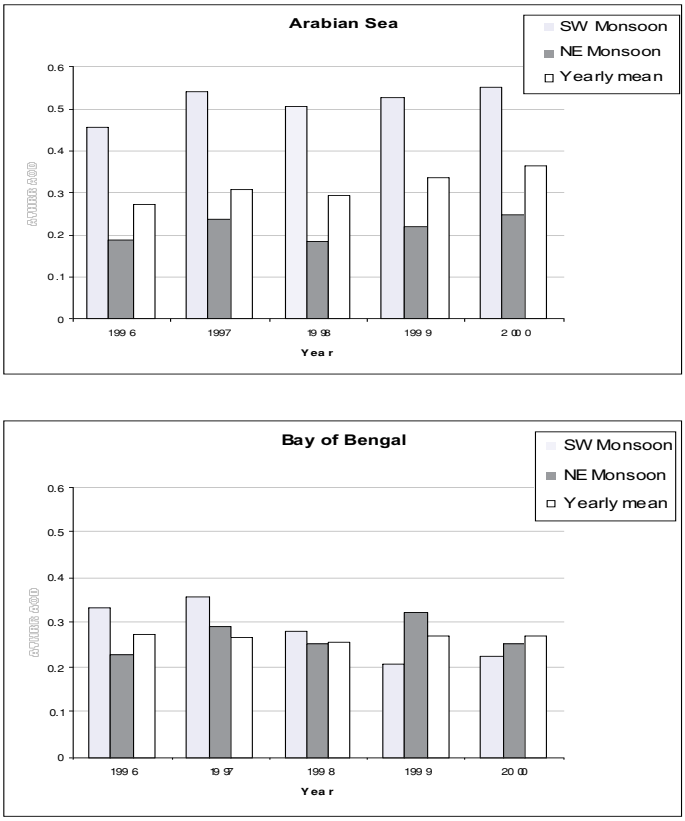

Figure 4.4: Interannual variations of aerosol optical depth (AOD) during the summer and winter monsoons and in yearly mean, over the regions of the Arabian Sea (10° N-25° N, 40° E-77° E) (top), and the Bay of Bengal (10° N-25° N, 77° E-100° E) (bottom), (Li and Ramanathan, 2002).

4.3. Relationship of aerosol optical properties to black carbon

At ambient humidity, the single-scattering albedo (SSA) is approximately 0.86 to 0.9 for aerosols in the northern Indian Ocean. Several independent methods have been used to determine SSA from surface, ship-borne, and airborne instruments and from MACR calculations. The observed column averages span 0.86 to 0.9 and are remarkably consistent with the model estimates. These values are also consistent with column-average SSA obtained from surface stations at Goa and Dharwad in western India (Alfaro et al., 2001; Leon et al., 2001). The values of SSA derived for INDOEX indicate that the aerosols in this region are a strong absorber of sunlight. Of the major aerosol species (sea-salt, dust, sulfate, and black and organic carbon), only dust and black carbon are sufficiently absorptive to produce these low values of SSA. Black carbon is approximately 3.5 times as absorptive as dust, and the fine-particle concentration of black carbon exceeds that of dust by 40% (Satheesh and Ramanathan, 2000). Therefore the relatively low values of SSA are explained primarily by the presence of black carbon. Observations of the chemical composition of the aerosols confirm that the strong absorption is directly related to significant concentrations of black carbon introduced by fossil fuel and biomass burning. The natural sources of black carbon are negligible compared to the anthropogenic sources (Cooke et al., 1999; and Novakov et al., 2000); and it is only 4% in the INDOEX region (Collins et al., 2000).

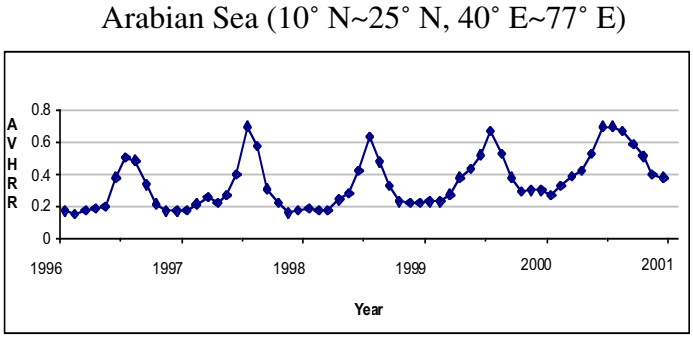

Figure 4.5: Time series (1996-2001) for monthly mean aerosol optical depth (AOD) (0.63 um) in the region of Arabian Sea (10° N-25° N, 40° E-77° E), The AOD values are retrieved from AVHRR data (Li and Ramanathan., 2002).

Part II: Climate and Environmental Impacts

5. Overview

Aerosols impact climate and the environment in many diiferent ways as illustrated in Figure 5.1 below. This figure describes schematically the various aerosol forcing terms, their impacts on atmospheric chemistry, cloud microphysics, large scale dynamics, global and regional climate and the hydrological cycle. The two major effects of air pollution are production of new particles and ozone in the lower atmosphere. The green boxes represent the various processes that impact climate. The gray shaded boxes denote atmospheric variables impacted by aerosols. The thick black arrows represent the most direct effect of aerosols and ozone. The thick green arrows represent the most direct effect between two processes. The thick red arrows are the feedback effects on the aerosol. The thick blue arrows represent the impact on temperatures. The thinner black and green arrows have the same meaning as their thicker counterparts but are less well understood.

Aerosols impact the micro physical (the left green box) processes which in turn influence the radiative processes (the right green box). Aerosols reduce the precipitation efficiency which decreases the thermodynamic forcing (i.e release of latent heat to the atmosphere during condensation). The change in the atmospheric radiative heating due to aerosols is the atmospheric forcing and the change in surface radiative fluxes is the surface forcing. The sum of the two is the well known top-of-the-atmosphere or TOA forcing. The atmospheric forcing is mostly due to absorbing aerosols such as black carbon, dust and some organics.

Since aerosols are regionally concentrated, absorbing aerosols can impose a large horizontal gradient in radiative heating which can directly alter the general circulation, which in turn can perturb the precipitation amounts and patterns. Another major impact of anthropogenic aerosols is the suppression of rain drops in shallow and deep convective clouds, which are the major sources of thermodynamic forcing of the general circulation. In addition, transport of aerosols and aerosol precursor gases to the upper troposphere can impact the concentration of several trace gases including water vapor and population of ice crystals in cirrus clouds.

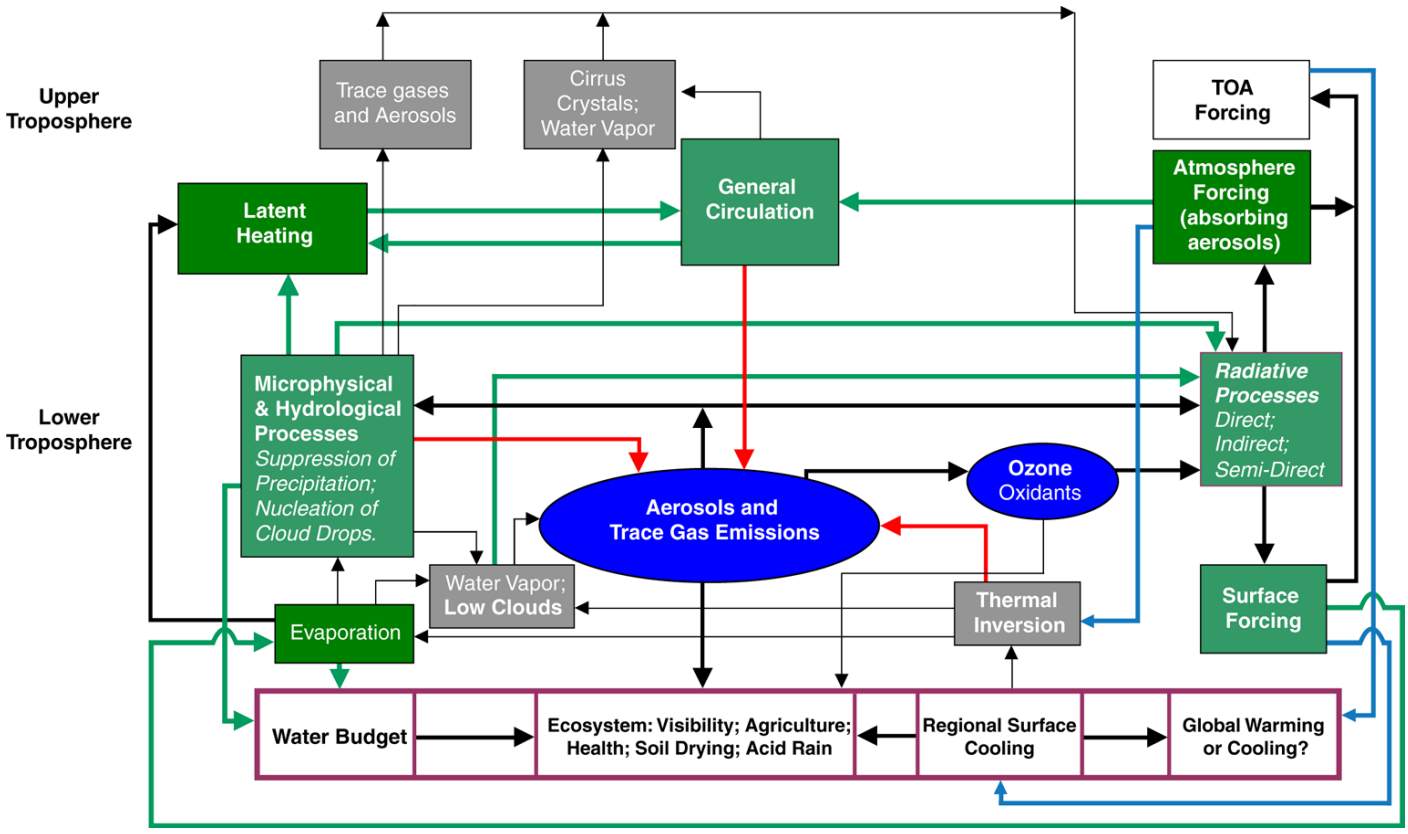

Figure 5.1

The black carbon heating of the boundary layer can strengthen the low level inversion which can in turn perturb low level clouds, enhance aerosol life times and alter the boundary layer moisture. Aerosol induced reduction of solar radiation to the surface reduces visibility and agriculture productivity. In addition, the inhalation of particles can have adverse health while the acidity of the aerosols impacts the ecosystem.

5.1. Comparison with Greenhouse Forcing

The climate forcing of GHG arises solely and directly from its radiative forcing of the earth-atmosphere system. Another simplifying factor is that the vertical and the horizontal distribution of the greenhouse forcing is somewhat uniform. The aerosol climate forcing on the other hand is more complex, distributed more heterogeneously in space and time and involves many components of the system (Figure 5.1). GHG absorb upwelling infrared, IR also referred as longwave, radiation and reduce the outgoing longwave (> 4μm) radiation (OLR) at the top-of-the atmosphere. Aerosols, on the other hand, increase the reflection of solar radiation to space through a variety of complex radiative and microphysical processes.

The scattering and absorption of solar and long wave radiation by anthropogenic aerosols decreasing the surface radiative heating (surface forcing) and enhance the atmospheric radiative heating (atmospheric forcing). The TOA forcing is the sum of the surface and the atmospheric forcing (Figure 6.1). The global average of the TOA forcing is the aerosol direct forcing used in most global warming studies. Another direct effect of aerosols arises from its dominant influence on the cloud micro-structure. Anthropogenic aerosols can enhance the number of cloud drops, decrease the mean drop radius and increase the cloud life time and cloud fraction. Since clouds are significant modulators of the radiative heating of the planet, these changes in cloud microstructure lead to additional radiative heating. This indirect radiative forcing, according to some model estimate can be significantly larger than the direct forcing. The regional radiative forcing (direct plus indirect) of aerosols can exceed their global mean forcing by as much as a factor of 5 to 10 , and can also significantly exceed the greenhouse forcing.

Another major contrast with the greenhouse forcing is that the effect on cloud microstructure leads to a direct thermodynamic forcing. The production of more drops, but with smaller radii, suppresses stratiform and convective precipitation. Since the latent heating released within precipitating clouds provides the thermodynamic forcing for the global circulation, we have to account for the role of aerosols in the thermodynamic forcing as well.

Lastly, a unique characteristic of aerosol forcing arises from absorption of solar radiation , particularly by black carbon (BC). In more recent years, the role of sunlight absorbing BC containing particles derived from fossil fuel burning and biomass burning have come to the forefront, especially as a result of the findings of some major field programs such as Tropospheric Aerosol Radiative Forcing Observational eXperiment (TARFOX); Aerosol Characterization Experiment (ACE)-2; Smoke, Clouds And Radiation - Brazil (SCAR-B); and especially INDOEX. Solar absorption adds to the atmospheric heating; while both scattering and absorption blocks the radiation reaching the surface. Thus the more significant impact of absorbing aerosols such as BC and dust involves the vertical redistribution of the solar radiation between the surface and the lower atmosphere, qualitatively resembling the nuclear winter forcing. In tropical regions with highly absorbing aerosols, the reduction in solar radiation can be as large as 20 Wm^{-2} compared with the 0.5 to 1 Wm^{-2} surface forcing of GHG.

6. Radiative Forcing and Latent Heating

6.1. Definition and observation of aerosol radiative forcing and radiative properties

Solar energy entering the Earth's atmosphere can be absorbed within the atmosphere, scattered and transmitted toward the surface, or reflected back to space. The amount of solar energy involved in each of these processes is quantified as up and down fluxes in units of Watts per meter squared (Wm^{-2}). The change in each of these processes by the introduction of aerosols is called aerosol forcing. The changes in the solar energy absorbed in the atmosphere, transmitted to the surface, and reflected to space are atmospheric, surface, and top-of-atmosphere (TOA) forcing, respectively. Aerosols can also change the distribution of solar energy by altering the physical and microphysical properties of clouds in which the aerosols are mixed. The effects of aerosols that do not involve this interaction are called direct radiative forcing, and the effects that do involve the interaction are called indirect radiative forcing. The first indirect effect is the increase in cloud reflectivity, or albedo, when aerosols act to increase the number of cloud droplets while simultaneously decreasing the size of the droplets. The second indirect effect is the increase in time or area-averaged cloud albedo when more numerous aerosols leading to smaller cloud droplets act to decrease precipitation and increase cloud lifetime and/or condensed cloud water. The semi-direct effect is the reduction in cloud cover and cloud albedo when aerosols increase solar heating and evaporate low clouds (Ackerman et al., 2000). We will first consider the direct radiative forcing in the absence of clouds, then discuss the direct forcing in the presence of clouds, and subsequently add in the first indirect effects to estimate the total aerosol forcing. Estimation of the second indirect effect and semi-direct effect for the Indian Ocean is based (at this time) entirely upon model calculations, and as a result it is difficult to assign uncertainties to these effects.

Aerosols can also affect the propagation of thermal, or longwave, radiation emitted by the surface and atmosphere. For INDOEX, most of the longwave aerosol forcing is caused by coarse aerosols from sea salt and dust and is therefore natural in origin (Lubin et al., 2001). Although the change in downwelling thermal radiation is approximately 2 Wm^{-2} during INDOEX, the total aerosol forcing is dominated by changes in solar fluxes related to anthropogenic pollutants (Ramanathan et al., 2001a).

The IPCC definition of forcing only includes changes in aerosol effects related to anthropogenic activity (IPCC, 1995). The INDOEX forcing estimates include the effects of both natural and anthropogenic aerosols. However, the background dust and sea-salt aerosols constitute only 20+10% of the total aerosol optical depth (Satheesh et al., 1999) and contribute relatively minor components of the forcing.

Direct aerosol radiative forcing in the region has been characterized using several independent sets of surface observations (Jayaraman et al., 1998; Krishnamurti et al., 1998; Meywerk and Ramanathan, 1999; Jayaraman, 1999; and Conant, 2000) and combinations of surface and satellite data (Satheesh and Ramanathan, 2000; Rajeev and Ramanathan, 2001; and Ramanathan et al., 2001a). Observations of the chemical, physical, and optical properties of aerosols form the basis for a Monte Carlo model for computing aerosol and cloud radiative forcing called MACR (Podgorny et al., 2000). This model is consistent with the observed aerosol properties and the observed direct forcing. When observed cloud properties are input to MACR, it provides a mechanism for calculating the effects of clouds on direct radiative forcing and for computing the first indirect effect (Ramanathan et al., 2001a). The direct radiative forcing and solar heating over continental areas in the Indian Ocean region have been calculated with an aerosol assimilation model (Collins et al., 2001a). This model has been validated with the aerosol optical depth, chemical speciation, and TOA and surface forcing at the KCO site (Collins et al., 2001b).

6.2. Direct aerosol radiative forcing and heating under clear and cloudy conditions

For non-absorptive aerosols, e.g. sulfate, to first approximation, the direct aerosol forcing at the surface and TOA are nearly identical. In essence, the incident solar radiation reflected back to space by the aerosols (the TOA forcing) is removed from the sunlight incident on the surface (the surface forcing). When absorptive aerosols are present, the reduction in surface insolation is the sum of the solar radiation reflected back to space and absorbed in the atmosphere. Under these conditions, the direct aerosol radiative forcing at the surface is larger than the forcing at TOA. This effect is observed in the INDOEX region, and may be quantified using forcing efficiencies (radiative forcing change per unit of optical depth) for the surface and TOA forcing denoted by f_S and f_T, respectively. At the Kaashidhoo Climate Observatory (KCO), under clear-sky conditions, f_T, is approximately -25 Wm^{-2} and f_S is approximately -75 Wm^{-2} (Satheesh and Ramanathan, 2000). The minus

signs indicate that aerosols reduce the net sunlight absorbed by the surface and by the Earth-atmosphere system at TOA. For a non-absorptive aerosol, $f_S \approx f_T$, but since the aerosols in the INDOEX region are absorptive, this condition does not apply. In fact, f_S is approximately 3 times f_T. Analysis of satellite data for the whole northern Indian Ocean yields f_S of -22 Wm^{-2}, similar to the value obtained at KCO (Ramanathan et al., 2001a). Preliminary analysis of radiometric data from the INDOEX aircraft missions confirms that f_T is approximately -70 to -75 Wm^{-2}.

The aerosol forcing at TOA and surface are respectively equal to the product of f_T, and AOD and f_S and AOD in cloud-free conditions. Since the observed optical depth over the northern Indian Ocean during January to March, 1999 is 0.3, the TOA and surface forcing are -7±1 Wm^{-2} and - 23±2 Wm^{-2} over the Indian Ocean between 0° to 20° N and 40° E to 100° E (Figure 6.1). The forcing over adjacent continental areas has been computed from the INDOEX aerosol assimilation model (Collins et al., 2001a), which reproduces the observed forcing efficiencies f_T, and f_S (Collins et al., 2001b). The surface forcing by aerosols over central India, Southeast Asia, and southern China is –35 to 40 Wm^{-2} (Figure 6.2b). This represents a 15% reduction in surface insolation over central India and a 17 to 20% reduction for Southeast Asia and central China. The direct aerosol surface forcing over India during INDOEX actually exceeds climatological estimates for the reduction in insolation by clouds.

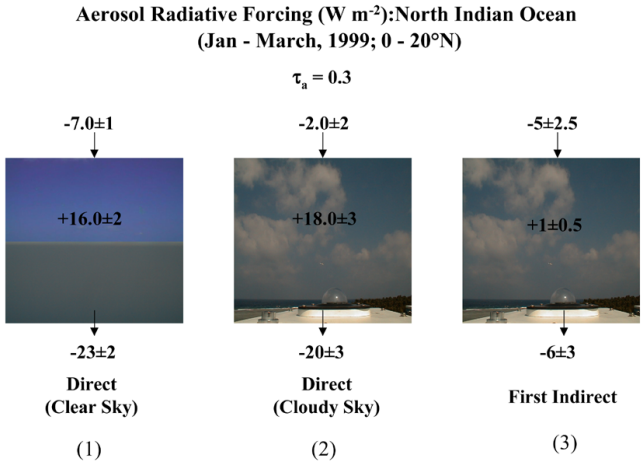

Figure 6.1 (Ramanathan et al., 2001a)

The presence of aerosols increases the heating of the atmosphere by absorption of solar radiation. The heating is expressed as a tendency Q in atmospheric temperature per day considering just the effects of solar absorption. The change, δQ, in the southern Indian Ocean produced by natural and anthropogenic aerosols is less than 0.01° C/day. However, between 15° N to 20° N δQ exceeds 0.7° C/day in the lower atmosphere (Collins et al., 2001b). This corresponds to an increase in the clear-sky heating of 130%, a significant change in the radiative heating of the atmosphere. Approximately 90% of δQ is associated with the carbonaceous aerosols.

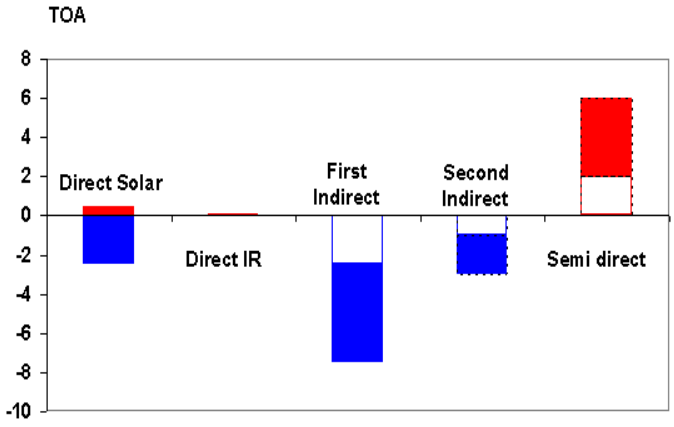

Figure 6.2.a

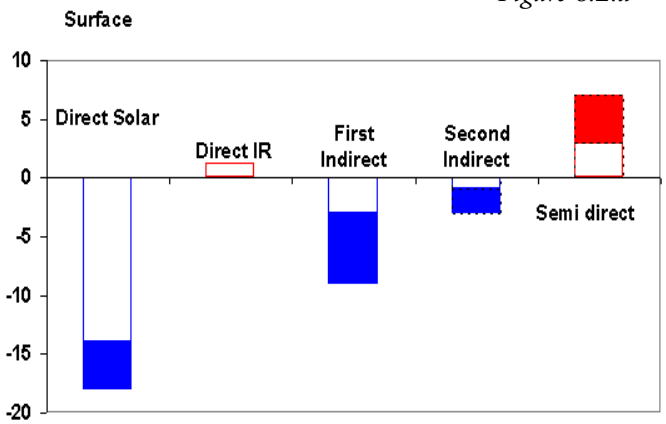

Figure 6.2.b

Figure 6.2: Anthropogenic Aerosol Radiative Forcing avrgaed over the North Indian ocean, Arabian sea and the bay of Bengal (0° to 20° N; 40° E to 100° E). The results are for the year 1999, from January to April. The range of the estimated forcing is shown by the shaded region (red or blue). The direct and the first indirect forcing values are from INDOEX observations and the results for the second indirect effect and the semi-direct are from a 3-d cloud model study by Ackerman et al. (2000). The top panel shows the forcing at TOA and the bottom panel shows it at the surface. The difference between the TOA and the surface forcing yields the atmospheric forcing. The mean for the individual forcing terms should lie within the blue or red shaded region. (Ramanathan et al., 2001a)

The direct radiative forcing in the presence of clouds has been computed using the MACR model with cloud properties and distributions derived from in situ data and satellite imagery. For cloudy conditions over the northern Indian Ocean, the average TOA and surface direct forcing are -2±2 Wm^{-2} and -20±3 Wm^{-2}, respectively (Figure 6.1). Compared to the cloud-free conditions, the magnitudes of the TOA and surface forcing have been reduced by 5 Wm^{-2} and 3 Wm^{-2} by addition of clouds.

We will now consider the radiative forcing due to anthropogenic aerosols shown in Figure 6.2. The first step is to estimate the AOD for the northern Indian Ocean without any anthropogenic influence, i.e, the background natural aerosol over the tropical Indian Ocean, subject to the continental outflow. If we adopt the result given in Chapter 3 for the anthropogenic contribution of 75% to the column aerosol optical depth, we obtain the background to be 0.07 (25% of the 0.3 mean value for the northern Indian Ocean, shown in Figure 4.2). In addition to the direct and the first indirect effect, we also include the second indirect effect and the semi-direct effect. Lastly, we also include the infrared (IR) forcing. The individual forcing values are shown in Figure 6.2. Given the large uncertainty and the opposing signs of the various effects, we do not give a mean value, but instead show a gray shaded region that must contain the mean value.

The clear sky TOA forcing is -5 Wm^{-2}, but the enhanced aerosol solar absorption in cloudy regions cancels out as much as 3 to 5 Wm^{-2}. Thus the TOA direct effect (+0.5 to -2.5 Wm^{-2}) is a small difference between two large numbers. The surface forcing, however, is as large as –14 to -18 Wm^{-2}. In view of the large uncertainty in the satellite retrieved low cloud cover and the competing nature of the various aerosol forcing terms, the total aerosol forcing is not shown in Figure 6.2. The regional distribution of the sum of the direct and the first indirect forcing is shown in Figure 6.3.

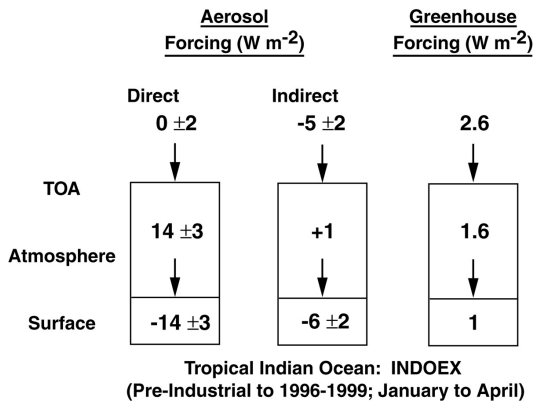

Figure 6.3: A comparison of aerosol forcing with greenhouse forcing (including the cloud effect) for the Indo-Asian region (50-100° E and 25° N to 10° S).

The first indirect effect is related to the increase in the number of cloud droplets with increasing aerosol concentrations, as some of the aerosol particles act as sites for condensation of moisture to form additional droplets. The increase in droplet number is accompanied by a decrease in the diameter of the droplets. The variation of these cloud properties with aerosol concentration has been estimated directly from INDOEX aircraft measurements collected in clouds under polluted conditions. In turn, the concentration of aerosol particles can be related to aerosol optical depth, which can be derived from satellite imagery for the INDOEX region. The relationships between cloud properties and aerosol optical depth together with satellite-derived optical depths are used in MACR to compute the first indirect effect. Over the northern Indian Ocean, the first indirect effect changes the aerosol forcing by -5±2 Wm^{-2} at TOA and -6±2 Wm^{-2} at the surface (Figure 6.3).

For the second indirect effect and the semi-direct effect, we rely on a 3-Dimensional eddy resolving trade Cumulus model described in Ackerman et al., 2000. Two independent model studies (Ackerman et al., 2000 and Kiehl et al., 1999) of the INDOEX soot heating show that it leads to a reduction in the trade cumuli prevalent over the tropical oceans. Ackerman et al. (2000) insert the INDOEX aerosol with soot and estimate the forcing for various cloud drop concentrations (their Plate 5). We adopt here their simulations for *Nc* (cloud drop number density) of 90 cm^{-3} (pristine) and 315 cm^{-3} (polluted), consistent with the composite indirect-effect scheme shown in Figure 4.2. The inclusion of soot heating (semi-direct effect) reduces the low cloud fraction by about 0.04 (day-night average). The TOA forcing due to this increase is about +4 Wm^{-2} (day-night average). Their model also shows that addition of cloud drops (due to second indirect effect) enhances cloud lifetime, which in turn increases the low cloud fraction by about 2% and a forcing of –2 Wm^{-2}. Given our poor knowledge of how the various uncertainties accumulate, we prefer not to attribute an overall uncertainty range to the total forcing.

6.4. Important aspects of the forcing

6.4.1. Comparison with the Greenhouse Forcing: The average aerosol forcing is compared with the greenhouse forcing in Figure 6.3. This figure shows just the anthropogenic aerosol forcing. The sum of the direct and indirect aerosol forcing is a net cooling effect of 5 W m^{-2} compared with the positive greenhouse forcing of 2.6 Wm^{-2}. The major difference is in the atmosphere and at the surface, where the aerosol effects dominate.

The solar heating of the eastern Arabian sea and Bay of Bengal is reduced by as much as 20 to 30 Wm^{-2} (about 15%). The TOA forcing peaks in the cloudy and polluted Bay of Bengal region, with values between -6 to -15 Wm^{-2}. The sum of the direct and first indirect aerosol forcings exhibits a large positive gradient of 25 Wm^{-2} in the solar heating of the atmosphere between 25° S to 25° N (Figure 6.4). This is accompanied by a corresponding reduction in insolation at the ocean surface. The implications of this gradient have been examined using state-of-the-art models of the general circulation, and the effects on regional climate are summarized elsewhere in this report.

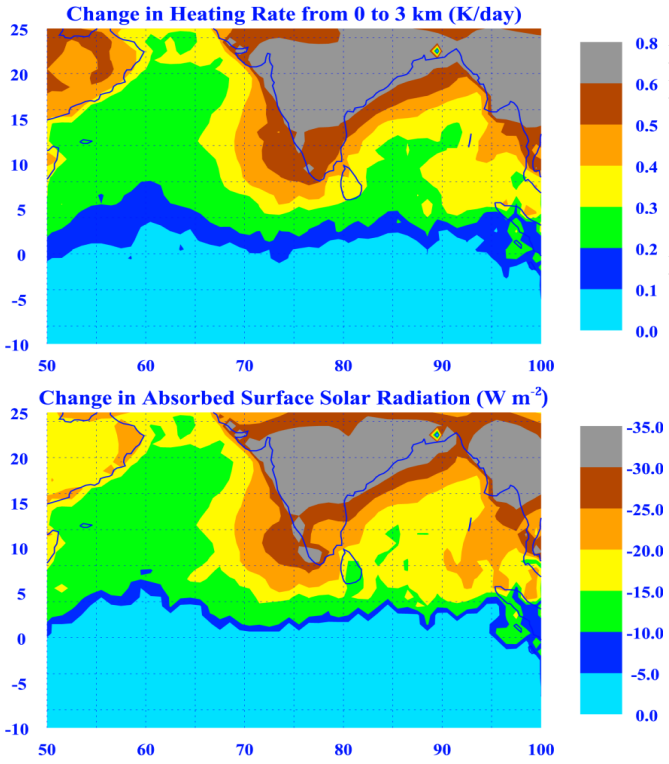

Figure 6.4: Regional distribution of aerosol forcing (Ramanathan et al., 2001b).

6.5. Thermodynamic forcing: The direct microphysical effect on precipitation

Aerosols containing large concentrations of small CCN nucleate many small cloud droplets, which coalesce very inefficiently into rain drops, one consequence of which is suppression of rain over polluted regions (Rosenfeld, 2000). The suppression of precipitation in turn will suppress the release of latent heating (over the polluted regions), which is an important forcing term for the tropical general circulation. This was recently confirmed by satellite observations of the Tropical Rainfall Measuring Mission (TRMM), showing tracks of reduced cloud particles emanating from forest fires (Rosenfeld et al., 2001) and from pollution sources such as coal power plants, refineries, smelters and urban areas (Rosenfeld et al., 2001). The clouds in and out of the pollution tracks had similar dimensions, and according to the TRMM passive Microwave Imager (TMI) contained similar amounts of water. The only difference was in the reduction of the cloud particle effective radius (r_e) within the pollution tracks to <14 μm, the precipitation threshold radius. Respectively, the TRMM Precipitation Radar (PR) observed precipitation outside the pollution tracks, but not in them. A similar behavior was seen on the INDOEX plumes (Figure 6.5; Rosenfeld, private communication). Figure 6.6 shows precipitation suppression of rain by aerosols in different parts of the world. Furthermore, satellite observations (Rosenfeld et al., 2001) showed consistently that the suppression of coalescence by smoke and air pollution induced lower freezing temperature of the cloud supercooled water and suppression of the ice precipitation processes as well.

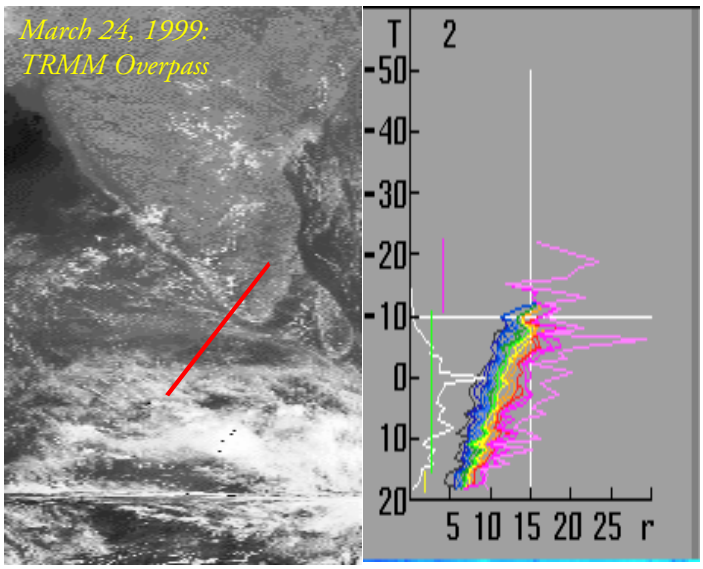

Figure 6.5: The effective particle radius along the red track is shown in the graph on the right panel. The track is along southern India, running through a pollution mass (left). The effective radius of clouds drops plotted against the temperature of the cloud tops (right). Data were obtained from TRMM satellite (Rosenfeld, private communication).

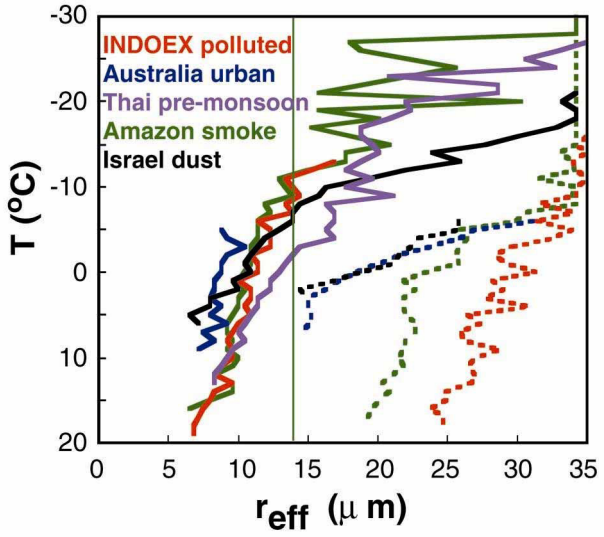

Figure 6.6: Satellite retrieved median effective radius of particles near the top of deep convective clouds at various stages of their vertical development, as a function of the cloud top temperature, which serves as a surrogate for cloud top height. The effective radius is the ratio of the integral of the third moment (r^3) of the radius weighted with the number concentration at that radius, to its second moment (r^2). This is shown for clouds forming in polluted (solid lines) and pristine air (broken lines) at: INDOEX, over southern India and over the southern Indian Ocean; Australia pollution tracks; Thailand pre-monsoon clouds with suppressed coalescence; Smoke over the Amazon; Desert dust over Israel. The vertical green line denotes the 14 μm precipitation threshold radius. (Ramanathan et al., 2001b)

7. Climate and the Hydrological Cycle

7.1. On assessing aerosol impacts on climate

The period of interest is the post-1960s, since before this period anthropogenic aerosols sources were signficantly smaller (Figure 1.1). Before we can examine aerosol impacts, we must recognize that aerosols are not the only agents of climate change in this region. Increase in the greenhouse gases, episodic forcing due to volcanic emision (e.g, El-Chichon in 1982 and Mt. Pinatubo in 1991), the impact of ENSO phenomenon in the Pacific through teleconnections, and other natural causes of interannual variability are other important forcing agents of regional climate change. A detailed discussion of these effects are beyond the scope of this report. We restrict our attention here to the haze and compare their effects with the GHG warming.

GHG and aerosols: Competing effects. GHG and aerosols have competing effects on climate and the hydrological cycle. Furthermore their competing effects depend on spatial and temporal scales. The GHGs warm the surface and the atmosphere, whereas, aerosols can warm or cool depending on the TOA forcing (positive or negative). Even if the TOA forcing is positive, the surface can cool regionally, if the aerosols lead to a large reduction in surface solar radiation and the atmosphere and the surface are weakly coupled, such as the South Asian region during the dry seasons. Regionally, the most important effect of aerosol may very well be on the water cycle. Most, if not all, Ocean-Atmosphere (OA) GCMs show that a global mean surface warming will be accompanied by an increase in global precipitation by about 1 to 2% per K (increase in surface temperature) because of the increase in evaporation, in particular, from the oceans. The evaporation increases because of the increase in saturation vapor pressure with temperature. Anthropogenic aerosols, on the other hand, can alter the regional precipitation in many different ways, including (to name just the important ones): the direct microphysical effect discussed earlier; increasing the lifetimes of low clouds through the indirect effect (again discussed earlier); and the strong spatial gradients in aerosol forcing patterns (e.g., Figure 6.4) will perturb the regional circulation which in turn can alter the regional precipitation patterns. The large difference between the TOA and the surface forcing due to the absorbing anthropogenic aerosols raises an important question related to the global hydrological cycle: How does the system adjust to the large reduction in surface solar absorption (Figures 6.1 - 6.3)?

At the surface, there is a balance between radiative flux, R, latent heat flux (evaporation, E) and sensible heat flux, S (Figure 7.1). One or all of these components will decrease to offset the reduction in surface solar radiation. Since 60% to 70% of the absorbed solar radiation at the surface is balanced (on a global annual mean basis) by evaporation, it is possible that a major fraction of the reduction in surface solar radiation is balanced by a reduction in evaporation. Reduction in the evaporation will have to be balanced by a reduction in rainfall and effectively spin down the hydrological cycle. The resulting decrease in the latent heat released by precipitation will also counter the aerosol induced increase in atmospheric solar heating.

In this regard it should be noted that there has been a downward trend in Asian rainfall over the last several decades (Fu et al., 1998). In addition, there has been a decrease in the tropical and subtropical mean rainfall during the last several decades (IPCC, 2001). While the subtropical decrease may be attributed to the observed global warming trend (based on GCM studies of greenhouse forcing), the tropical decrease requires other explanations and absorbing aerosols is a leading candidate for the observed drying.

We do not have global model studies of realistic absorbing aerosols to assess the quantitative importance of the aerosol effect on the global hydrological cycle. As a consequence, we do not know whether the aerosol effects on the precipitation are concentrated regionally close to the sources or distributed around the globe. However, the deduction that the aerosol induced reduction in surface solar radiation will be balanced by a decrease in evaporation and precipitation is supported by numerous OA-GCM studies. Most of

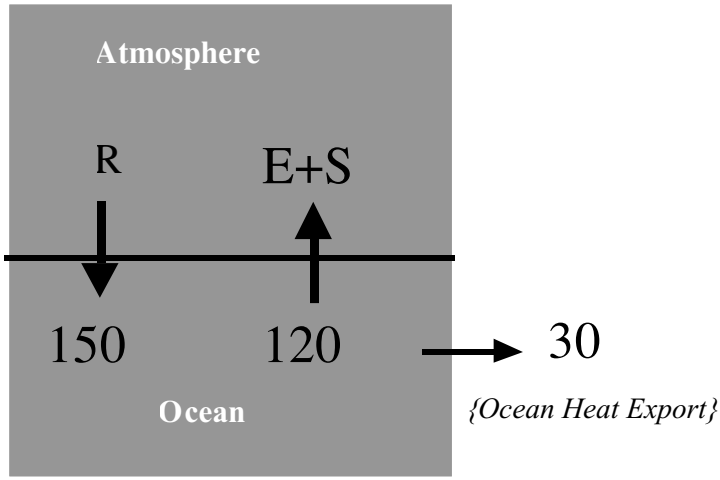

Figure 7.1: Annual Mean Heat Budget of the Tropical Indian Ocean (W m^{-2}).

the models have included only the radiative effect of sulfate aerosols. Nevertheless, inclusion of just the direct radiative forcing of sulfate aerosols (without the GHG forcing) leads to a net reduction in the hydrologic cycle in the OA-GCMs, with the reduction in solar insolation balanced by a reduction in the latent heat flux due to evaporation. In more recent studies that include both the direct and the indirect radiative effect of sulfate aerosols on the climate system, the strength of the hydrologic cycle decreased again, and this decrease was large enough to reverse the effect of GHG in one of the models.

A brief background of the climatic environment of South Asia is presented in the next section; followed by an assessment of the regional climate sensitivity to aerosol forcing as inferred from GCM experiments performed at SIO and NCAR. An analysis of the relevant observed climate variations is presented finally in order to describe the complexity of the climate change issue over South Asia.

7.2. Climatic environment

South Asia lies in the heart of the Asian Monsoon tropics. Latitudinally the region lies between the equator to 38° N and longitudinally between 65° E and 98° E, and covers a wide variety of climatic regimes. The winter and early spring months are characterized by moderate to strong northeasterly seasonal winds. The month of May is the transition period when the seasonal northeasterly winds are replaced by the southwest summer monsoon wind system. Associated with this seasonal cycle of the atmospheric winds and stability conditions, the anthropogenic aerosol load builds up from October; peaks during February and March; decreases in May and June; and decreases further during July to September under the washout and scavenging influence of the summer monsoon clouds and precipitation processes. During winter months the duration of sunshine over northern India is about 6-7 hours, while over southern India it is about 9-10 hours. The soil moisture and evaporation rates are low during winter months over the entire Indian subcontinent. The spatial distribution of surface-air temperature (Figure 7.2) during the January-April months shows strong north-south gradient with the northern Indian region being significantly colder than the southern peninsular region.

The annual cycle of rainfall for whole India (Parthasarathy et al., 1995) and also for different homogeneous regions of India is shown in Figure 7.3a. The bulk of the annual rainfall for the most region is concentrated during the June-September months of the monsoon season. However the region of Peninsular India receives considerable rainfall during the October-December season that is comparable with that of the summer monsoon season. The winter and spring rainfall is generally low over most of the regions of India with the exception of North-East, Peninsular India, and also parts of Northwest India and Pakistan. Rainfall during the winter season is important for the cultivation of wheat crop over Northwest India and Pakistan. The spatial distribution of the total seasonal (January-April) rainfall over North India and Pakistan is illustrated in Figure 7.3 (b, c). The rainfall amounts within the Indo-Pakistan region are generally higher in the northern parts (Jammu and Kashmir and north Pakistan) than south of 30° N. The area-averaged total rainfall during January-April over the Indo-Pakistan region is typically around 110 mm. There is also considerable interannual variability (~30% of normal) in the total seasonal rainfall amounts.

7.3. Assessment of regional climate change from modeling experiments

The aerosol effects on climate have been addressed quite recently. General Circulation Model (GCM) study by Haywood et al. (1997), and a similar study by Tett et al. (1999) demonstrated that inclusion of sulfate aerosols counteracts GHG induced warming considerably. In contrast with sulfate, carbonaceous aerosols absorb solar radiation and are a source of atmospheric diabatic heating. Accordingly, while scattering aerosol such as sulfate apparently works against global warming, absorbing aerosol may not. As pointed out earlier, INDOEX aerosols are highly absorptive to solar radiation due to a substantial black-carbon component. Thus, their direct effect is characterized by heating of the lower-troposphere and cooling of the surface.

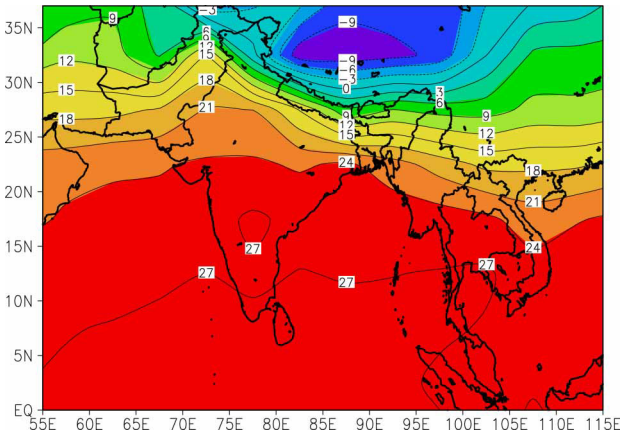

Figure 7.2: The climatological distribution of surface temperature (° C) during January-April. The dataset of surface-air temperature over land is based on Jones (1994) and the sea-surface temperature in the oceans is based on Parker et al. (1995).

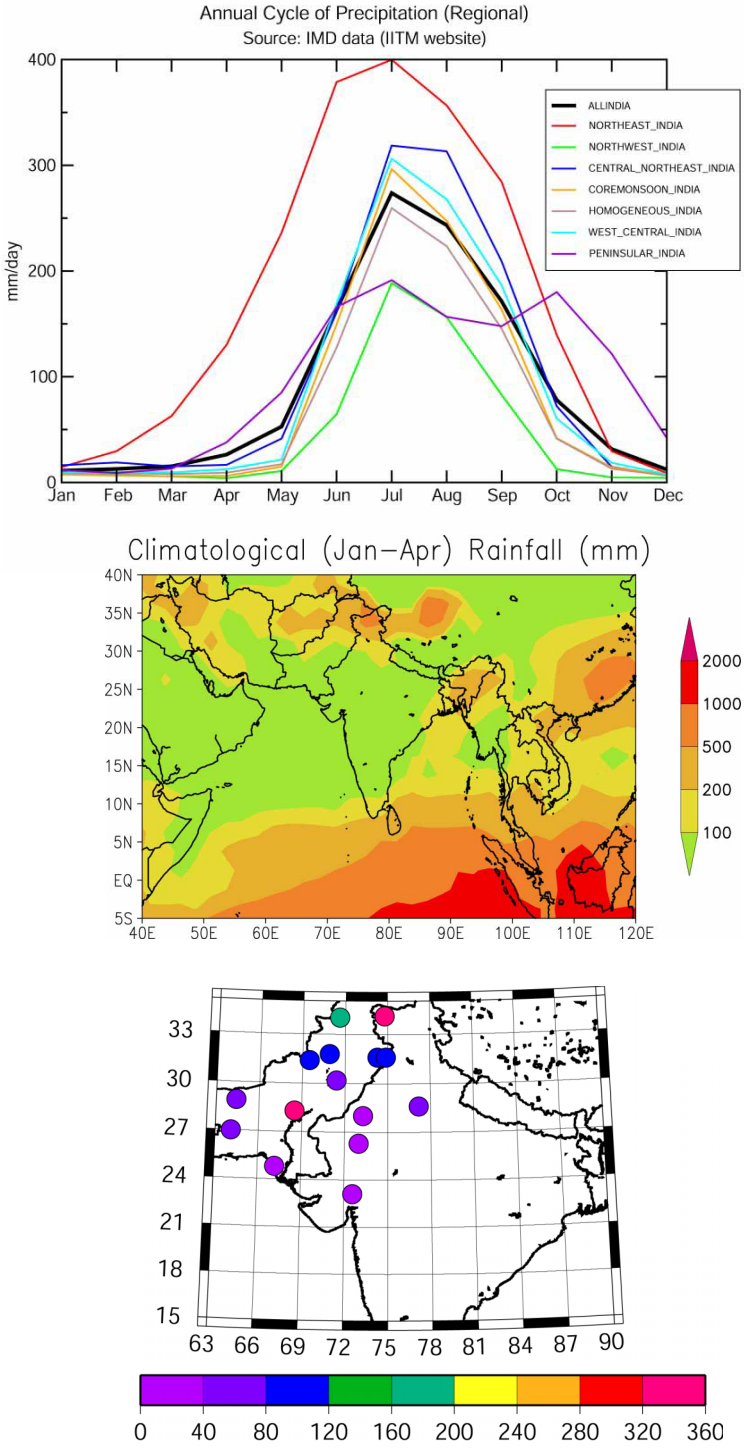

Figure 7.3: (a) The annual cycle of precipitation for different regions of India. The rainfall dataset is obtained from Indian Institute of Tropical Meteorology, Pune, India (Parthasarathy, et al., 1995). (b) The climatological distribution of total rainfall (mm) for the (January-April) season. The precipitation dataset from the Climate Prediction Center (CPC) is obtained by merging raingauge observations and precipitation estimates from satellites (Xie and Arkin, 1997). (c) Same as (b) except for rainfall over stations in Northwest India and Pakistan. This dataset is obtained from the Global Historical Climatology Network (GHCN) archives (Vose et al., 1992).

The direct effect of this regionally confined aerosol on the regional climate was estimated by Ramanathan et al. (2001a), Chung et al. (2002), and Kiehl et al. (2000). The numerical experiments of Chung et al. (2002) were carried out using the National Center for Atmospheric Research-Community Climate Model Version-3 (CCM3). This study imposes a regional distribution of solar heating perturbation due to S. Asian haze as estimated by Ramanathan et al. (2001a) from the observed aerosol optical depths, aerosol composition and cloud distribution. On the other hand, while using the same climate model, Kiehl et al. (2000) prescribe the observed aerosol properties and optical depths, and allow the model radiation code to generate the radiative forcing, using the model generated cloud fields. Thus, a comparison with Chung et al. (2002) will bracket the effects of uncertainties in the radiation code of the CCM3 model and its calculated cloud fraction. Kiehl et al. (2000), furthermore, allow the sea surface to respond to the aerosol forcing, using a mixed-layer slab ocean model, thereby assessing SST change and its impact on the regional climate. We denote the Chung et al. study (2002) as GCM-FO (for fixed ocean temperatures) and the Kiehl et al. study (2000) as GCM-MO (for mixed layer ocean). In addition, in collaboration with W.M. Washington (private communication), we have just completed simulations of the haze with a fully coupled ocean-atmosphere model and the analysis is underway. The temperature changes estimated with the GCM-CO are in good agreement with those estimated by GCM-FO and GCM-MO.

These studies find cooling of the land surface, and warming of the atmosphere during the dry monsoon season (Figure 7.4). These temperature change features lead to the stabilization of boundary layer that results in a reduction of evaporation and sensible heat fluxes. As Figure 7.4 shows, the land surface temperature change is very sensitive to the ratio of the surface, f_S, to the atmospheric forcing, f_T, thus pointing to the importance of estimating the surface forcing in addition to the TOA forcing (Chung et al., 2002); the area-mean cooling amplitude was found to vary from 0.2 K (for $R = f_S/f_T = -0.6$ case) to 1.0 K (for R = -1.5). For the standard experiment ($R \cong -0.9$) the magnitude of cooling was about 0.4 K. The last panel of Figure 7.4 shows a relatively large decrease in the daily maximum temperature as compared to the daily minimum temperature.

Figure 7.5a depicts a 2D temperature change with the standard experiment (from a 85 years of the control run and 60 years of experiment; Chung et al., 2002).

The surface temperature decreases are about 0.5~1.5 K over India, and the lower atmospheric warming is comparable. Kiehl et al.'s study (2000, Figure 7.6) finds somewhat larger land surface cooling and a moderate adjacent ocean cooling.

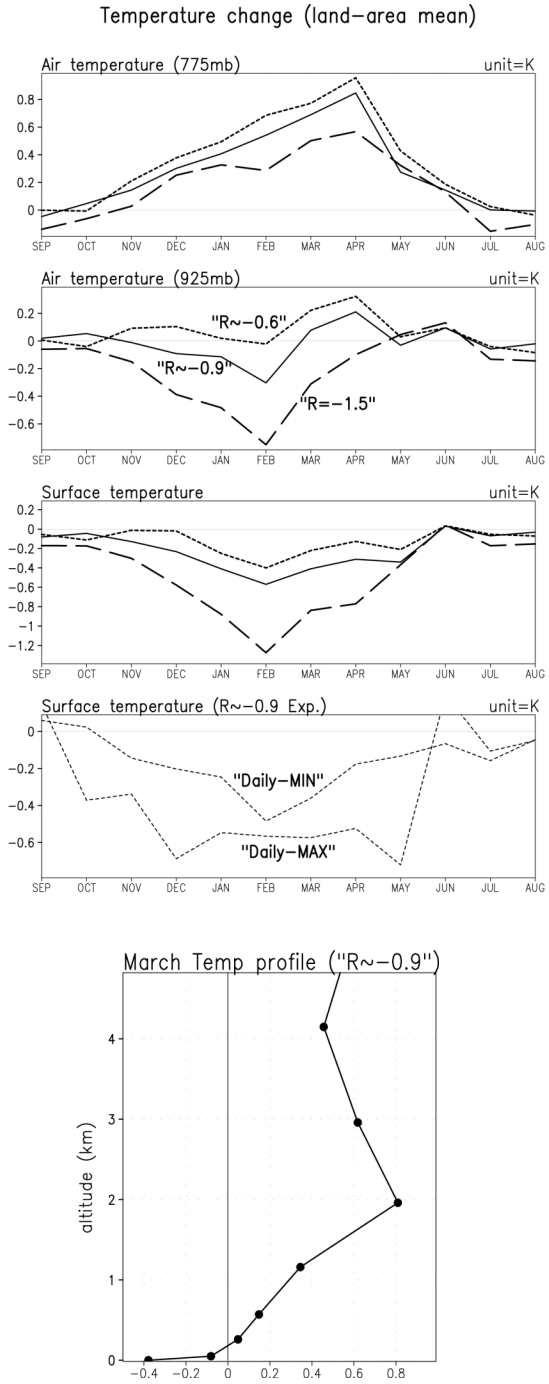

Figure 7.4: Surface and air temperature change, averaged over the land area where the prescribed atmospheric aerosol forcing exceeds 3 W m^{-2} between the control run and each of the 3 sensitivity experiments (Chung et al., 2002). The aerosol forcing was prescribed over India and Southeast Asia as well (see Fig. 6.4). Three experiments (all from GCM-FO), differing in the ratio "R" of fS to fA, are presented here. The standard experiment is the "R~-0.9" case.

The rainfall perturbation (Figure 7.5b) is characterized mainly by a northward widening of the convective region leading to a net enhancement of precipitation therein. In addition, Figure 7.5b shows compensated drying during the wintertime over areas northwest of India and over the western Pacific. These precipitation change features are somewhat similar to the recent trend derived from observation. In particular, the regions northwest of India have been suffering wintertime drought in the recent years. The convection suppression in the western Pacific has implications to El Niño/ Southern Oscillation (ENSO) since the suppressed convection in the western Pacific can amplify El Niño phase and weaken La Niña variability. Clearly, we are at the very early stages of understanding how absorbing aerosols affect climate.

The interannual variability of rainfall over the INDOEX region is large and is comparable to the changes shown in Figures 7.5 and 7.6. A reliable method for ensuring statistical significance is through ensemble simulations of the haze effects with different initial conditions. Such ensemble simulations have not been attempted thus far. However, the FO and the MO versions of CCMs as well as the three *R* values (-0.6,-0.9 and -1.5) of the haze forcing simulate patterns of precipitation response (to the haze forcing) that are similar to those shown in Figures 7.5 and 7.6. Furthermore, the CCMs simulations of the winter precipitation is in good agreement with observed estimates (Figure 7.7).

The enhancement of rainfall in the near-equatorial region has driven the drying over the regions of Northwest India, Pakistan, Afghanistan and the western equatorial Pacific (Figure 7.5b) in the context of the Indian-western Pacific Walker circulation cell. Chung et al.'s (2002) diagnosis using Lindzen and Nigam's simple model (1987) offers an explanation for this rainfall enhancement. The lower layer is heated north of the Indian ITCZ (typically located around 5° S during boreal winter), which leads to a northward widening of the warmest air area in the Indian Ocean. The areal extent of the low layer warm air sector, and its warming amplitude determine the gross features of the large-scale Indian convection. The widening of the warmest area enhances the convection, which is intensified by convergence feedback.

These modeling studies argue for the following conclusions/issues:

• The South Asian haze stablizes the boundary layer in the landmass, leading to a reduction in sensible/

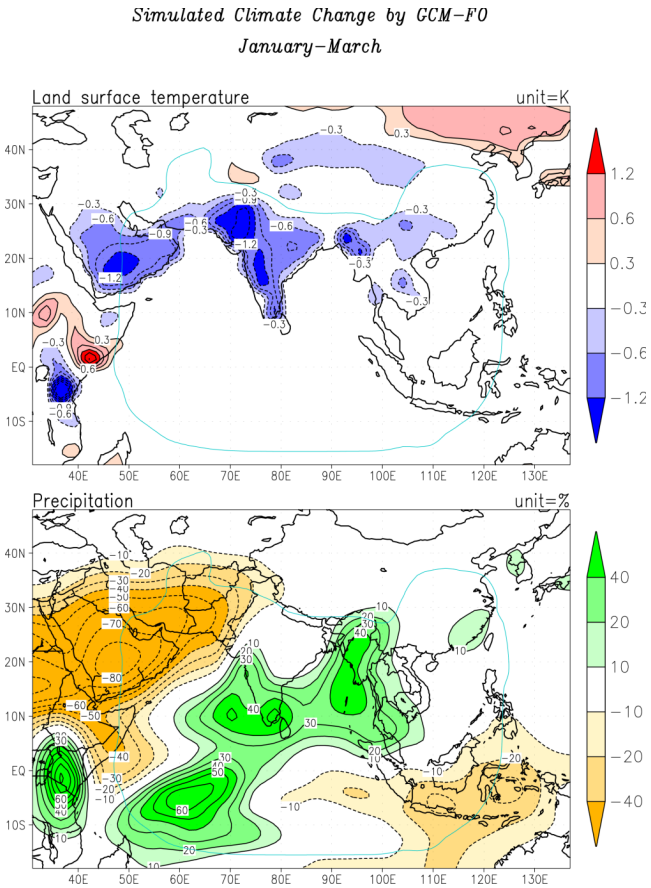

Figure 7.5: Simulated climate change (January-March) with NCAR/CCM3 + observed SST. (a) Land surface temperature change (upper panel) in units of K (b) Precipitation change (lower panel) is displayed in units of percentage. (Chung et al., 2002)

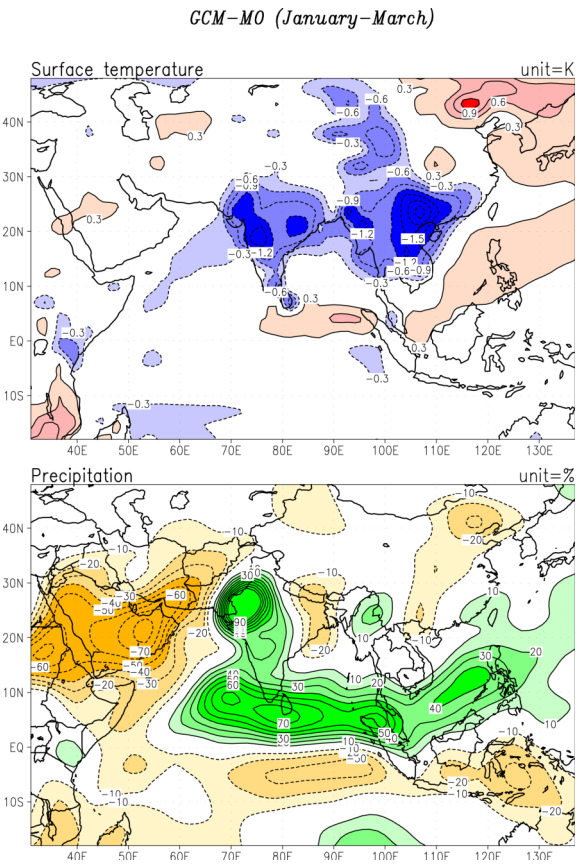

Figure 7.6: Surface temperature change (January-March) simulated with the CCM3 + Slab Ocean Model (Kiehl et al., 2000).

evaporation flux from surface. The stablized boundary layer makes the pollutants harder to remove.

• The haze disrupts the rainfall pattern substantially, with the main characteristics of the convection enhancement north of ITCZ, and a drying northwest of India and over the western equatorial Pacific. The convection suppression in the western Pacific has an implication to ENSO variability and thus to the global climate.

Lastly, both the GCM-FO and GCM-MO show that the tropical mean (20° N to 20° S) evaporation and precipitation decreases by 1 to 2% depending on the season. This decrease is consistent with our expectation that reduction in solar radiation at the surface will be balanced, in part, by a reduction in evaporation.

7.4. Trends in observed atmospheric and surface parameters

Aerosol Optical Depth (AOD) measurements over Peninsular Indian stations (Pune, Trivandrum and Mysore) available for over 10 years now show an increase in AOD over the years (Devara, 2000; Krishnamoorthy, 1999). Turbidity measurements using sunphotometers at several stations in India indicate an increase in turbidity over the years (Srivatsava et al., 1992; Datar et al., 1996). Visibility observations at airports have shown signatures of increased anthropogenic aerosol load over the Indian sub-continent. Significant deterioration of visibility at Mumbai airport due to pollution has also been reported (Chandiramani et al., 1975; Mukherjee et al., 1980).

Analysis of long-term trends of surface-air temperature over a large number of Indian stations by Rupakumar and Hingane (1988) and Rupakumar et al., (1994) suggest a positive trend, consistent with the global trend, having magnitude of about 0.6° C in 100 years. We have analyzed the temperature variations for the January-April months over the Indian region from two different datasets. The plot in Figure 7.8a is the time-series of the daily-mean temperature for the 1990s based on a University of East Anglia dataset (Jones, 1994). The time-series in Figure 7.8b corresponds to the daily-maximum temperature over whole of India for the 1901-1990 period. The similarity in the nature of variations among the two time-series indicates the consistency between the two temperature records.

The correlation coefficient between the two temperature records for the common period (1901-1990) is 0.87. An important feature in Figure 7.8 is the appearance of a long-term positive trend upto about 1960, which leveled off after the 1960s. The superposition of interannual to multi-decadal variabilities on the long-term trends increases the complexity in detecting the signatures of climate change associated with the anthropogenic aerosol forcing. Figure 7.9 shows the NCAR-GCM estimated greenhouse warming and the estimated cooling effect (as part of this UNEP report) due to the South Asian dry season haze. The two effects are about the same but of opposite signs. Furthermore, the haze effect was very small before the 1960s. This suggests that one possible explanation for the near zero trend in the observed temperature records (Figure 7.8) is the near cancellation of the GHG warming and the haze cooling effect.

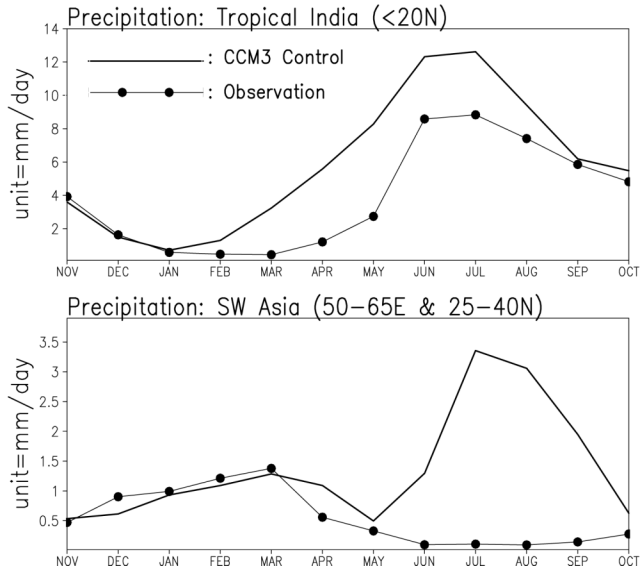

Figure 7.7: Climatological seasonal cycle of precipitation: CCM3 Control Run case was produced with 84 model years of simulation in which the CCM3 was forced repeatedly with the observed SST seasonal cycle. The observation is 21 years (1979-99) of the analyzed precipitation by Xie and Arkin (1997). This observation is currently the state-of-the-art product for precipitation, and is often called CMAP (CPC Merged Analysis of Precipitation).

Analysis of rainfall records during the January-April months over northwest India and Pakistan shows the presence of significant interannual and longer time-scale variations. The time-series of rainfall averaged over stations in the Indo-Pakistan region (Figure 7.10) shows that the winter rainfall in this region has been generally low in this region since the early 1980s, consistent with the model study results in section 7.3 (see Figure 7.5). However, no significant long-term trend is discernable in the rainfall time-series. Krishna Rao (2001) carried out a detailed analysis of rainfall variability over different regions of India and examined their relationship with SST variations in the global oceans. He noted that the rainfall variations over most regions of India are weakly correlated with SST variations during the January-April months. He also noted that although there has been an increase in the ENSO variability in the Pacific Ocean during the recent years, the rainfall over most regions of India has remained in a relatively stable period of low variability.

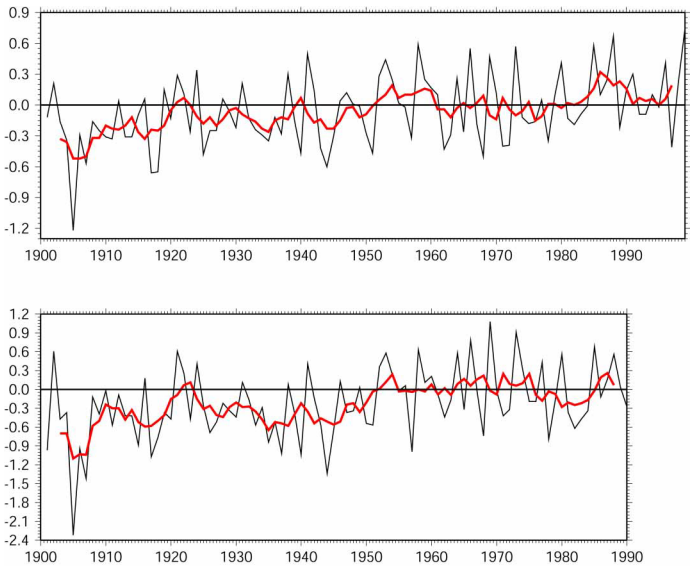

Figure 7.8: Time-series of surface temperature (°C) for the (January-April) season. The red-curve is the 5-year running mean. (a) The daily-mean temperature data from Jones (1994) averaged over Indian region (75–95° E; 10–30° N) for the period (1901-99). (b) The All India daily-maximum temperature data averaged over stations covering the whole of India for the period (1901-90) (Rupkumar, et al., 1994, Indian Institute of Tropical Meteorology, Pune, India).

Impact of GHG and the South Asian Haze

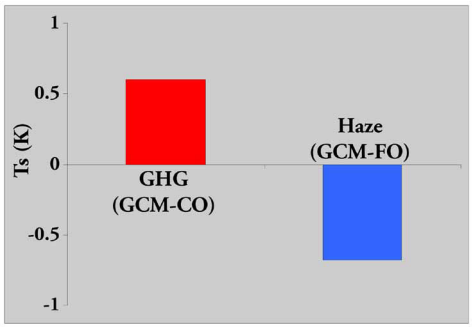

Figure 7.9: The relative impact of Greenhouse gases (GHG) and the South Asian Haze on the average (land only) Indian subcontinent surface temperature as estimated by a GCM-CO (for GHGs) and a GCM-FO. The GCM-CO is described in Washington and Meehl (1996) and the GCM-FO simulation with the South Asian haze is described in Chung, Ramanathan and Kiehl (2002). Both the GHG and the Haze temperature changes are for the January to March period. The values for both the GHG and haze are the difference in the model surface temperature between the pre-industrial to the 1990s.

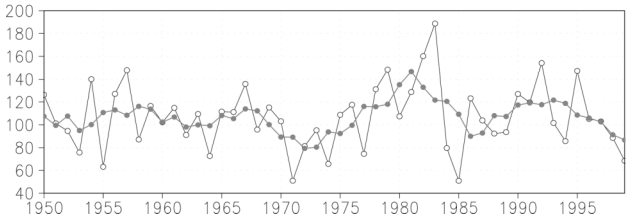

Figure 7.10: Time-series of total rainfall (mm) for (January-April) months over Pakistan and Northwest India. The 5-year running mean is shown by the dark line. The data source is from the GHCN archives (Vose et al., 1992).

8. Agriculture Effects

8.1. Overview

Asia is considered to be the largest agricultural continent. It has 60-90% of the world's agricultural population and contributes about 80-90% of the world's production of rice and tea (Fu et al., 1998). The development of agriculture is also rapid with more than 10% per year increase (The Yearbook of World Economy, 1994). The impact of global warming on Asian agriculture has received some attention recently (Rosenzweg et al., 1992; Hulme et al., 1992; and Zhao and Wang, 1994). These studies take into account the effect of warming on the hydrological cycle, water budget and CO_2 fertilization effect and suggest that by the year 2050, the total crop yield, averaged over the Asian region might decrease by 10-30%. These studies, however, have not accounted for the haze effects. We first describe the potential pathways by which the haze can impact agriculture.

Direct Effects

1) Reduction in total solar radiation can decrease crop productivity (e.g., Chameides et al., 1999).

2) In addition to reducing the total solar radiation, aerosols have a much larger impact on the direct and the scattered radiation. Aerosols lead to a large reduction in direct solar radiation (by as much 30% for the South Asian haze) and enhance the diffuse radiation (by a factor of two or more). Plants whose solar absorption is directionally dependent will be impacted significantly more by the haze than those, which depend on just the total (sum of direct and diffuse; also referred as global radiation) solar radiation.

3) Suppression of rain by the haze (by nucleating more drops of smaller effective radii) can also have large localized effects.

4) Settling of aerosols, such as dust, soot and fly ash, on the leaves can shield them from solar radiation and reduce photosynthesis and may even cause localized heating due to solar absorption by the soot.

5) The other major direct effect is impact of the acidity of the haze, the so-called acid rain problem.

Indirect Effects

1) Potentially, the most important of all of the effects, can arise from the impact of the haze radiative forcing on the hydrological cycle, since water availability is a major limiting factor for agriculture.

2) Change in surface temperature (from the haze radiative forcing) can increase productivity by changing surface evaporation. In addition, a surface cooling by the haze can reduce evaporation of moisture, decrease heat stress on plants and hence increase productivity.

It has been difficult to identify the haze effects on crop yields in Asia (Stanhill and Cohen, 2001), since the rapid growth in agricultural production has been achieved in the last decades due to improved agricultural practice, cultivation and irrigation along with increasing fertilizer usage. In what follows, we summarize the results of a first attempt to estimate the impact of the South Asian haze on Indian agriculture. The results summarized below are based on a crop model developed by the Indian Agriculture Research Institute in New Delhi (Aggarwal and Kalra, 1994). We have restricted our attention to just the direct effect 1 (above). Data on all other effects are insufficient to factor into this analysis.

8.2. Agricultural Consequences of Aerosol Pollution during INDOEX

Global radiation is the major factor regulating carbon assimilation by plants (visible part of the solar spectrum), water loss to the atmosphere and, to a major extent, the temperature of crop canopies (mostly near infrared part of the solar spectrum). Aerosols reduce both the direct and global (the sum of direct and diffuse) radiation at the surface by absorbing and scattering solar light (Figure 8.1) and increasing amount and life-time of clouds.

Data on radiation measurements over several stations in India (e.g. Shende and Chivate, 2000, and references therein) show increasing trends in diffuse radiation during December to May and more than 5% reduction in global radiation. A reduction in global radiation is documented for most of industrial regions over the globe (Stanhill and Cohen, 2001) and attributed to anthropogenic aerosol production.

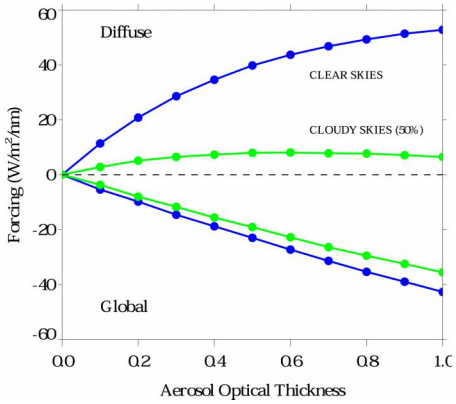

Figure 8.1: Aerosol effect on diffuse and global surface fluxes (direct aerosol forcing) in the PAR (Photosynthetically Active Radiation, 400-700 nm) spectral region. Calculations are made for the case of grassland using the INDOEX aerosol model (Satheesh et al., 1999; Podgorny et al., 2000).

In order to link the region's agriculture with the direct effect (radiative forcing), this study employs three original crop models for simulating growth and productivity of winter wheat, rice and sugarcane in India. To this goal, daily mean aerosol forcing was calculated for Punjab, Maharashtra and Tamil Nadu (Figure 8.2) and used as inputs to the crop models. The models were used to quantify aerosol impact on growth and yield of wheat (Indo-Gangetic alluvial plains and Central India), rice (Coimbatore and Hyderabad in South India) and sugarcane (Delhi, Lucknow and Coimbatore in Indo-Gangetic alluvial plains and South India). The Punjab, Maharashtra and Tamil Nadu datasets were used for Indo-Gangetic Plains, and Central and Southern regions, respectively.

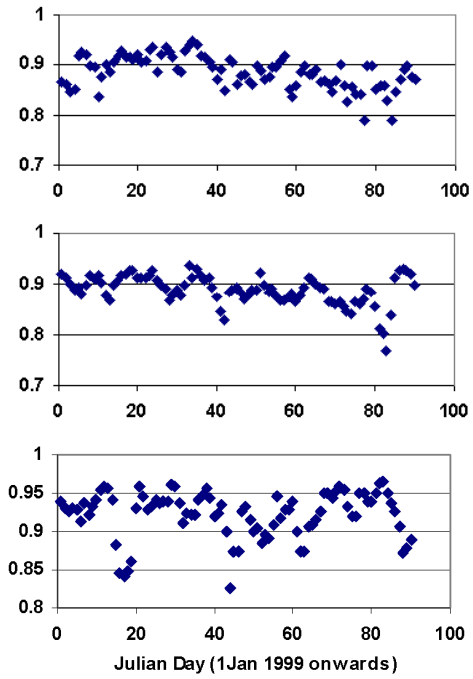

Figure 8.2: Reduction in radiation amounts (direct aerosol forcing) versus Julian day (upper panels) (January-March, 1999) and aerosol induced weather anomalies (lower panels) at Punjab (29.5° N, 76.9° E - 1st and 4th panels), Maharashtra (20.0° N, 76.9° E - 2nd and 5th panels) and Tamil Nadu (10.5° N, 76.9° E - 3rd and 6th panels). The aerosol forcing is estimated from NCAR Aerosol Assimilation Model (Collins et al., 2001) and MACR (Ramanathan et al., 2001a).

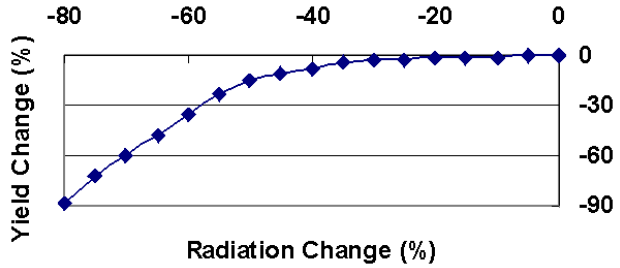

Figure 8.3: Winter wheat crop yield in New Delhi environment versus radiation change at the surface.

8.2.1 Winter Wheat

Wheat is an important food crop of India and is grown during winter season (November to April) in Indo-Gangetic alluvial plains and Central parts of India. In the North Western India, the main cropping system is rice-wheat, which results in a delay in sowing of wheat. To avoid the delay, farmers go for minimum or zero tillage for wheat, burning rice and sugarcane residues from November to March. During the INDOEX event (January to March, 1999), the wheat crop in the region was under tillering to vegetative stage, and thereby the effects on crop processes are expected. Impact of the aerosol event was studied on met. sub-division scale.

Wheat Growth Simulator (WTGROWS) has been developed at the Indian Agriculture Research Institute (Aggarwal and Kalra, 1994) and validated for Indian environments. This model was used to evaluate the effect of radiation reduction from the normal values during the entire growing period on growth and yield of wheat grown under adequate resource inputs. The results for the New Delhi environment (Figure 8.3) show a non-linear response of the yield to the magnitude of radiation reduction. The degree of reduction in total biomass (not shown) was smaller. A weak reaction of wheat yield to 20% radiation reduction from the normal level means that the radiation requirement by the crop is satisfied even under radiation reduction scenario.

WTGROWS was run for the INDOEX event for different wheat growing meteorological sub-divisions under adequately irrigated condition (Figure 8.4). A slight decrease in the grain yield was noticed, but the differences were statistically non-significant.

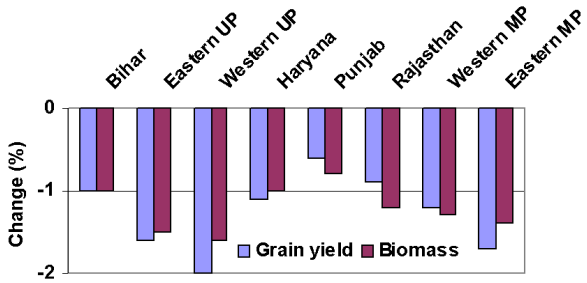

Figure 8.4: Direct effects of aerosol layer (January - March 1999) on biomass and yield of irrigated wheat.

8.2.2 Rice

Rice is the most important cereal crop in India, which occupy nearly 35% of the total area under foodgrain and contribute about more than 40% of the total foodgrain requirement of the country. It is mainly grown in kharif (rainy) season as more than 90% of its acreage comes in this season. In northwestern plains it is mostly grown as kharif crop, as extreme climate prevail over this region. In south and northeastern part of the country rice is grown in all the three seasons due to milder weather during winter season. The growth period generally spans over four months. Limited solar radiation due to cloudy conditions and lack of proper water and nutrient management during the kharif season cause an appreciable decrease in yield as compared to that during the boro and rabi (dry) seasons. That's why with assured irrigation, the winter crop (November - December to March-April) is gaining popularity in South Coastal belts. A reduction in radiation during winter time can decrease the yield adversely and further aggravate the conditions arising because of rice-wheat rotation in different parts of the country.

In the present study, CERES (Crop Estimation Through Resource and Environment Synthesis) Rice model in the DSSAT (Decision Support System for Agrotechnology Transfer) was used for simulating the crop behavior under both scenarios of aerosol impact. DSSAT is a program shell developed under International Benchmark Sites Network for Agrotechnology Transfer (IBSNAT) project which links three major element: crop model, a data base management system and a management/risk assessment program. CERES simulates the effects of weather, soil, water, cultivar, and nitrogen dynamics in the soil and the crop in order to predict the crop growth and yield at a daily time step.

The impact of INDOEX aerosol event was evaluated for Coimbatore and Hyderabad. The water and fertilizer were assumed to be at optimal rates, as farmers generally grow the winter rice under optimal input conditions in these locations. Due to the large range in the date of sowing/transplanting, the two dates were assumed for simulating the impact of aerosol presence on the growth and yield. As seen from Figure 8.5, aerosol can reduce the yield by 6-10% for both dates of sowing. The effect is stronger for the second date of sowing because crop goes through a critical growth phases during the aerosol event.

8.2.3 Sugarcane

Sugarcane is the second most important cash crop in the country, growing in diverse agro-environments both as sub-tropical and tropical crop and occupying an area of about 4.1 million hectares. Uttar Pradesh, Bihar, Haryana and Punjab are the major cane-growing zone in the subtropical region. The crop in this zone grown for about a year compared to 12-18 months in the tropical belt. The productivity of North Indian cane is about 60 t/ha compared to 105 t/ha in South India. Untimely sowing, improper management of irrigation water and fertilizer, and insect-pest infestation are the major causes of its low productivity. The harvest of sugarcane is mainly forced harvesting, dictated by the demand and supply situation. The trash is generally burnt in the field, and the byproduct of the sugarcane industry is used as fertilizer. The radiation use efficiency of sugarcane is relatively high, but the reduction in the radiation during the growth phase can cause a considerable damage in the final yield formation.

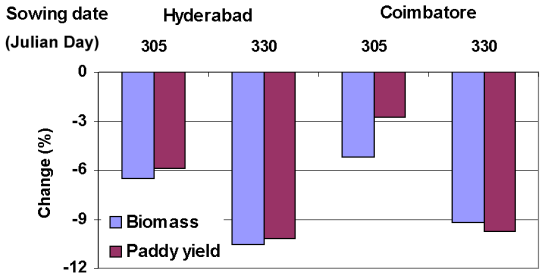

Figure 8.5: Percent change in biomass and yield of rice (rabi season) due to the direct effect of haze.

CANEGRO Module of DSSAT recently validated and calibrated under different production systems for Indian environments and was employed for this study. The impact of the INDOEX aerosol event was evaluated for Delhi, Lucknow and Coimbatore. The simulation runs were carried out for optimal conditions. Aerosol decreases sugarcane yield in all the locations (Figure 8.6).

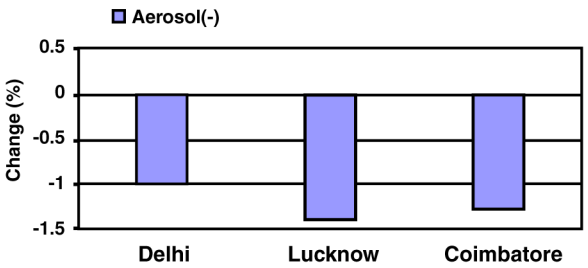

Figure 8.6: Percent change in cane yield.

8.3. Discussion of the INDOEX Case Study

From the INDOEX case study, it appears that without aerosol load the crop yield would increase due to enhanced amount of radiation reaching Earth's surface. The modeling results reported for other regions of the globe (e.g. Stanhill and Cohen, 2001) indicate that a 10-20% decrease in solar radiation, if unaccompanied by significant climatic changes, would generally have minor effect on crop yields and plant productivity. Moreover, the experimental studies (Stanhill and Cohen, 2001, and references therein) point out that where and when crop productivity is limited by water (e.g. arid and semi-arid regions), small decreases in solar radiation may either have little impact on productivity, or may even increase it. In wet climates with low radiative heat load to the plants, a decrease in solar radiation in likely to result in a small decrease in productivity. The results of other studies are, therefore, consistent with those of the INDOEX case study. It should be stressed out, however, that a further increase in aerosol pollution in South Asia may result in a reduction in surface radiation much larger than 20% and trigger a non-linear response in terms of crop yield (see Figure 8.3) with yet unknown negative consequences for food supply in South Asia.

In addition to their radiative impact, aerosols may affect the environment in a variety of ways, most notoriously through acid deposition (also known as "acid rain"). The latter has two parts, specifically, wet deposition (acidic rain, fog, and snow) and dry deposition (acidic gases and particles). Sulfur dioxide (SO_2) and nitrogen oxides (NO_x), are the primary causes of the acid deposition (Lelieveld et al., 2001). Results of the various modeling studies show that the majority of the emissions and damages relevant to acid deposition in Asia currently lie within one country, namely, China (Shah et al., 2000, and references therein). Acid deposition may cause slower growth, injury, or even death of forests, by damaging leaves, limiting nutrients available to trees, and exposing the trees to toxic substances slowly released from the soil. Of course, acid deposition can harm other plants in the same way it does trees. However, food crops are not usually seriously affected because farmers frequently add fertilizers to the soil to replace nutrients that have washed away.

Closely linked to the problem of acid deposition is that of fly ash generated during the combustion of coal in thermal power plants. Ash incorporation in the agricultural fields due to variety of climatic and human actions may affect soil and hence crop productivity. Recent study by Kalra and Jain (1998) concluded that fly ash incorporation in soil at rates matching the ash/dust fall around power plants do not reduce yields of major rabi and kharif crops in India. The shading effects of fly ash and other aerosols deposited on leaves on carbon assimilation by plants still remain to be addressed.

An important issue of enormous concern for agricultural production is the adverse impacts of aerosol on the regional hydrological cycle. As mentioned earlier, winter wheat in India is sown in November-December and harvested in April-May. During the entire wheat season, the average rainfall is between 25 and 150 mm only (see Figure 7.3) so that irrigated conditions are required for achieving an optimum yield. Thus, wheat crop yield in India as well as in other semi-arid regions in Asia may be particularly vulnerable to a non-adequate water supply, one of possible consequences of the haze (see previous sections). Similarly, rice, by far the biggest consumer of water in the Indo-Asia-Pacific region, can be at risk to water shortages due to disruptions in monsoonal circulation.

According to a recent report issued by the Food and Agriculture Organization of the United Nations (FAO/WFP, 2001), a three-year long drought severely affected fruit and rainfed cereal production in Balochistan, Sindh and Punjab provinces of Pakistan. The drought spread over the Central Asia as well including such countries as Afghanistan, Tajikistan and Uzbekistan. More scientific efforts are needed to understand the mechanisms regulating the monsoon rainfall reduction in the region, one of which can be man made aerosols originating from Indo-Pakistan desert. Further spreading of the drought over the Northern India would have catastrophic consequences for the South Asia region in terms of food supply. We conclude therefore that effect of Asian Haze on the region's water supply should be paid most attention when addressing the aerosol impact on region's agriculture.

9. Health Effects

Overview

The health effects of outdoor air pollution have been a topic of investigation for nearly half a century, with much of the original motivation for this research coming from the well-chronicled air pollution disasters - Donora, Pennsylvania 1948 and the London fog of 1952, for example. The resulting body of evidence, coming from application of the research disciplines of toxicology, epidemiology, and exposure assessment is voluminous. It documents a wide array of adverse health effects of air pollution that extend from reduced well-being and increased symptoms to causation and exacerbation of chronic diseases and even premature death. Air pollution typically exists as a complex mixture, reflecting the multiplicity of sources and the many pollutants released by combustion processes, the principal source of pollutants generated by man's activities. Key components of combustion-related air pollution mixtures include particles, emitted as primary particles or formed secondarily from gaseous species, sulfur oxides (SO_x), nitrogen oxides (NO_x), carbon monoxide (CO), and numerous organic chemicals, including carcinogens, e.g., benzo(a)pyrene, and irritants, e.g., formaldehyde. In many urban and rural areas of the world, photochemical reactions involving hydrocarbons and NO_x emitted by biomass burning, vehicles and industry lead to high levels of ozone (O_3).

The respiratory tract is the major entry point of the pollutants and lungs are the ultimate target organs for their adverse health effects. The various complex health effects include bronchitis, pulmonary edema, chronic bronchoitis, emphysema, cancer, asphyxiation and even death in cases of high doses. Most commonly observed effects at lower doses are eye, nose and throat irritation. Dose-response studies provide useful information regarding the threshold limit values (TLVs), maximum allowable concentration for short-term exposure, dangerous short term exposure concentrations and lethal doses for various air pollutants. The TLVs for nitric oxide (NO), NO_2, O_3 and SO_2 are 25, 5, 0.1 and 5 (ppm) respectively.

Although the concentrations of some of the constituents are rather small, the physiological effects can be dangerous. The chemical nature of a number of gases changes in presence of water in the humid atmosphere. Thus, NO_x forms nitric acid and O_3. Such changes may occur on the surface lining of the bronchi. Similarly, SO_2 and other acid mists increase the acidity of the respiratory tissues and O_3 causes intense oxidation and irritation.

The particulates larger than 10 μm are mainly deposited in the extrathoracic part of the respiratory tract. Particles in the range of 2.5 to 6 μm will deposit primarily in the conducting airways below the larynx and particles in the range of 0.5 to 2.5 μm will deposit in the distal airways and alveoli. Particles < 0.5 μm are exhaled without significant deposition. Particles deposited distal to the terminal bronchioles are cleared by alveolar macrophages (AM, an established biomarker for lung response to air pollution) and/or dissolution. AMs will ingest particles and migrate to the mucociliary escalator or into lymphatics. With mouth breathing, the proportion of tracheobronchial and pulmonary deposition increases.

In part driven by regulatory approaches that have emphasized individual pollutants, much of the epidemiologic and toxicologic evidence addresses the adverse health effects of specific pollutants, rather than attempting to characterize the toxicity of ambient pollutant mixtures or classes of mixtures. The literature tends to follow the U.S. Environmental Protection Agency's designation of five major combustion-related pollutants as "criteria pollutants", for which a review of the evidence related to health effects is mandated every five years by the Clean Air Act. These pollutants include particulate matter (PM), sulfur dioxide (SO_2), nitrogen dioxide (NO_2), CO and O_3. Lead is also a criteria pollutant. Interpretation of the literature on these pollutants, particularly that coming from epidemiologic investigation, is complicated by the correlation among the concentrations of these pollutants, reflecting common sources and the transformation of the gaseous pollutants into PM. Attributions of adverse effects to a single pollutant rather than to the full mixture are subject to uncertainty in many instances.

Nonetheless, an extensive literature documents adverse health effects of specific pollutants. This literature has been well summarized elsewhere and in this brief review, we touch on those findings most relevant to the developing country setting (see Bascom et al. 1995, 1996a, 1996b, and Holgate et al. 1999 for comprehensive reviews). Table 9.1 provides an overview of the adverse health effects of air pollution, as summarized in a recent review carried out by a committee of the American Thoracic Society (Bascom et al., 1996a and 1996b). The effects range from increased frequency of respiratory symptoms to increased risk for premature death. For most of the effects, risk increases with increasing concentrations of ambient pollutants, following approximately linear dose-response relationships.

For public health protection, the shape of the dose-response relationship is particularly relevant, as the presence of a threshold implies that some concentrations would not be expected to convey increased risk. However, observational data may give only an imprecise picture of dose-response relationships. Laboratory exposures of volunteers, as carried out, for example, for CO and O_3 can characterize dose-response relationships under the controlled circumstances of exposure to one or several pollutants. Newer techniques for statistical analysis are providing more informative descriptions of dose-response relationships from observational data.

Table 9.1. Air Pollution and Health Threats
(United Nations Population Fund, The State of World Population 2001.)

- Air pollution kills an estimated 2.7 – 3 million people every year, about 90% of them in the developing countries.
- Outdoor pollution harms more than 1.1 billion people and kills an estimated half million people per year, mostly in cities. About 70% of these deaths are in the developing countries.
- Asian mega cities exceed WHO standards for suspended particulate matter and sulfur dioxide (e.g. Beijing, Delhi, Jakarta, Kolkata and Mumbai).
- Indoor air pollution, from the burning of wood, dung, crop residues and coal for cooking and heating - affects about 2.5 billion people, mostly women and girls and is estimated to kill more than 2.2 million each year, over 98% of them in the developing countries.

Since the review carried out by the American Thoracic Society, substantial new evidence has been reported on PM. In urban areas of developed countries, most PM in the respirable size range originates from combustion sources. It is variable in physical and chemical characteristics, depending on its sources. A rapidly enlarging body of toxicologic and epidemiologic evidence links PM to a wide range of adverse health effects, even at concentrations present in many cities of the United States and Europe. PM has been associated with increased risk for mortality, both in studies on shorter-term (days to weeks) and longer-term (years) timeframes. Epidemiological studies have also associated airborne PM with numerous effects on morbidity, including increased risk for hospitalization for pneumonia, heart disease, and chronic obstructive pulmonary disease (COPD), adverse cardiovascular consequences, and exacerbation of asthma.

Considerations Related to Asia Pacific

While extensive epidemiological data have been reported from studies in the United States, Europe and other developed countries, the data from developing countries are far more limited. Can the data from developed countries be generalized to developing countries with reasonable certainty? In extrapolating from the evidence gathered in developed countries, there are inherent uncertainties, reflecting differences in pollutant mixtures and concentration ranges, differing patterns of exposure, and possibly differing levels and distributions of susceptibility. The generally higher levels of indoor air pollution may also modify the risks of outdoor air pollution, perhaps acting to synergistically increase risk. Additionally, even the definition of "an adverse health effect" of air pollution is not an absolute and there may be differing societal judgements as to the acceptability of some consequences of air pollution. A committee of the American Thoracic Society recently provided a commentary on this issue, noting the impossibility of offering a single definition of an adverse health effect of air pollution that would be appropriate for all settings.

Nonetheless, the developed country data offer a basis for estimating the potential hazard of air pollution in developing countries as a prudent basis for controlling air pollution. Levels of pollutants in many cities, particularly the emerging megacities, reach concentrations at which adverse health effects have been well documented. For PM, the developed country studies show surprising homogeneity of risk across a range of particle sources, suggesting that the effects of PM may be general rather than reflecting some specific chemical or physical characteristic. If this hypothesis is correct, then PM would be anticipated to have the same range of effects in developing as in developed countries. Some studies support adverse consequences of PM. Available data from developing countries indicate increased mortality risk associated with PM and also increased risk for acute respiratory infections in children.

Air Pollution Related Health Effects in India

Overview

With the growing population and increasing urbanization/industrialization, several cities in India are faced with the problem of air pollution affecting the daily lives of millions. Air pollution, both indoors as well as outdoors pose serious health risk to the large population living in the Indian cities. The World Bank estimated that in 1991-92 some 40,000 people died from air pollution (caused only by PM in the air) in the

36 cities in India (Brandon and Hommann, 1995). In each of the 23 cities with a million plus population, air pollution levels exceed the WHO standards. In 1995, the total number of deaths due to pollution went up to 52,000 (Kumar, 1997). Table 9.2 shows the number of premature deaths in selected Indian cities. Emissions from the transport vehicles form major source of pollution in urban India, due to use of two-stroke operated and diesel driven vehicles. Apart from transport, industrial boilers, household stoves, municipal refuse burning are also responsible for air pollution in India.

India Scenario

Indian studies, though limited, cover both effects of outdoor pollution as well as indoor pollution.

The estimated annual health effects of indoor air pollution exposure in India is provided in Table 9.3 (adapted from Smith, 2000). Smith (2000) estimates ill health from indoor air pollution to be as large as 4.2-6.1% of the national total, and 6.3-9.21 for women and children under 5. The most serious hazard is acute respiratory infection (ARI), the single largest disease category in India (1/9th of the natural burden). Smith estimates that children below 5 years account for 85% of ARI in India. For TB in women, a study near Lucknow found that male and female householders using wood or dungcakes are 3 times more likely to have someone reporting TB.

Shally et al. (2000) studied the association between ambient air pollution and respiratory symptoms in nearly 700 under-five children leaving in slums in a longitudinal follow-up for 6 months. Ambient air SO_2, NO_x and SPM, and exposure to burning were monitored. The pollutants covaried with each other. Increases in SO_2 and SPM were associated with increased incidence of respiratory symptoms, increased duration of symptoms, or both.

Kamat (2000) carried out studies on the health effects of SPM, SO_2 and NO_x in the seventies. Serial studies of randomly selected matched communities revealed children below 5 years and elderly above 60 years to suffer more. The morbidity for cough, dyspnoea, common colds, eye irritation, headache and dermatitis strongly correlated with the three pollutants. Lung functions were lower with greater pollution. Mortality due to cardiorespiratory causes varied according to SPM levels.

Pande et al. (2000) carried out a study in Delhi between January 1997 to December 1998 to study the relationship between outdoor air pollution and emergency room visits. Daily counts for visits by patients suffering from acute asthma, acute exacerbation of chronic obstructive pulmonary disease and acute coronary events were obtained. Ambient air SPM, SO_2 and NO_x were measured along with temperature and humidity. Data was analyzed using one day time lag for events of interest. It was observed that emergency

Table 9.2. Estimates of annual premature deaths in select Indian cities due to suspended particulate matter (SPM), (The Citizens' Fifth Report, 1999).

City	1991-92	1995
Ahmedabad	2,979	3,006
Kolkata	5,726	10,647
Chennai	863	1,291
Delhi	7,491	9,859
Hyderabad	768	1,961
Kanpur	1,894	3,639
Mumbai	4,477	7,023

Table 9.3. Estimated annual health effects of indoor air pollution exposure in India (Smith, 2000).

	Disease	Deaths (thousands)	Disability Adjusted Life Year (DALY; millions)
Strong Evidence	Acute Respiratory Infections (ARI; >5 years; 880,000)	270-400	9.6-14
	Chronic Obstructive Pulmonary Disease (COPD; 160,000)	20-35	0.39-0.68
	Lung Cancer (6,000)	0.42-0.79	0.0048-0.0090
Moderate Evidence	TB (250,000)	53-130	1.1-2.6
	Asthma (20,000)	3.6-9.0	0.27-0.68
Suggestive Evidence	IHD (1,100,000)	54-200	0.55-2.1
	Possible total (2,300,000)	400-780	12-20
Range used		400-550	12-17

room visits due to acute asthma, acute exacerbation of chronic obstructive pulmonary disease and acute coronary events increased by 21.3%, 24.9% and 24.3% respectively on account of higher than acceptable levels of pollutants.

Chhabra et al. (2001) carried out a cross-sectional study among the residents of Delhi to determine the role of ambient air pollution in chronic respiratory morbidity in Delhi. A random stratified sample (n = 4171) was selected from among the permanent residents, for at least 10 years, around each of the nine permanent air quality monitoring stations in the city. Air quality data for the last ten years was obtained and based on the differences in total suspended particulates (TSP), the study areas were categorized into lower and higher pollution zones. Lung function of asymptomatic non-smokers, however, was consistently and significantly better among residents of lower pollution zones, both in males and females.

Kolkata (Calcutta) is one of the most prominent cities in Asia with over population of over 10 million in an area of about 104 km^2. Like several other cities in India, Kolkata is one of the most polluted cities with nearly 100 pollutants. The city is reported to have very high concentration of total SPM in its air, particularly during winter (Chakraborty, 1988).

Lahiri et al. (1999) evaluated the lung responses to the city air pollution by examining the number of AM and leucocytes in sputum samples at the individual level. The study, based on a survey of over 500 residents of the Kolkata area, notes remarkable correlations between increases in AM counts and air pollution across a diverse population.

Summary

While the available data on the health effects of air pollution for developing countries in Asia Pacific region are limited, the high concentrations of PM in many cities there (Figures 9.1 and 9.2 from Holgate et al., 1999) would be anticipated to increase risk for mortality and morbidity events. A substantial proportion of inhabitants may be susceptible and at increased risk because of malnutrition, infectious diseases, and underlying chronic lung disease, as well as the additional burden of exposure to indoor air pollution.

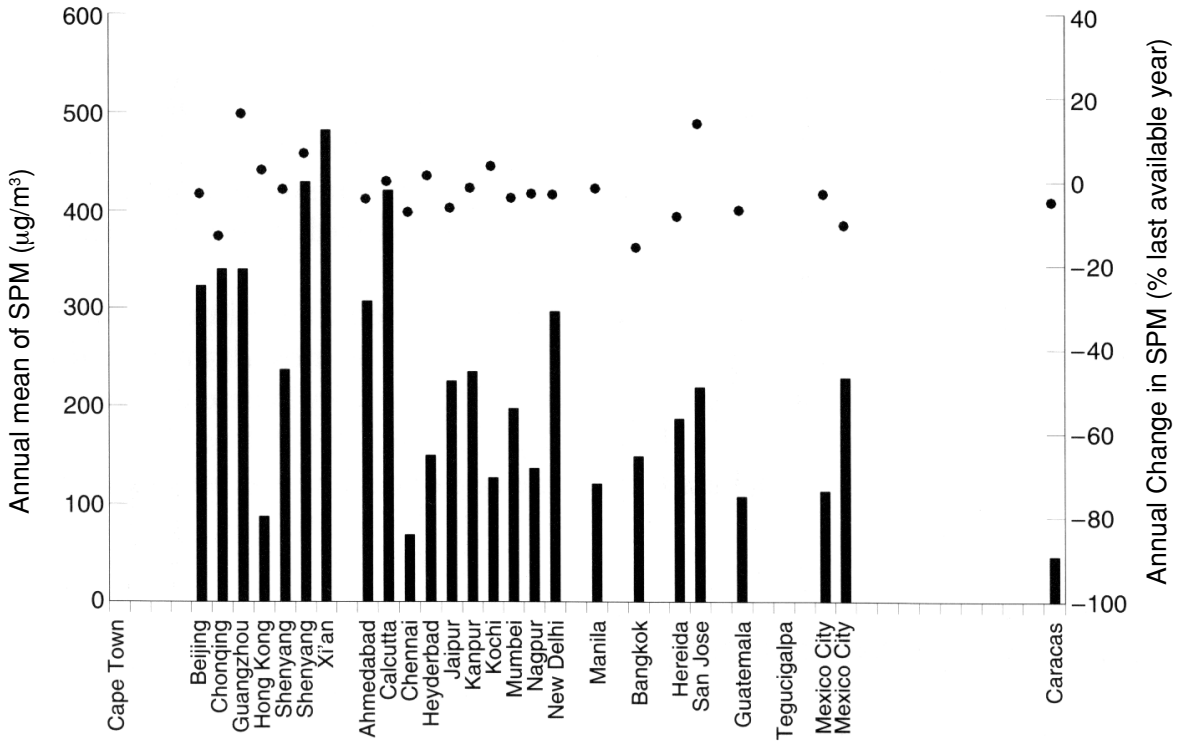

Figure 9.1. Annual mean in last available year (bars) and annual change of total suspended particulate matter concentrations (•) in residential areas of cities in developing countries. Annual change is given as a percentage of the last available year mean (Holgate et al., 1999).

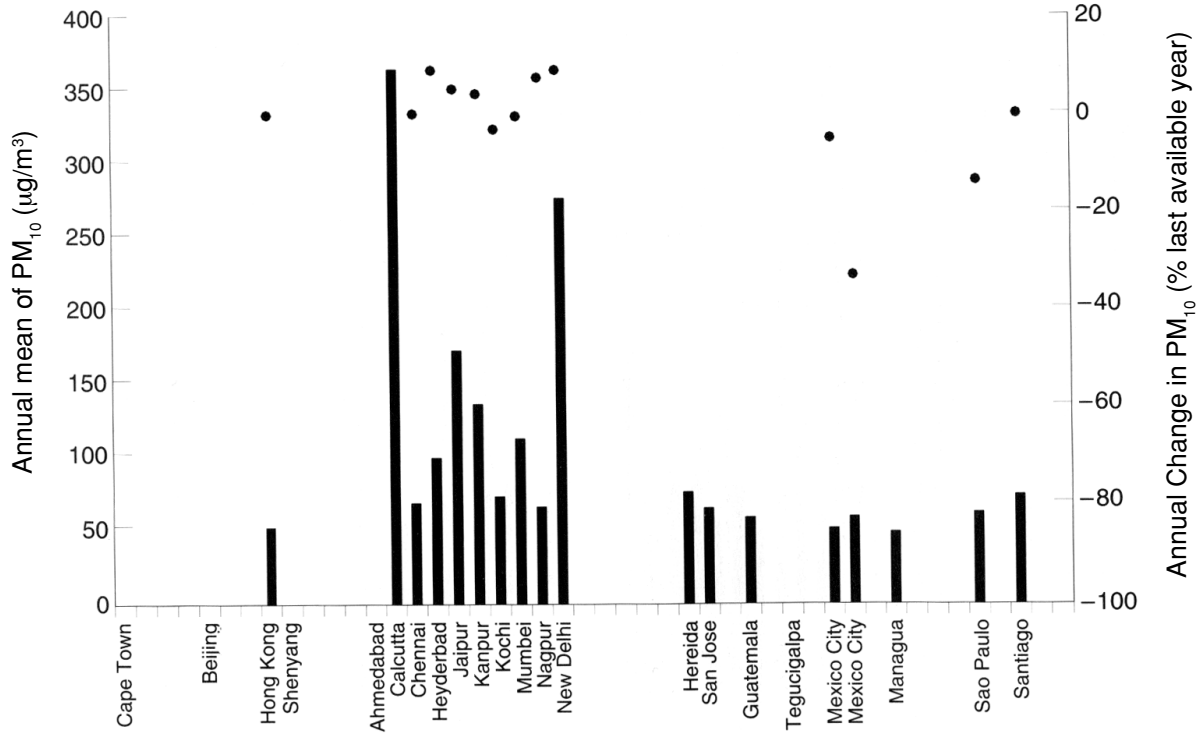

Figure 9.2. Annual mean in last available year (bars) and annual change of respirable particulate matter (PM_{10}) concentration (•) in residential areas of cities in developing countries. Annual change is given as percentage of the last available year mean (Holgate et al., 1999).

Part III: Global and Future Implications

10. Global and Future Implications

10.1. Global

Climate change: It is important to differentiate the decadal to centennial time scales involved in greenhouse gases (GHG) warming from the several days time scale of aerosol life times. On the regional scale, anthropogenic aerosols are already affecting surface forcing, atmospheric heating, and precipitation. It is important to recognize that Asia is not the only source of manmade particles. Anthropogenic aerosol sources are distributed worldwide. Globally averaged, the aerosol net radiative cooling effect may currently be quite comparable with the forcing due to GHG emissions. The role of GHG in global warming will increase because of their accumulation in the atmosphere. For the next decades, the regional aerosol effects will continue to play a major role as long as such strong sources of air pollution remain. It appears that the strongest GHG effect (on surface temperature) will be felt in the southern hemisphere and at the extra-tropical latitudes, whereas the effects from aerosols will be felt most in the tropics and the sub-tropics, particularly in view of the large tropical and sub-tropical aerosol emission sources in the Asian region.

Transcontinental nature of the haze: Life times of most anthropogenic aerosols (sulfates, black carbon, dust) are in the range of 5 to 10 days. If the aerosol is mostly confined to the first 1 kilometer, the transport will be limited to a thousand kilometers or less. However during INDOEX the haze was elevated to higher layers with a peak concentarion at about 3 kilometers. An air parcel at 3 kilometers can travel half way around the globe within a week (Figure 10.1) thus raising the possibility of hemispheric wide dispersal for particles such as black carbon. In addition, gaseous air pollutants, such as CO and O_3, having substantially longer lifetimes can be strongly involved in transcontinental pollutant transport.

Hydrological Cycle: The large reduction in solar radiation at the surface by black carbon has potential implications for spinning down the hydrological cycle. This issue is particularly important in view of the longrange transport of black carbon.

Potential Transcontinental Nature of the "Haze"
Forward Trajectories from 700 mb, March 14-21, 1999

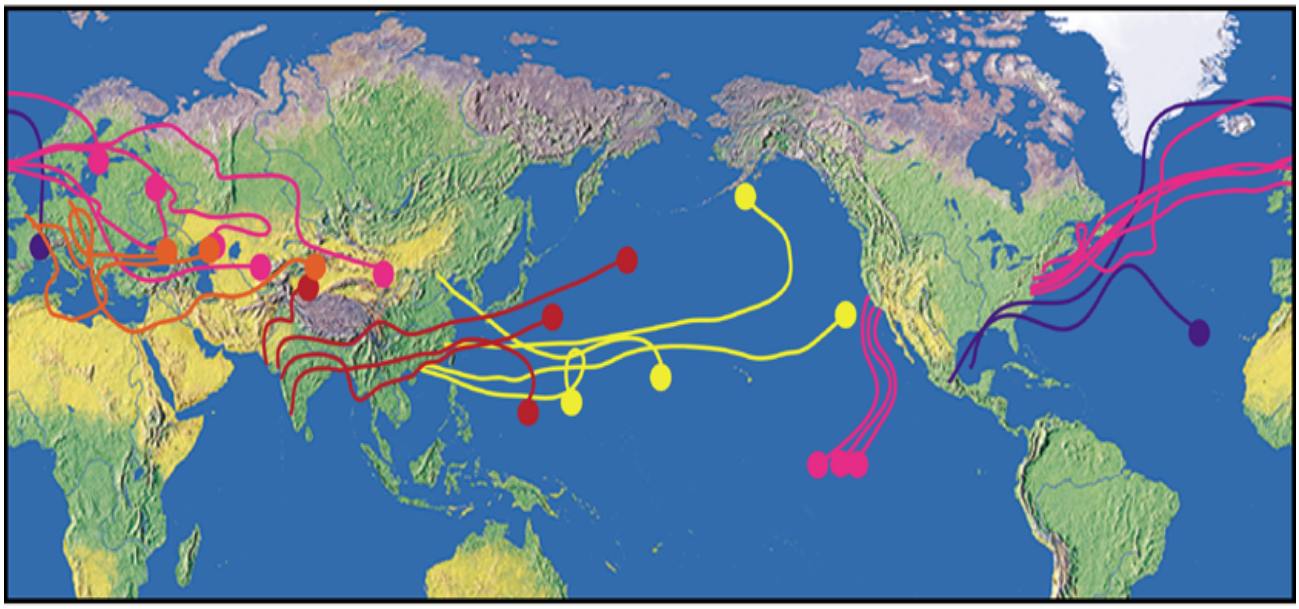

Figure 10.1: Trajectories are from India, China, Mexico, US east and west coasts, London, Paris and Berlin (courtesy of T.N. Krishnamurti).

10.2. Recommendations

A new approach: A more complete picture of the roles and interactions of GHG, aerosols and ozone is urgently needed. Problems such as haze, smog, and acid deposition fall under the general category of air pollution. The aerosols and high level of ozone that result from rural and urban air pollution are part of the global warming issue since they could induce climate change by altering the radiative balance of the planet. Their presence can also have ecosystem impacts, notably on agriculture and public health. Thus, there is a need to assess the impacts under one common framework (Figure 10.2), which is the goal of the proposed strategy for *Project Asian Brown Cloud (ABC)*.

It is now undisputed that primary air pollutants and their chemical products can be transported over distances of many thousands of kilometers. Thus, emissions in one country can cause damage in other countries through transnational and even transcontinental transport. This transport of pollutants converts local issues into regional and global concerns. Thus this issue cannot be addressed by individual national efforts alone. Past experience has demonstrated that the most effective way of tackling air pollution is through international cooperation which is the essence of this proposed strategy. To aid policy actions, we urgently need scientific data on the sources of primary and secondary aerosols from various regions within Asia. In particular we need to characterize the relative strengths of biomass burning and fossil fuel combustion. Such data for India and China are needed first since they contribute the bulk of the total emissions.

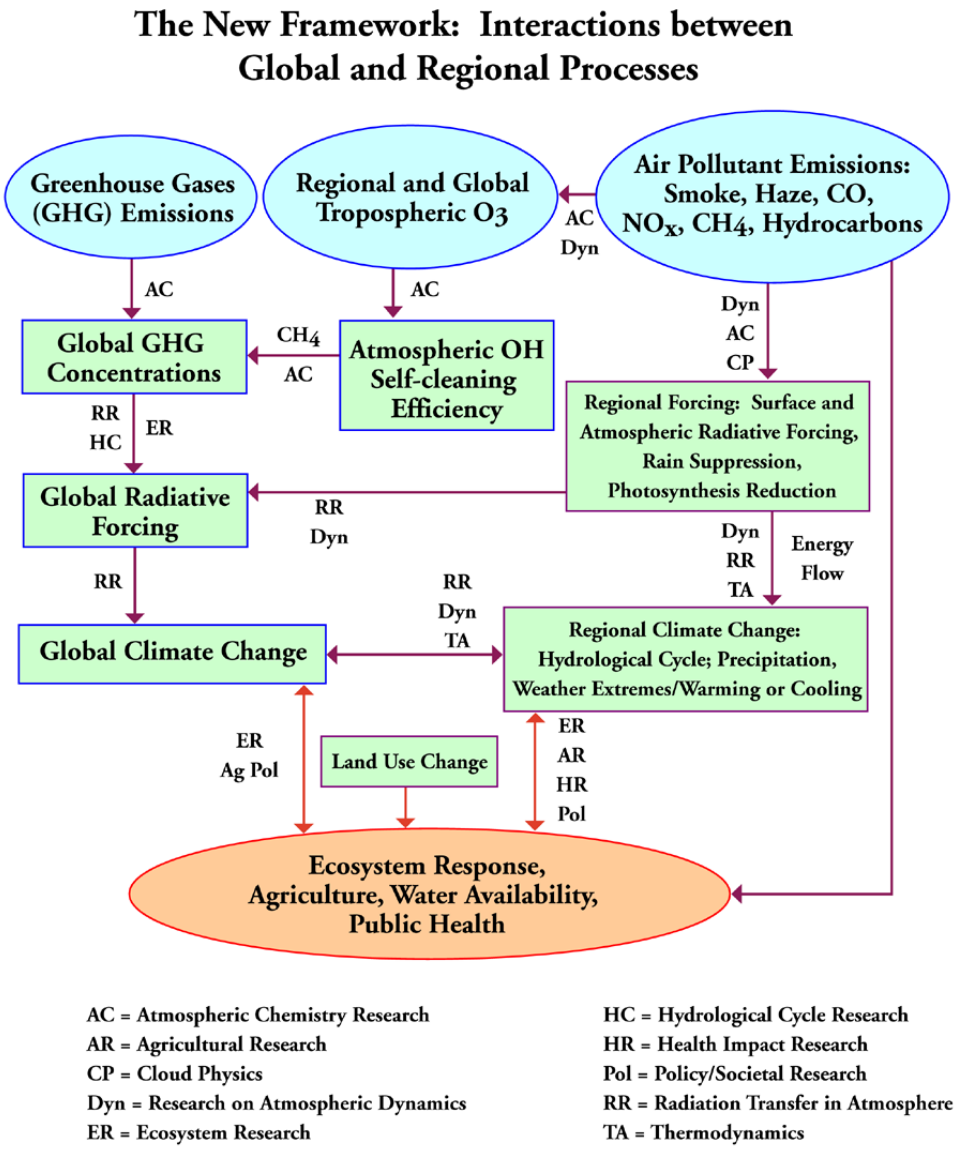

Figure 10.2

A comprehensive program needs to be developed and implemented for understanding the nature and scope of environmental issues facing Indo-Asia-Pacific, and develop a framework for assessing past and future impacts. Such a program should include integration of satellite data with regional surface data, global atmospheric chemistry and climate models in correlation with critical data from public health, agriculture, and marine and terrestrial ecology. Specifically, in the area of capacity building, it should include field experiments to facilitate active collaboration with regional scientists and practical training for regional students and post graduates.

The agriculture assessment should be gradually expanded to include Pakistan, China and particularly Indonesia, Thailand and Vietnam, the region's main rice producers. Of particular interest, to complement and to validate modeling studies, in-situ observations should be set up to provide critical data input for the models. Together with satellite observations, data from these sites should provide critical coverage to understand the long-term build up of atmospheric pollutants in the Indian Ocean/South Asian region and gain insights on the role of transboundary transport of pollutants. When these data are integrated with air pollution data from various cities and surface stations in Asia, we will have a much better understanding of how air pollution is transported and how it impacts on the South Asia-Pacific region.

By the year 2030, the Asian region will house about 5,000 million people (Figure 10.3). According to one projection (Figure 10.4), SO_2 emissions could double during that period. A corresponding increase in the concentration of black carbon and other aerosols can have major negative impacts on the radiation, temperatures and water budget of Asia and of the planet. It is important that steps be taken to slow down the growth of pollutants.

Lastly, given the importance of the South Asian region, we recommend that UNEP undertake such regional assessments periodically. Such an enterprise should be expanded to other parts in the developing world, such as Africa and South America.

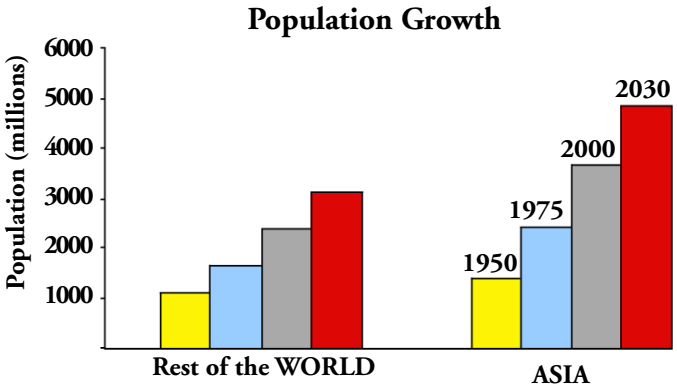

Source: World Population Prospects: The 2000 Revision; United Nations New York.

Figure 10.3

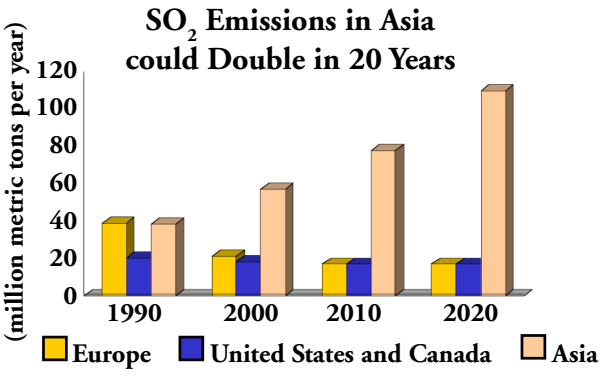

Source: World Resources Institute, Global Environmental Trends, *http://www.wri.org/wri/trends*, R. Downing, R. Ramankutty, and J. Shah, RAINS-ASIA: An Assessment Model for Acid Deposition in Asia (The World Bank, Washington, D.C. 1997), p. 11.

Figure 10.4

References

References

Ackerman, A. S., O. B. Toon, D. E. Stevens, A. J. Heymsfield, V. Ramanathan, and E. J. Welton, Reduction of tropical cloudiness by soot, *Science*, **288**:1042-1047, 2000.

Ackerman, S. A., and S. K. Cox, Radiative energy budget estimates for the 1979 southwest summer monsoon, *J. Atmos. Sci.*, **44**:3052-3078, 1987.

Ackerman, S. A., and S. K. Cox, The Saudi Arabian Heat Low: Aerosol distributions and thermodynamic structure, *J. Geophys. Res.*, **87**:8991-9002, 1982.

Aggarwal, P.K., and N. Kalra (Eds.), Simulating the effect of climatic factors, genotype and management on productivity of wheat in India, Indian Agriculture Research Institute, New Delhi, India, 1994.

Ahmad Q.K., A.K.A. Chowdhury, S.A. Imam and M. Sarker (Eds.), Perspective on flood, 1998, University Press Limited, Dhaka, 2000.

Alfaro, S., L. Gomes, A. Gaudichet, J.L. Rajot, J.F. Leon, H. Cachier, P. Chazette, F. Dulac, P.R. Sarode, S.R. Inamdar, and J.S. Kadadevarmath, Aerosol model derived from measurements performed at an Indian coastal site during the INDOEX intensive field phase: Size distribution and composition, *J. Geophys. Res.*, 2001, submitted.

Asia Least Cost Greenhouse Gas Abatement Strategy (ALGAS), Asian Development Bank, Manila, 1998.

Bascom, R., J. Kesavanathan, and D.L. Swift, Human Susceptibility to Indoor Contaminants, *Occupational Med.-State of the Art Rev.*, **10**(1):119-132, 1995.

Bascom, R., P.A. Bromberg, D.A. Costa, R. Devlin, D.W. Dockery, M.W. Frampton, W. Lambert, J.M. Samet, F.E. Speizer, M. Utell, Health Effects of Outdoor Air Pollution. *Am. J. Respir. Crit. Care Med.*, **153**(1):3-50, 1996a.

Bascom, R., P.A. Bromberg, C. Hill, D.L. Costa, R. Devlin, D.W. Dockery, M.W. Frampton, W. Lambert, J.M. Samet, F.E. Speizer, M. Utell, Health Effects of Outdoor Air Pollution. *Am. J. Respir. Crit. Care Med.*, **153**(2):477-498, 1996b.

Bhattacharya, S. and A.P. Mitra, Greenhouse gas emissions in India for the base year 1990. Scientific Report 11, Centre for Global Change, National Physical Laboratory, New Delhi, 1998.

Brandon, C. and K. Hommann, The cost of inaction: valuing the economy-wide cost of environmental degradation in India. In conference on the Sustainable Future of the Global System, United Nations University, Tokyo, 1995.

Central Pollution Control Board, Delhi, 1998-99. Ambient Air Quality Status-India 1996, Ambient air quality monitoring series: NAAQMS/16/1998-99.

Chakraborty, C., Urban air pollution with special reference to Calcutta, NEERI, 1988.

Chameides, W.L., H. Yu, S.C. Liu, M. Bergin, X. Zhou, L. Mearns, G. Wang, C.S. Kiang, R.D. Saylor, C. Lio, Y. Huang, A. Steiner, and F. Giorgi, Case study of the effects of atmospheric aerosols and regional haze on agriculture: An opportunity to enhance crop yields in China through emission controls? *Proceedings of the US National Academy of Sciences,* **96**:13626-13633, 1999.

Chandiramani, W.G., S.K. Pradhan, et al., A case study of poor visibility over Bombay airport. *Ind. J. Met. Hydrol. Geophys.*, **26**:208-210, 1975.

Chhabra, S.K., P. Chhabra, S. Rajpal and R.K. Gupta, Ambient air pollution and chronic respiratory morbidity in Delhi, Archives of Environmental Health, **56**(1):58-64, 2001.

Chung, C.E., V. Ramanathan, and J.T. Kiehl, Effects of the South-Asian absorbing haze on the monsoon and the surface-air heat exchange, *J. Climate*, Accepted, 2002.

Collins, W.D., A. Bucholtz, P. Flatau, D. Lubin, F.P.J. Valero, C.P. Weaver, and P. Pilewski, Determination of surface heating by convective cloud systems in the central equatorial Pacific from surface and satellite measurements, *J. Geophys. Res. Atmos.*, **105**(D11):14807-14821, 2000.

Collins, W.D., P.J. Rasch, B.E. Eaton, B. Khattatov, J.-F. Lamarque, and C.S. Zender, Simulating aerosols using a chemical transport model with assimilation of satellite aerosol retrievals: Methodology for INDOEX, *J. Geophys. Res.*, **106**(D7):7313-7336, 2001a.

Collins, W.D., P.J. Rasch, B.E. Eaton, D.W. Fillmore, J.T. Kiehl, T.C. Beck, and C.S. Zender, Simulation of aerosol distributions and radiative forcing for INDOEX: Regional climate impacts, *J. Geophys. Res.*, Submitted, 2001b.

Conant, W.C., An observational approach for determining aerosol surface radiative forcing: Results from the first field phase of INDOEX, *J. Geophys. Res.*, **105**(D12):15,347-15,360, 2000.

Cooke, W.F., C. Liousse, H. Cachier, and J. Feichter, Construction of a 1 degrees x 1 degrees fossil fuel emission data set for carbonaceous aerosol and implementation and radiative impact in the ECHAM4 model, *J. Geophys. Res.*, **104**(D18):22,137-22,162, 1999.

Crutzen, P.J. and V. Ramanathan, Foreword, *J. Geophys. Res.*, **106**(D22):28369, 2001.

Datar, S.V., B. Mukhopadhyay and H.N. Srivastava, Trends in background air pollution parameters over India. *Atmos-Environment*, **30**(21):3677-3682, 1996.

Desikan, V., R. Chivate and V.V. Abhyankar, Reaction of radiometric parameters to atmospheric pollution: Part I: Variation over time. *Mausam*, **45**:79-86, 1994a.

Desikan, V., R. Chivate, and V.V. Abhyankar, Reaction of radiometric parameters to atmospheric pollution. Part II: A comparative study between pair of stations. *Mausam*, **55**:139-148, 1994b.

Devara, P.C.S., Long-term trends in the atmosphere. A review with future needs. Long-term changes and trends in atmospheric aerosols in India (Ed. G. Beig). Inst. Pub. New Delhi, 172-202, 2000.

Ellingson, R.G., and G.N. Serafino, Observations and calculations of aerosol heating over the Arabian Sea during MONEX, *J. Atmos. Sci.*, **41**:575-589, 1984.

FAO/WFP crop and food supply assessment mission to Pakistan, Special Report, 11 July 2001. URL= *http://www.fao.org*).

Florig, K.H., China's Air Pollution Risks. *Am. Chem. Soc. Envir. Sci. & Tech.*, **31**(6):274-279, 1997.

Fu, C.B., J-W. Kim and Z.C. Zhao, Preliminary assessment of impacts of global change on Asia. Asian Change in the Context of Global Climate Change, J.N. Galloway and Jerry M. Melillo (Eds.), Cambridge Univ. Press, 1998.

Fuchs, R.J. et al. (Eds.), Mega-city Growth and Future, UNU Press, Tokyo, 1994.

Graedel, T.E. and P.J. Crutzen, Atmospheric Change: An Earth System Perspective, W.H. Freeman & Co., New York, 1993.

Haywood, J.M., R.J. Stouffer, R.T. Wetherald, S. Manabe, and V. Ramaswamy, Transient response of a coupled model to estimated changes in greenhouse gas and sulfate concentrations. *Geophys. Res. Lett.*, **24**(11):1335-1338, 1997.

Holgate, S.T., J.M. Samet, H.S. Koren and R.L. Maynard (Eds.), Air Pollution and Health. Academic Press, San Diego, 1065 pp., 1999.

Hulme, M.,T. Wigley, T. Jiang, Z.C. Zhao, F.T. Wang, Y.H. Ding, R. Leemans and A. Markham, Climatic change due to greenhouse effect and implication for China, Banson Production, 57 pp., 1992.

India Meteorology Department (IMD), Precipitation chemisty and atmospheric turbidity data form Indian BAPMON stations (1973-1980), 1982.

Intergovernmental Panel on Climate Change, *Climate Change 1995: The Science of Climate Change*. Houghton, J.T., L.G. Meira Filho, B.A. Callander, N. Harris, A. Kattenberg, and K. Maskell (Eds.), Cambridge University Press, 1996.

Intergovernmental Panel on Climate Change, *Climate Change 2001: Impacts, Adaptation, and Vulnerability*. Contribution of Working Group II to the Third Assessment. McCarthy, J.J., O.F. Canziani, N.A. Leary, D.J. Dokken, and K.S. White (Eds.), Cambridge University Press, 1032 pp., 2001.

Iyer, N.V., Transparency of atmosphere over Jodhpur, *Mausam*, **36**:250-252, 1985.

Jayaraman, A., D. Lubin, S. Ramachandran, V. Ramanathan, E. Woodbridge, W.D. Collins, and K.S. Zalpuri, Direct observations of aerosol radiative forcing over the tropical Indian Ocean during the Jan.-Feb. 1996 Pre-INDOEX cruise, *J. Geophys. Res.*, **103**:13,827-13,836, 1998.

Jayaraman, A., Results on direct radiative forcing of aerosols obtained over the Indian Ocean, *Current Science*, **76**:924-930, 1999.

Jones, P.D., Hemispheric surface-air temperature variations: A reanalysis and an update to 1993, *J. Climate*, **7**:1794-1802, 1994.

Kalra, N. and M.C. Jain (Eds.), Effect of flyash incorporation on soil properties and crop productivity, Indian Agriculture Research Institute, New Delhi, India, 79 pp., 1998.

Kamat, S.R., Mumbai studies of urban air pollution and health resulting synergistic effects of SPM, SO_2 and NO_x, In: International Conference on Environmental & Occupational Respiratory Diseases, Indian Toxocological Research Centre, Lucknow, India, 2000.

Kiehl, J.T., V. Ramanathan, J.J. Hack, A. Huffman and K. Swett, The role of aerosol absorption in determing the atmospheric thermodynamic state during INDOEX. *EOS Transactions*, AGU, 80, F184, 1999.

Kiehl, J.T., J.J. Hack and V. Ramanathan, AGU Meeting Presentation, San Francisco, 2000.

Krisha Rao, A., Influence of sea-surface temperatures on rainfall over the Indian sub-continent, Under publication, 2001.

Krishnamoorthy, K., Aerosol climatology over India. Indian Space Research Organization, 1999.

Krishnamurti, T.N., B. Jha, J.M. Prospero, A. Jayaraman, and V. Ramanathan, Aerosol and pollutant transport over the tropical Indian Ocean during the 1996 northeast monsoon and the impact on radiative forcing, *Tellus*, **50B**:521-542, 1998.

Krishnamurti, T.N., B. Jha, P.J. Rasch, and V. Ramanathan, A high resolution global reanalysis highlighting the winter monsoon. 1: Reanalysis fields, *Meteor. Atmos. Physics*, **64**:123-150, 1997a.

Krishnamurti, T.N., B. Jha, P.J. Rasch, and V. Ramanathan, A high resolution global reanalysis highlighting the winter monsoon. 2: Transients and passive tracer transports, *Meteor. Atmos. Physics*, **64**:151-171, 1997b.

Krishnand and S.J. Maske, Atmospheric turbidity measurements at a few BAPMON network stations in India, *Mausam*, **34**:327-330, 1983.

Kumar, P., Death in the air. In "Down to Earth, Society for Environmental Communications", New Delhi, (**6**)12:29-43, 1997.

Lahiri P., T. Lahiri and M.R. Ray, Assessment of health impacts of indoor air pollution in Calcutta. Report submitted to Department of Environment of Government of Bengal, India, 1999.

Lal, S. and M.G. Lawrence, Elevated mixing ratios of surface ozone over the Arabian Sea, *Geophys. Res. Lett.*, **28**(8):1487-1490, 2001.

Lal, S., M. Naja and B.H. Subbaraya, Seasonal variations in surface ozone and its precursors over an urban site in India, *Atmos. Environ.*, **34**(17):2713-2724, 2000.

Lelieveld, J., P.J. Crutzen, V. Ramanathan, M.O. Andreae, C.A.M. Brenninkmeijer, T. Campos, G.R. Cass, R.R. Dickerson, H. Fischer, J.A. de Gouw, A. Hansel, A. Jefferson, D. Kley, A.T.J. de Laat, S. Lal, M.G. Lawrence, J.M. Lobert, O.L. Mayol-Bracero, A.P. Mitra, T. Novakov, S.J. Oltmans, K.A. Prather, T. Reiner, H. Rodhe, H.A. Scheeren, D. Sikka, and J. Williams, The Indian Ocean Experiment: Widespread air pollution from South and Southeast Asia, *Science*, **291**(5506):1031-1036, 2001.

Leon, J.-F., P. Chazette, F. Dulac, J. Pelon, C. Flamant, M. Bonazzola, G. Foret, S.C. Alfaro, H. Cachier, S. Cautenet, E. Hamonou, A. Gaudichet, L. Gomes, J.L. Rajot, F. Lavenu, S.R. Inamdar, P.R. Sarode, and J.S. Kadadevarmath, Large scale advection of continental aerosols during INDOEX, *J. Geophys. Res.*, **106**(D22):28,427-28,439, November 27, 2001.

Li, F. and V. Ramanathan, Winter to Summer Monsoon Variation of Aerosol Optical Depth Over the Tropical Indian Ocean, *J. Geophys. Res.*, Submitted, 2002.

Lindzen, R. S., and S. Nigam, On the role of sea surface temperature gradients in forcing low-level winds and convergence in the tropics. *J. Atmos. Sci.*, **45**:2440-2458, 1987.

Lubin, D., S.K. Satheesh, A. Heymsfield, and G. McFarquhar, The longwave radiative forcing of Indian Ocean tropospheric aerosol, *J. Geophys. Res.*, Submitted, 2001.

Mahapatra, A.K. and C.P. Mitchell, Biofuel consumption, deforestation, and farm level tree growing in rural India, *Biomass and Bioenergy*, **17(4)**:291-303, 1999.

Mani, A., O. Chacko and N.V. Iyer, Atmospheric transparency over India from solar radiation measurements, *Solar Energy*, **14**:185-195, 1973.

Meywerk, J., and V. Ramanathan, Observations of the spectral clear-sky aerosol forcing over the tropical Indian Ocean, *J. Geophys. Res.*, **104**:24,359-24,370, 1999.

Mitra, A.P. and C. Sharma, Inventorization of Greenhouse Gas Emissions from Different Sectors in Indian Mega-cities of Delhi and Calcutta, Global Change Open Science Conference, Abstract 815, 2001.

Mukherjee, A.K., C.E.J. Daniel and K. Sethumadhavan, Deteriorating visibility at Bombay airport due to atmospheric pollutants. *Mausam*, **31**:287-290, 1980.

Murray, C.J., and A.D. Lopez, The global burden of diseases, Harvard University Press, 990 pp., 1996.

N.H. Ravindranath and J. Ramakrishna, *Energy Policy*, **25**:63, 1997.

Nakicenovic, N., and R. Swart (Eds.), Special Report of the Intergovernmental Panel on Climate Change on Emissions Scenarios. Cambridge University Press, The Edinburgh Building, Shaftesbury Road, Cambridge, CB2 2RU, England, 2000. URL=*http://www.grida.no/climate/ipcc/emission/index.htm*.

Novakov, T., M.O. Andreae, R. Gabriel, T.W. Kirchstetter, O.L. Mayol-Bracero, and V. Ramanathan, Origin of carbonaceous aerosols over the tropical Indian Ocean: Biomass burning or fossil fuels?, *Geophys. Res. Lett.*, **27**:4061-4064, 2000.

Pande, J.N., N. Bhatta, D. Biswas, R.M. Pandey, G. Ahluwalia, N.H. Siddaramaiah and G.C. Khilnani, Outdoor air pollution and emergency room visits at a hospital in Delhi, In: International Conference on Environmental & Occupational Respiratory Diseases, Indian Toxocological Research Centre, Lucknow, India, 2000.

Parker, D.E., C.K. Folland and M. Jackson, Marine surface temperature: Observed variations and data requirements. *Climatic Change*, **31**:559-600, 1995.

Paroda, R.S., Food, Nutrition and Environmental Security, Presidential address, 88th Session of Indian Science Congress Association, New Delhi, 2001.

Parthasarathy, B., A.A. Munot and D.R. Kothawale, Monthly and seasonal rainfall series for All-India homogeneous regions and meteorological sub-divisions: 1871-1994. Research Report RR-065, Indian Institute of Tropical Meteorology, Pune, India, 1995.

Podgorny, I.A., W. C. Conant, V. Ramanathan, and S.K. Satheesh, Aerosol modulation of atmospheric and surface solar heating over the tropical Indian Ocean, *Tellus*, **52B**:947-958, 2000.

Rajeev, K., V. Ramanathan, and J. Meywerk, Regional aerosol distribution and its long-range transport over the Indian Ocean. *J. Geophys. Res. Atmos.*, **105**(D2):2029-2043, 2000.

Rajeev, K. and V. Ramanathan, Direct observations of clear-sky aerosol radiative forcing from space during the Indian Ocean Experiment, *J. Geophys. Res. Atmos.*, **106**(D15): 17,221-17,235, 2001.

Ramanathan, V., P.J. Crutzen, J.A. Coakley, A. Clarke, W.D. Collins, R. Dickerson, D. Fahey, B. Gandrud, A. Heymsfield, J.T. Kiehl, J. Kuettner, T. Krishnamurti, D. Lubin, H. Maring, J. Ogren, J. Prospero, P.J. Rasch, D. Savoie, G. Shaw, A. Tuck, F.P.J. Valero, E.L. Woodbridge, and G. Zhang, Indian Ocean Experiment (INDOEX), A multi-agency proposal for a field experiment in the Indian Ocean, Technical report, Center for Clouds, Chemistry, and Climate (C^4), Scripps Institution of Oceanography, URL = *http://www-indoex.ucsd.edu/publications/proposal*, June, 1996.

Ramanathan, V., P.J. Crutzen, J. Lelieveld, A.P. Mitra, D. Althausen, J. Anderson, M.O. Andreae, W. Cantrell, G.R. Cass, C.E. Chung, A.D. Clarke, J.A. Coakley, W.D. Collins, W.C. Conant, F. Dulac, J. Heintzenberg, A.J. Heymsfield, B. Holben, S. Howell, J. Hudson, A. Jayaraman, J.T. Kiehl, T.N. Krishnamurti, D. Lubin, G. McFarquhar, T. Novakov, J.A. Ogren, I.A. Podgorny, K. Prather, K. Priestley, J.M. Prospero, P.K. Quinn, K. Rajeev, P. Rasch, S. Rupert, R. Sadourny, S.K. Satheesh, G.E. Shaw, P. Sheridan, and F.P.J. Valero, Indian Ocean Experiment: An integrated analysis of the climate forcing and effects of the great Indo-Asian haze, *J. Geophys. Res.*, **106**(D22):28,371-28,398, November 27, 2001a.

Ramanathan, V., P.J. Crutzen, J.T. Kiehl, and D. Rosenfeld, Aerosols, Climate, and the Hydrological Cycle, *Science*, **294**(5549):2119-2124, December 7, 2001b.

Ramanathan, V. and P.J. Crutzen, Asian Brown Cloud Concept Paper, 2001.

Ravindranath, N.H. and J. Ramakrishna, Energy options for cooking in India, *Energy Policy*, **25**(1): 63-75, 1997.

Rangarjan S., and A. Mani, A new method for determination of atmospheric turbidity, *Tellus*, **36B**:50-54, 1984.

Rao, K.N. and H.R Ganesan, Global and Diffuse solar radiation over India, Indian Meteorology Department, *Monogr. Climatology* - 2, 1972.

Reddy, M.S., and C. Venkataraman, Direct radiative forcing from anthropogenic carbonaceous aerosols over India, *Current Science*, **76**:1005-1011, 1999.

Rhoads, K.P., P. Kelley, R. Dickerson, T. Carsey, M. Farmer, D. Savoie, and J. Prospero, The composition of the troposphere over the Indian Ocean during the monsoonal transition, *J. Geophys. Res.*, **102**:18,981-18,995, 1997.

Rosenfeld, D., Suppression of rain and snow by urban and industrial air pollution, *Science*, **287**(5459):1793-1796, 2000.

Rosenfeld, Y. Rudich and R. Lahav, Desert dust suppressing precipitaiton: A possible desertification feedback loop, *Proceedings of the US National Academy of Sciences*, **98**(11):5975-5980, 2001.

Rosenzweg, C., M. Parry, G. Fisher and K. Frohberg, Climate change and world food supply, Oxford, UK, Environmental Change Unit, University of Oxford, 40 pp., 1992.

Rupakumar, K., K. Krishna Kumar and G.B. Pant, Diurnal asymmetry of surface temperature trends over India. *Geophy. Res. Lett.*, **21**:677-680, 1994.

Rupakumar, K., and L.S. Hingane, Long-term variations of surface air temperatures at major industrial cities of India. *Climate Change*, **13**:287-307, 1988.

Satheesh, S.K., and V. Ramanathan, Large differences in tropical aerosol forcing at the top of the atmosphere and Earth's surface, *Nature*, **405**:60-63, 2000.

Satheesh, S.K., V. Ramanathan, X. Li-Jones, J.M. Lobert, I.A. Podgorny, J.M. Prospero, B.N. Holben, and N.G. Loeb, A model for the natural and anthropogenic aerosols over the tropical Indian Ocean derived from Indian Ocean Experiment data, *J. Geophys. Res.*, **104**(D22):27,421-27,440, 1999.

Shah, J., T. Nagpal, T. Johnson, M. Amann, G. Carmichael, W. Foell, C. Green, J.-P. Hettelingh, L. Hordijk, J. Li, C. Peng, Y. Pu, R. Ramankutty, and D. Streets, Integrated analysis for acid rain in Asia: Policy implications and results of RAINS-ASIA model, *Ann. Rev. Energy Environ.*, **25**:339-375, 2000.

Shally, A., H.A. Glick, R.H. Fletcher and N. Ahmed, Ambient air pollution and symptoms of respiratory disease in preschool children, In: International Conference on Environmental & Occupational Respiratory Diseases, Indian Toxocological Research Centre, Lucknow, India, 2000.

Shende, R.R., and V.R. Chivate, Global and diffuse solar radiant exposures at Pune, *Mausam*, **51**:349-358, 2000.

Sinha, C.S., S. Sinha, and V. Joshi, Energy use in the rural areas of India: Setting up a rural energy data base, *Biomass and Bioenergy*, **14**(5-6):489-503, 1998.

Smith, K.R, National burden of disease in India from indoor air pollution, *Proceedings of the US National Academy of Sciences*, **97(24)**:13,286-13,293, 2000.

Smith, S.J., H. Pitcher, T.M.L. Wigley, Global and regional anthropogenic sulfur dioxide emissions. *Global and Planetary Change,* **29**:99-119, 2001.

Srivastava, H.N., S.V. Dattar and B. Mukhopadhyay, Trends in atmospheric turbidity over India. *Mausam*, **43**:183-190, 1992.

Stanhill, G., and S. Cohen, Global dimming: a review of the evidence for a widespread and significant reduction in global radiation with discussion of its probable causes and possible agricultural consequences, *Agricultural and Forest Meteorology*, **107**:255-278, 2001.

Tahnk, W.R., and J.A. Coakley, Aerosol optical depths and direct radiative forcing for INDOEX derived from AVHRR: Observations, January-March, 1996-1999, *J. Geophys. Res.*, Submitted, 2001.

Tett, S. F. B., P. A. Stott, M. R. Allen, W. J. Ingram and J. F. B. Mitchell, Causes of twentieth century temperature change near the earth's surface, *Nature*, **399**:569-572, 1999.

The Yearbook of World Economy, World Economy Press, 1994.

The Citizens' Fifth Report, A. Agrawal and S. Narain (Eds.), Center for Science and Environment, New Delhi, 1999.

United Nations Development Programme, 2000.

United Nations Population Fund, The State of World Population 2001, Footprints and Milestones: Population and Environmental Change, 2001.

van Aardenne, J.A., F.J. Dentener, J.G.J. Olivier, C.G.M.K. Goldewijk and J. Lelieveld. A 1 degrees x 1 degrees resolution data set of historical anthropogenic trace gas emissions for the period 1890-1990, *Global Biogeochem. Cycles,* 15(4):909-928, 2001.

Vashistha, R.D., R.Madan and S.K.Srivastav, Spectral (direct) solar irradiance at Pune, *Mausam*, **49**:487-492, 1994.

Vashistha, R.D. and S.K. Dikshit, Automatic Weather Stations in India - Recent Trends, In: Papers presented at the WMO Technical Conference on Meteorological and Environmental Instruments and Methods of Observation (TECO-2000), Beijing, China, 23-27 October 2000, WMO/TD - No. 1028, 2000.

Venkataraman, C., B. Chandramouli, and A. Patwardhan, Anthropogenic sulphate aerosol from India: Estimates of burden and direct radiative forcing, *Atmos. Environ.*, **33**(19):3225-3235, 1999.

Vose, R.S., R.L. Schmoyer, P.M. Steurer, T.C. Peterson, R. Heim, T.R. Karl and J.K. Eischeid, The Global Historical Climatology Network. Tech. Rep., ORNL/CDIAC-53, NDP-041, (Carbon Dioxide Analysis Center, USA), 1992.

White Paper on Pollution in Delhi, 2000.

Washington W.M. and G.A. Meehl, High-latitude climate change in a global coupled ocean-atmosphere-sea ice model with increased atmospheric CO_2, *J. Geophys. Res. Atmos.*, **101**(D8):12,795-12,801, 1996.

Working Group 1, Climate Change 2001: The Scientific Basis, Technical report, Intergovernmental Panel on Climate Change, URL=*http://www.ipcc.ch*, 2001.

Working Group on Public Health and Fossil Fuel Combustion, *Lancet*, **350**:1341, 1997, URL=*http://www.epa.gov/oppeoee1/globalwarming/greenhouse/greenhouse6/part.html.*

World Population Prospects: The 2000 Revision; United Nations, New York.

World Resources Institute, Global Environmental Trends, *http://www.wri.org/wri/trends*, R. Downing, R. Ramankutty, and J. Shah, RAINS-ASIA: An Assessment Model for Acid Deposition in Asia (The World Bank, Washington, D.C. 1997), p. 11.

World Resources Institute, 1998.

Xie, P.P., and P.A. Arkin, Global precipitation: A 17-year monthly analysis based on gauge observations, satellite estimates, and numerical model outputs. *Bull. Amer. Met. Soc.*, **78(11)**: 2539-2558, 1997.

Zhao, Z.C. and F. Wang, Climate change and cropping systems in China. Bulletin of CNC-IGBP, **3**:52-62, 1994.

Cover photographs are from:

Focus on Your World
UNEP International Photographic Competition on the Environment 1999-2000

1. Adult Division Honorary Mention No. 54
"Sea of Wonder Thailand" David Fleetham [Canada]

2. Junior Division Honorary Mention No. 8
"Threatened Beauty" Austria Martina Dobrusky [Germany]

3. Adult Division Honorary Mention No. 50
"Reflections of Infinity" Bolivia Mitchell Rogers [USA]

4. Junior Division The International Photographic Scholarship
"Lovely Little Goose" China Xun Wang [China]

5. Adult Division Honorary Mention No. 39
"Paper Mill" Finland Kerttu Lohua [Finland]

Tophoto.co.uk

6. No. 0010112
Gary Brill

www.unep.org
United Nations Environment Programme
P.O. Box 30552-00100, Nairobi, Kenya
Tel: (254 2) 624105
Fax: (254 2) 624269
E-mail: dewainfo@unep.org
Web: www.unep.org
www.unep.net

UNEP

For further information

Director, Division of Early Warning and Assessment
United Nations Environment Programme
P.O. Box 30552-00100, Nairobi, Kenya
Tel: (254-2) 624028 Fax: (254-2) 623943 Email: dewa@unep.org
Web: www.unep.org, www.unep.net